THE DEVELOPMENT OF UNMODIFIED SILVER NANOPARTICLES (AgNPs) AS COLORIMETRIC Hg(II) SENSOR FOR A NEW APPROACH TO SENSITIVE AND HIGH SAMPLE THROUGHPUT DETERMINATION OF Hg(II) UNDER HIGH INFLUENCE OF IONIC MATRIX

SODSAI PUCHUM

A THESIS SUBMITTED IN PARTIAL FULFILLMENT OF THE
REQUIREMENTS FOR THE DEGREE OF MASTER OF SCIENCE
MAJOR IN CHEMISTRY
FACULTY OF SCIENCE
UBON RATCHATHANI UNIVERSITY
ACADEMIC YEAR 2018

UBON RATCHATHANI UNIVERSITY
THESIS APPROVAL
MASTER OF SCIENCE
MAJOR IN CHEMISTRY FACULTY OF SCIENCE

TITLE THE DEVELOPMENT OF UNMODIFIED SILVER NANOPARTICLES (AgNPs) AS COLORIMETRIC Hg(II) SENSOR FOR A NEW APPROACH TO SENSITIVE AND HIGH SAMPLE THROUGHPUT DETERMINATION OF Hg(II) UNDER HIGH INFLUENCE OF IONIC MATRIX

AUTHOR MR. SODSAI PUCHUM

EXAMINATION COMMITTEE

ASSOC. PROF. DR. ATITAYA SIRIPINYANOND	CHAIRPERSON
ASST. PROF. DR. PURIM JARUJAMRUS	MEMBER
DR.HOOI LING LEE	MEMBER
ASST. PROF. DR. MALIWAN AMATATONGCHAI	MEMBER
DR.SUPARB TAMUANG	MEMBER

ADVISORS

………………………………………………….. ADVISOR
(ASST. PROF. DR. PURIM JARUJAMRUS)

………………………………………………….. CO-ADVISOR
(DR.HOOI LING LEE)

……………….…………….…………...…......
(ASST. PROF. DR. CHARIDA PUKAHUTA)
DEAN, FACULTY OF SCIENCE

……………….…………….…………...…......
(ASSOC. PROF. DR. ARIYAPORN PONGRAT)
VICE PRESIDENT FOR ACADEMIC AFFAIRS

ACADEMIC YEAR 2018

ACKNOWLEDGMENTS

I would like to appreciative thank to Asst. Prof. Dr. Purim Jarujamrus my advisor for his excellent suggestions, sharing his extensive chemistry knowledge and to help me achievement my master study. I'd like to thank my co advisor Dr. Hooi Ling Lee who gave me for valuable and fruitful suggestions in the part of synthesis of AgNPs with new approach. Moreover, I would like to give a special thanks to Assoc. Prof. Dr. Atitaya Siripinyanond as the external committee, Asst. Prof. Dr. Maliwan Amatatongchai and Dr.Suparb Tamuang internal committees for their constructive comments in this thesis.

The Center of Excellence for Innovation in Chemistry (PERCH-CIC), Office of the Higher Education Commission (OHEC), Ministry of Education. The research scholarships and instrumental facilities of Department of Chemistry, Faculty of Science, Ubon Ratchathani University are gratefully acknowledged. My appreciation is extended to all the lecturers of the Department of Chemistry, Faculty of Science, Ubon Ratchathani University. Furthermore, I feel thankful to my friends, sisters and brothers here in PJ Group under Nanomaterials Science, Sensors & Catalysis for Problem-based projects for all kind supports.

Finally, and most importantly, I do appreciate my beloved family for their lifetime supports and encouragement on my Master degree pursuing.

Sodsai Puchum
Researcher

บทคัดย่อ

เรื่อง : การพัฒนาใช้อนุภาคเงินนาโนที่ไม่ปรับปรุงพื้นผิวสำหรับตรวจวัดทางสีแบบใหม่ที่จำเพาะต่อปรอท (II) โดยที่ไอออนตัวรบกวนอื่นไม่ส่งผลต่อการวิเคราะห์และสามารถวิเคราะห์ได้หลายตัวอย่างต่อการวิเคราะห์หนึ่งครั้ง
ผู้วิจัย : สดใส ภูชุม
ชื่อปริญญา : วิทยาศาสตรมหาบัณฑิต
สาขาวิชา : เคมี
อาจารย์ที่ปรึกษา: ผู้ช่วยศาสตราจารย์ ดร. ปุริม จารุจำรัส
อาจารย์ที่ปรึกษาร่วม: Dr. Hooi Ling Lee
คำสำคัญ : อนุภาคเงินนาโน, ไอออนปรอท, เซนเซอร์ทางสี, กรดฟอร์มิก, สมาร์ตโฟน

วิทยานิพนธ์นี้นำเสนอการพัฒนาใช้อนุภาคเงินนาโนที่ไม่ปรับปรุงพื้นผิวสำหรับตรวจวัดทางสีเพื่อวิเคราะห์หาปริมาณปรอท (II) ในตัวอย่างน้ำด้วยเทคนิคยูวี วิสิเบิล สเปกโทรโฟโตมิทรี โดยวัดการเปลี่ยนแปลงสีของอนุภาคเงินนาโนออกมาเป็นค่าการดูดกลืนแสง ซึ่งค่าการดูดกลืนแสงของอนุภาคเงินนาโนจะลดลงเมื่อความเข้มข้นของปรอท (II) เพิ่มขึ้นส่งผลทำให้ค่าความยาวคลื่นแสงเลื่อนไปทางความยาวคลื่นแสงสีฟ้าเนื่องจากอนุภาคเงินนาโนถูกออกซิไดซ์โดยปรอท (II) ไอออน ทำให้อนุภาคเงินนาโนลดลงพร้อมกับการเกิดเป็นปรอทอะตอมเกาะบนพื้นผิวของอนุภาคเงินนาโนนำไปสู่การเกิดอนุภาคอมัลกัม (Hg-Ag) มากไปกว่านั้นการใช้กรดฟอร์มิกสามารถเพิ่มประสิทธิภาพและสภาพไวในการตรวจวัดหาปริมาณของปรอท (II) ได้ซึ่งให้ความเป็นเส้นตรงอยู่ในช่วง 0.01 – 10 มิลลิกรัมต่อลิตร (ค่าสัมประสิทธิ์สหสัมพันธ์เท่ากับ 0.999) โดยมีขีดจำกัดต่ำสุดของการตรวจวัดที่ 0.007 มิลลิกรัมต่อลิตร (คำนวณจาก สามเท่าของค่าเบี่ยงเบนมาตรฐานของสัญญาณแบลงค์) นอกจากนี้เซนเซอร์ที่พัฒนาขึ้นมีความจำเพาะเจาะจงต่อปรอทมากกว่าไอออนชนิดอื่นรวมไปถึงตัวรบกวนจากสีย้อมเนื่องจากในงานวิจัยนี้ได้ใช้สารพอลิเมอร์ชนิดโพลีไวนิลไพโรลิโดนเป็นตัวรักษาสภาพพื้นผิวของอนุภาคเงินนาโนที่มีความแข็งแรงส่งผลทำให้อนุภาคเงินนาโนที่พัฒนาขึ้นสามารถทนต่อตัวรบกวนต่างๆที่ปนเปื้อนในตัวอย่างสารละลาย นอกจากนั้นงานวิจัยนี้ได้มีการประยุกต์ใช้สมาร์ตโฟนโดยอาศัยแอปพลิเคชันที่พัฒนาขึ้นสำหรับใช้ในการตรวจวัดทางสีเพื่อวิเคราะห์หาปริมาณของปรอท (II) โดยอาศัยไมโครเพลตขนาดเล็กที่ประกอบไปด้วย 96 หลุมเกิดปฏิกิริยาสำหรับการตรวจวัดเป็นพื้นที่รองรับการเกิดปฏิกิริยาโดยทำการถ่ายรูปปฏิกิริยาที่เกิดขึ้นด้วยสมาร์ตโฟนภายใต้สภาวะที่มีการควบคุมแสงแล้ววิเคราะห์หาปริมาณความเข้มข้นของปรอท (II) ด้วยแอปพลิเคชันที่พัฒนาขึ้นซึ่งสามารถวิเคราะห์ได้หลายตัวอย่างต่อการวิเคราะห์หนึ่งครั้ง (128 ตัวอย่างต่อชั่วโมง) นอกจากนี้เมื่อนำไปวิเคราะห์ด้วยตัวอย่างจริงที่มีการเติมสารละลายมาตรฐานปรอท (II) ที่ทราบความเข้มข้นที่แน่นอนพบว่ามีร้อยละการได้กลับคืนมาในช่วงที่ยอมรับได้และให้ผลสอดคล้องกับผลการทดลองที่ได้จากเทคนิคยูวี วิสิเบิล สเปกโทรโฟโตมิทรี ดังนั้นวิธีการตรวจวัดทางสีที่พัฒนาขึ้นนี้สามารถวิเคราะห์ได้ง่าย รวดเร็ว และมี

สภาพไวในการตรวจวัดรวมถึงมีความจำเพาะเจาะจงต่อการตรวจวัดหาปริมาณปรอท (II) ในตัวอย่างสารละลายที่หลากหลาย

ABSTRACT

TITLE : THE DEVELOPMENT OF UNMODIFIED SILVER NANOPARTICLES (AgNPs) AS COLORIMETRIC Hg(II) SENSOR FOR A NEW APPROACH TO SENSITIVE AND HIGH SAMPLE THROUGHPUT DETERMINATION OF Hg(II) UNDER HIGH INFLUENCE OF IONIC MATRIX
AUTHOR : SODSAI PUCHUM
DEGREE : MASTER OF SCIENCE
MAJOR : CHEMISTRY
ADVISOR : ASST. PROF. PURIM JARUJAMRUS, Ph.D.
CO-ADVISOR : HOOI LING LEE, Ph.D.
KEYWORDS : SILVER NANOPARTICLES (AgNPs), MERCURY (Hg(II)), COLORIMETRIC SENSORS, FORMIC ACID, SMARTPHONE

In this thesis presents an unmodified silver nanoparticles (AgNPs) as colorimetric sensor prepared by green and facile method for determination of Hg(II) ions in aqueous samples which is developed using UV-Vis spectrophotometry. Abrupt change in absorbance of the AgNPs is observed, which progressively decreased and slightly shifted to the blue wavelength as the concentration of Hg(II) increased. It appears that the AgNPs were oxidized by Hg(II), resulting in disintegration of the AgNPs and Hg(0). Deposition of Hg(0) on the surface of AgNPs also occurred, resulting in amalgam particles of mercury (Hg-Ag). Interestingly, the developed approach showed a significant enhancement in the Hg(II) analytical sensitivity when formic acid was doped onto the AgNPs, with the linearity range of 0.01-10 mg L^{-1} (r^2 = 0.999) providing the quantitative detection limit of 0.007 mg L^{-1} (3SD blank/slope of the calibration curve). Greater selectivity toward Hg(II) over other ions and color dyes was also observed, likely a result of stabilization by polyvinylpyrrolidone (PVP), which kept the AgNPs well-stabilized and dispersed in the bulk aqueous environment making them resistant to ionic matrix. Under using a 96-well microplate and a smartphone equipped with homemade application as a colorimetric analyzer under controlled lighting, high sample throughput (128 sample h^{-1}) was achieved, establishing its potential for practical analysis. The percentage recoveries of spiked aqueous samples obtained from the microplate-based system were in acceptable range, in agreement with the values obtained from the UV-Vis spectrophotometry-based system. The proposed colorimetric sensor has been demonstrated to provide a rapid, simple, sensitive and selective detection of Hg(II) ions in various aqueous samples.

CONTENTS

PAGE

ACKNOWLEDGMENTS I
THAI ABSTRACT II
ENGLISH ABSTRACT IV
CONTENTS VI
LIST OF TABLES IX
LIST OF FIGURES XI

CHAPTER 1 INTRODUCTION

1.1 The importance and origin of this research 1
1.2 Objective 3
1.3 Research scope 3
1.4 Research site 3

CHAPTER 2 LITERATURE REVIEWS

2.1 The colorimetric method for the Hg(II) detection based on unmodified AgNPs 4
2.2 Chromatic analysis based on RGB color system 6

CHAPTER 3 EXPERIMENTAL

3.1 Instrumentation 12
3.2 Chemicals and materials 12
3.3 Synthesis of PVP-stabilized AgNPs 14
3.4 Characterizations of PVP-stabilized AgNPs 15
3.5 Optimization of experimental conditions for colorimetric detection of Hg(II) (based on UV-Vis spectrophotometry system) using unmodified silver nanoparticles (AgNPs) as colorimetric probe 17
3.6 Optimization of experimental conditions for colorimetric detection of Hg(II) (based on smartphone as a colorimetric analyzer) using unmodified silver nanoparticles (AgNPs) as colorimetric probe 18

CONTENTS (CONTINUED)

PAGE

3.7 Colorimetric detection of Hg(II) using AgNPs as a probe in the presence of formic acid 21
3.8 The analytical characteristic of the Hg(II) sensor (based on UV-Vis spectrophotometry and smartphone as a colorimetric analyzer) 27
3.9 Study of selectivity of the Hg(II) sensor based on UV-Vis spectrophotometry 27
3.10 Real samples preparation 28
3.11 Study of stability of unmodified AgNPs as a probe for the Hg(II) sensor 28

CHAPTER 4 RESULTS AND DISCUSSION

4.1 Synthesis and their mechanism of PVP-stabilized AgNPs 29
4.2 Characterizations and their mechanism of PVP-stabilized AgNPs as a probe for colorimetric detection of Hg(II) ions 31
4.3 Optimization of experimental conditions for colorimetric detection of Hg(II) (based on UV-Vis spectrophotometry system) 34
4.4 Optimization of experimental conditions for colorimetric detection of Hg(II) (based on smartphone as a colorimetric analyzer) 38
4.5 Using optimized condition for colorimetric detection of Hg(II) using AgNPs as a probe 40
4.6 Study of selectivity of the Hg(II) sensor based on UV-Vis spectrophotometry 47
4.7 Real samples application 52
4.8 The stability of PVP-stabilized AgNPs 54

CONTENTS (CONTINUED)

PAGE

CHAPTER 5 CONCLUSION **56**

REFFERENCES **60**

APPENDIX **66**

CURRICULUM VITAE **100**

LIST OF TABLES

TABLE		PAGE
2.1	Comparison of the sensing performance of reported unmodified AgNPs for Hg(II) detection	12
3.1	The instrumentation for the determination of Hg(II) and characterizations	13
3.2	Chemicals and materials	14
3.3	The operating conditions of UV-Vis spectrophotometer, TEM, SEM-EDS and Zetasizer parameter	17
3.4	The speciation of the smartphone camera	17
4.1	Effect of hydrodynamic size and zeta potential of the PVP-stabilized AgNPs, PVP-stabilized AgNPs in the presence of 0.5 mg L^{-1} Hg(II) and PVP-stabilized AgNPs in the presence of 0.5 mg L^{-1} Hg(II) and 0.5 M formic acid	33
4.2	Comparison between the performance of the current sensor for Hg(II) detection and that of our previous work	36
4.3	pH values of the solution containing various concentrations of formic acid and their corresponding maximum wavelength values of in the presence of Hg(II) in the range 0.05 to 2.0 mg L^{-1}	38
4.4	Precision (%RSD) of the calibration curve of the developed AgNPs observed in three different synthesis batches of AgNPs at various concentration of Hg(II)	45
4.5	Comparison of the results of AgNPs-based colorimetric sensor for Hg(II) detection by using green intensity (Image processing, ImageJ) at different conditions (with formic acid and without formic acid)	46

LIST OF TABLES (CONTINUED)

TABLE **PAGE**

4.6 Percentages of recovery for Hg(II) determination in the presence of methylene blue 51

4.7 Determination of Hg(II) concentration in real aqueous samples application and Standard Reference Material (SRM) 1641d using the UV-Vis spectrophotometry system and smartphone as colorimetric sensor (n=3) 53

4.8 Stability of the AgNPs at room temperature observed on three replicates. Four different batches of the nanoparticles were synthesized. The maximum absorption of AgNPs roughly occurred at 424-433 nm for all synthesis batches, suggesting that our synthesis method provided a good reproducibility. The nanoparticles were also stable at room temperature for several months despite being stored in a transparent vial 54

5.1 Comparison of the sensing performance of reported unmodified AgNPs for Hg(II) detection 58

LIST OF FIGURES

FIGURE **PAGE**

2.1 RGB color model (a) combination of primary light colors generates the new color depending on RGB ratio (b) 9

2.2 G intensity (0 – 255) vs. protein concentration [P]. Data are from triplicate intra-assay measurements. Dashed line: G =G_0exp (-k[P]), k = 0.0993 dl/g, where G_0 is the average G intensity for the 0% protein standard. Inset: Transformed data, V = log(G_0/G) vs. [P]. By least-squares linear regression: V = 0.043[P]/(g/dl) 0.0059, r = 0.997 10

2.3 Real time on-mobile color analysis system for methamphetamine detection 11

3.1 The process of unmodified AgNPs synthesis 16

3.2 The volume of AgNPs solution at 50, 75 and 100 µL 19

3.3 The process of the optimization volume of AgNPs solution in the present of Hg(II) concentration at 0.1 and 1.0 mg L^{-1}, respectively 20

3.4 The instant change of visible color of unmodified AgNPs in the presence of Hg(II) concentration from 0.005 to 10.0 mg L^{-1}: absence of 0.5 M formic acid (a) and presence of 0.5 M formic acid (b) 22

3.5 Determination of Hg(II) using a smartphone equipped with software application CAnal as a colorimetric analyzer on a well plate-based system in the control light box 24

3.6 Flowchart of CAnal application processing 26

3.7 Screenshots of smartphone application CAnal detailing the processes of Hg(II) detection 27

LIST OF FIGURES (CONTINUED)

FIGURE **PAGE**

4.1 Partial electron donation of nitrogen to oxygen and Reduction and bond between Ag^+ ions and PVP molecules 29

4.2 UV-Vis absorption spectrum of unmodified AgNPs stabilized with PVP solution was recorded by adding of 50 µL of AgNPs into 5 mL of volumetric flask and final volume was adjusted at 5 mL by DI water. Inset: Photograph of unmodified AgNPs stabilized with PVP solution 31

4.3 EDS spectrum of the sample stub (a), TEM images and EDS spectra of the dispersion of PVP-stabilized AgNPs (b), PVP-stabilized AgNPs after addition of 5 mg L^{-1} Hg(II) (c), and PVP-stabilized AgNPs after addition of 5 mg L^{-1} Hg(II) and 0.5 M formic acid (d) 33

4.4 Optimization of the volume of AgNPs (50, 75 and 100 µL) using UV-Vis spectrophotometer: (a) spectra of AgNPs at different volumes and optimization of the volume of AgNPs (50, 75 and 100 µL) using UV-Vis spectrophotometer: (b) the calibration curves comparing different volumes of AgNPs (50 , 75 and 100 µL) with A_0/A plotted against the different concentrations of Hg(II) ions 35

4.5 Calibration curves showing the effect of different concentrations (0-2.0 M) of formic acid used as a enhancer reagent for reduction of mercury. Absorbance ratios are plotted against various concentrations of Hg(II) (0.01-2.0 mg L^{-1}) 37

LIST OF FIGURES (CONTINUED)

FIGURE **PAGE**

4.6 Optimal volume of AgNPs studied in the range of 5-50 µL for detecting Hg(II) under different devices (smart phone and scanner) in the presence of Hg(II) in the range of 0.10 to 1.0 mg L^{-1} 39

4.7 Calibration curve showing optimization of different colors based on the RGB system, ●R (red), ■G (green), ◆B (blue), ▲(R + G + B)/3 for average gray and △(0.299R + 0.587G + 0.114B) for gray with luminosity 40

4.8 UV-Vis absorption spectra of the unmodified AgNPs solution upon addition of different concentrations of Hg(II) in the absence, inset: the calibration curve of the A_0/A versus the concentration of Hg(II) (a) and presence of 0.5 M formic acid, inset: the two calibration curves of the A_0/A versus the concentration of Hg(II) (high and low linearity) (b) and the calibration curve of A_0/A value versus the concentration of Hg(II) before and after the addition 0.5 M formic acid (c) Where, A_0 and A represent the absorption intensity of AgNPs roughly occurred at 424-433 nm before and after reaction with different concentrations of Hg(II), respectively 42

4.9 Calibration curve of AgNPs-based colorimetric sensor for Hg(II) detection by using green intensity (image processing, ImageJ) at different conditions (▲ with formic acid and ■ without formic acid) 46

LIST OF FIGURES (CONTINUED)

FIGURE		PAGE
4.10	Calibration curve of the smartphone-based colorimetric analyzer where differences in the green color intensity (G_0-G) are plotted against difference concentrations of Hg(II) (0.05-0.5 mg L^{-1})	47
4.11	Comparison between the selectivity of the newly developed sensor (PVP-stabilized AgNPs) **(a)** and that of our previous work (citrate-based AgNPs) **(b);** AgNPs + 0.1 mg L^{-1} Hg(II) (A), AgNPs + 1mg L^{-1} Hg(II) (B), AgNPs + 10 mg L^{-1} Hg(II) (C), AgNPs + 0.1 mg L^{-1} Hg(II) + 10 mg L^{-1} anions (D-H; chloride, fluoride, nitrate, sulfate, sulfide, respectively) and cations (I-R; Ba(II), Ca(II), Cd(II), Cu(II), Fe(II), Mg(II), Mn(II), Pb(II), Zn(II), Ni(II), respectively)	48
4.12	UV-Vis absorption spectra (a) showing the effect of organic dye (MB) on the maximum absorption wavelength of AgNPs, the absorbance versus the concentration of MB(mg L^{-1}) (b)	50
4.13	UV-Vis spectra showing the effect of organic dyes on the absorption intensity of AgNPs: (a) methyl orange (MO) and (b) neutral red (NR)	51

CHAPTER 1
INTRODUCTION

1.1 The importance and origin of this research

Environmental pollution caused by heavy metals, especially mercury, is a cause for concern around the world. Mercury has been shown to pollute soil, food and even water, originating from diverse sources including increasing human activities, rapid industrialization of cosmetics as well as pharmaceutical and battery manufacturing [1-2]. The toxic effects of Hg(II) greatly harm the digestive, nervous and immune systems as well as organs like kidneys, skin and eyes, and lungs [3]. Mercury exists in various forms which are all toxic to the environment and human beings. Inorganic mercury is one of the most stable and commonly used forms due to its high solubility, existing mostly in water and living systems (mercuric ion, Hg(II)). The World Health Organization (WHO) and US Environmental Protection Agency (USEPA) guidelines recommend that the total maximum mercury content in drinking water should be less than 0.006 mg L^{-1} and 0.002 mg L^{-1}, respectively [2]. Therefore, it is of necessity to have a highly selective and rapid method to monitor Hg(II) levels in various samples under aqueous conditions.

There are various conventional analytical approaches to estimate Hg(II) concentration in aqueous samples including cold vapor atomic absorption spectrometry (CVAAS) and inductively coupled plasma mass spectrometry (ICP-MS) [4-5]. Despite having high selectivity, these methods are costly and time-consuming, and require advanced instruments. Recently, portable instrumentation has attracted considerable research attention whereby detection of an analyte can be done with high simplicity, rapidity, reliability and precision. One of the most simple methods successfully applied to the detection of Hg(II) takes advantage of the color change upon the interaction of nanoparticles and the target analytes. Gold nanoparticles (AuNPs) and silver nanoparticles (AgNPs) have been developed as colorimetric sensors for Hg(II) determination due to their optical and high extinction coefficients of their surface plasmon resonance (SPR) absorption band [6]. AgNPs, in particular, are more favorable because of their low cost and higher extinction coefficients of their surface plasmon resonance (SPR) absorption band (approximately 100-fold) compared to those of gold nanoparticles (AuNPs) of the same size [7].

Up to now, most nanoparticles-based colorimetric sensors for analyte ions detection rely on the interaction between surface modification of AuNPs or AgNPs and the analyte ions inducing “non-cross linking aggregation” or “interparticles crosslinking aggregation” of nanoparticles giving characteristic colorimetric responses [6]. Although these sensors can be used to successfully detect metal ions with high sensitivity, Hg(II) included, their syntheses involve expensive and complicated procedures to modify the surface with recognition molecules such as thymine [8], oligonucleotides [9], L-cysteine [10], protein and DNA [11]. Despite their high sensitivity, the modified NPs lose their superior optical properties through surface modification due to the effects of adsorbed species or capping on the wavelength position and intensity of the SPR band [12].

In this thesis, we reported the use of unmodified silver nanoparticles (AgNPs) prepared by green and facile method as colorimetric sensor for sensitive and high sample throughput determination of Hg(II) ions in aqueous samples. The AgNPs were stabilized with polyvinylpyrrolidone (PVP) leading to good stabilization and dispersion of the nanoparticles in the bulk aqueous environment making them resistant to the influence of ionic suppression, without any need for toxic and hazardous reducing agents like sodium borohydride ($NaBH_4$). Moreover, the effect of formic acid as a catalytic enhancer was investigated with a first view to enhance Hg(II) detection sensitivity based on UV-Vis spectrophotometry. In addition, high sample throughput of Hg(II) determination based on 96-well microplate using a smartphone as a colorimetric analyzer with our homemade application under a housing light controlling system was successfully applied to analyze Hg(II) ions in various real samples.

1.2 Objectives

1.2.1. To use of an unmodified silver nanoparticles (AgNPs) synthesized by green and facile method as colorimetric Hg(II) sensor for a new approach to sensitive determination of Hg(II) under high influence of ionic matrix based on UV-Vis spectrophotometry.

1.2.2. To develop an analysis of Hg(II) in various real samples using a smartphone colorimetric analyzer on 96-well microplate with our homemade application (CAnal) under a housing light controlling system.

1.3 Research scope

1.3.1 Characterizations and stability of PVP-stabilized AgNPs

1.3.2 Optimization of experimental conditions for colorimetric detection of Hg(II) (based on UV-Vis spectrophotometry system) using unmodified silver nanoparticles (AgNPs) as colorimetric probe

1.3.3 Optimization of experimental conditions for colorimetric detection of Hg(II) (based on smartphone as a colorimetric analyzer using developed CAnal application) using unmodified silver nanoparticles (AgNPs) as colorimetric probe

1.3.4 The analytical characteristics of the Hg(II) sensor (based on UV-Vis spectrophotometry and smartphone as a colorimetric analyzer)

1.3.5 Selectivity study of the Hg(II) sensor (based on UV-Vis spectrophotometry)

1.3.6 The determination of Hg(II) in various real samples (based on UV-Vis spectrophotometry and smartphone as a colorimetric analyzer)

1.4 Research site

Department of Chemistry, Faculty of Science, Ubon Ratchathani University, Ubon Ratchathani, Thailand.

CHAPTER 2
LITERATURE REVIEWS

2.1 The colorimetric method for the Hg(II) detection based on unmodified AgNPs

Development of new analytical methods from alternative techniques with simplicity, rapidity, cost-effectiveness is thus considered to be a key target in this thesis. To date, colorimetry is well known, and commonly used for routine analysis without requirement of any complicated instrumentation. Lately, colorimetric sensors providing the rapid optical reaction have been greatly attended being excellent candidates for such simple, economic and high performance analytical methods.

Successful use of unmodified silver nanoparticles (AgNPs)-based sensors for monitoring the level of mercury has been reported [13-15]. A research group led by Huang reported a colorimetric detection method for mercury ions in aqueous medium using graphene oxide (GO)-modified AgNPs [13]. GO was found to be an excellent stabilizer for AgNPs and the invented sensors provided a LOD for Hg(II) of 0.068 mg L^{-1}. However, their synthesis involved the use of sodium borohydride ($NaBH_4$), a toxic agent to reduce GO and Ag(I). In their other publication, they proposed a greener method whereby (GO)-modified AgNPs were prepared by the horn sonication method [14]. Through this method, the LOD for Hg(II) was 0.12 mg L^{-1}. Although no hazardous agents were involved, the green method was time-consuming and complicated. In another study, Mehdinia et al. used AgNPs capped with a biomolecule for determination of inorganic mercury in environmental aqueous media and the LOD of the developed sensor was found to be 0.54 mg L^{-1} [15], Farhadi et al. used soap-root plant as a stabilizing agent for AgNPs to achieve a LOD of 0.44 mg L^{-1} [16] and Gao et al. reported the use of a yogurt-mediated silver nanostructure for label-free and colorimetric mercury ions detection with a LOD as low as 0.002 mg L^{-1} [17] and reported works as demonstrated in Table 2.1 [18-19]. Although highly sensitive, the synthesized biomolecule-linked nanoparticles needed to be freshly prepared and the preparation of these biomolecules was often a complicated and expensive process. Despite their high stability and sensitivity, in general the unmodified

AgNPs as mentioned above were difficult to prepare as their synthesis usually involved a complicated process. In 2015, our recent work reported a selective colorimetric sensor based on unmodified AgNPs to detect Hg(II) using tri-sodium citrate as a stabilizing agent, which achieved a LOD of 0.008 mg L^{-1} using Cu(II) as sensitivity enhancer [20]. However, our previous method involved the use of sodium borohydride ($NaBH_4$) [21-23] and hydrazine [24], a toxic reducing agent. There is also another drawback associated with the aforementioned work in that the unmodified AgNPs may fail in their application on real samples because of the negative incidence of the ionic strength and the presence of exchangeable ligands [12]. Comparison of the sensing performance of reported unmodified AgNPs for Hg(II) detection was summarized in Table 2.1. The goal therefore has been to develop a colorimetric sensor based on “unmodified AgNPs” for Hg(II) detection through a simple and cost-effective method.

To solve that problems, in this thesis, an unmodified AgNPs as colorimetric sensor for sensitive and high sample throughput determination of Hg(II) ions in aqueous samples was proposed. The AgNPs stabilized with polyvinylpyrrolidone (PVP) were synthesized by green and facile method leading to good stabilization and dispersion of the nanoparticles in the bulk aqueous environment making them resistant to the influence of ionic suppression, without any need for toxic and hazardous reducing agents like sodium borohydride ($NaBH_4$). Moreover, the effect of formic acid as a catalytic enhancer was investigated with a first view to enhancing Hg(II) detection sensitivity based on UV-Vis spectrophotometry. In addition, high sample throughput of Hg(II) determination based on 96-well microplate using a smartphone as a colorimetric analyzer with our homemade application (using chromatic analysis based on RGB color system) under a housing light controlling system was successfully applied to analyzing Hg(II) ions in various real samples.

Recently, the chromatic analysis based on RGB color system has attracted interest as an alternative method due to its rapidity, simplicity, low cost and practicality in on-site analysis and high sample throughput. The chromatic analysis based on RGB color system is now obtained increasing.

2.2 Chromatic analysis based on RGB color system

The chromatic analysis is described based on the light spectrum theory, any visible light colors in the RGB system consist of three primary components being red (R), green (G) and blue (B) as illustrated in Figure 2.1a. The combination of primary light colors generates a new color depending on a RGB intensity ratio. For the RGB system applied in 8-bitdigital images, there are 256 different levels of colors (0-255). Each color of a pixel in a digital image is described by the intensity of each primary color represented by the (R, G, B) coordinate which is reported by image analysis software (Figure 2.1b). The coordinates of white and black light colors are (255, 255, 255) and (0, 0, 0), respectively. The total color intensity (V) is calculated from the equation $R + 255G + 255^2B$ [25-26]. The gray scale system is the two tone system of white and black colors which can be calculated from a RGB coordinate by using a white filter (255, 255, 255). Each RGB coordinate is projected on to the direction of a line passing through the black and white coordinates. This results in a new coordinate with the same RGB intensity values ($R = G = B$) and the gray scale also contains 256 levels within the range of 0 - 255 of the 8-bitimage as that in the RGB system. The ideal average grayscale is calculated by $(R + G + B)/3$. However, this is not the true value in the grayscale system. In addition, actual luminosity and human perception of each light color are different. Humans perceive red and green light being brighter than blue light. Luminance factors are thus added in to the grayscale (grayscale with luminosity) calculation for each light color as $0.299R + 0.587G + 0.114B$. Moreover, a RGB color must be converted in to the grayscale in each color channel before use for calculation of the ideal average grayscale and grayscale with luminosity [27]. Image J, image processing software based on the RGB system, was applied to analyze the light color of detection zones through the grayscale system. Thus, all of the color intensities were investigated in the grayscale with different channels being red (G_R), green (G_G) and blue (G_B). Application of Image J allows all colors to be converted into the grayscale for the chromatic analysis (Figure 2.1b). It should be noted that the colors obtained from the three channels (RGB) are subtractive colors and selectively absorb certain wavelengths of light (i.e. blue, green and red light as the wavelength ranges of 400–500, 500–580 and 580–700 nm, respectively), thus affecting the observed colors [28–34]. Humans perceive the converse of the color component that is primarily absorbed [33] such as the bright yellow were expected to reflect red and green light (slight alter) and absorb blue light (significant alter) [35]. The relationship between the subtractive color and wavelength selectivity to light absorption was explained in the previous studies [28-30].

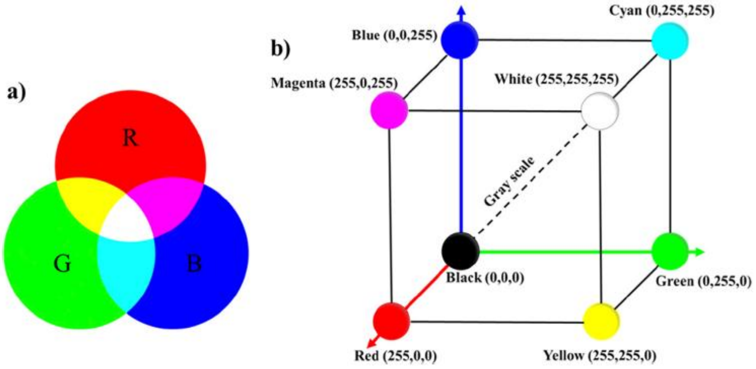

Figure 2.1 RGB color model (a) combination of primary light colors generates the new color depending on RGB ratio (b) [35]**.**

The chromatic analysis based on RGB color system is now obtained increasing for the determination of the various analytes which provide simplicity, rapidity and inexpensive method, example of the reported works [25, 28-30] are as following.

In 2003, Birch et al. [28] reported the use of a desktop scanner for data acquisition in a colorimetric assay. The color scanners typically use charge-coupled device (CCD) arrays to register reflected light intensities for wavelengths corresponding to red (R), green (G) and blue (B) segments of the visible electromagnetic spectrum. They investigated whether a desktop scanner could be used as a data collection device for a quantitative, colorimetric assay. They demonstrate a specific example in which ‘‘RGB’’ data from a color scanner image was used to produce a standard curve for protein concentration using the biuret reagent assay. Biuret reagent turns from light blue to deep purple in relation to protein concentration by binding of cupric ions to peptide bonds, with an absorbance peak at 550 nm (green color). Aliquots of the reaction mixtures were dropped into a 96-well plate and place on the scanner with visual basic program as an image processor based on RGB color system. The calibration curve was plotted between green color intensity against concentration of protein, and the transformed scanner data were correlated with measurements of change in absorbance at 550 nm are shown in Figure 2.2.

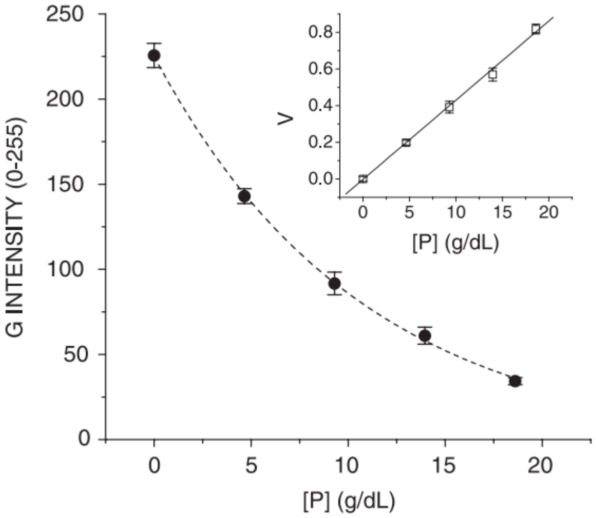

Figure 2.2 G intensity (0 – 255) vs. protein concentration [P]. Data are from triplicate intra-assay measurements. Dashed line: G =G_0exp (-k[P]), k = 0.0993 dl/g, where G_0 is the average G intensity for the 0% protein standard. Inset: Transformed data, V = log(G_0/G) vs. [P]. By least-squares linear regression: V = 0.043[P]/(g/dl) 0.0059, r = 0.997.

In 2011, Chooduma and Niamh Nic Daeid [25] proposed a rapid and semi-quantitative presumptive tests for opiate drugs. They used of the Adobe Photoshop software for color analysis to obtain analytical data in the form of a Red Green Blue (RGB) value. The proposed method were successfully applied to seize heroin samples to demonstrate the application of the technique in a forensic case context. The result shows good agreement with gas chromatographic quantification results was obtained for the illicit samples analysed with a wide linear range and low detection limit for all drugs under test facilitated the application to illicit samples.

In 2012, Choodum et al. [29] reported a rapid quantitative colorimetric test for the determination of 2,4,6-trinitrotoluene (TNT) in soil by using an innovative application of photography where the relationship between the Red Green Blue (RGB) value and concentration of colorimetric product, respectively. The proposed method provides a wide linear range (1–50 mg L^{-1}) and low detection limit (0.73 ± 0.01 mg L^{-1} to 3.5 ± 0.4

mg L^{-1}) achieved was comparable with spectrophotometric quantification methods. The proposed method is providing the accurate, rapid, portable and economically viable quantitative test for the analysis of TNT in soil.

In 2014, Choodum et al. [30] reported the real time quantitative colorimetric test for methamphetamine detection using digital and mobile phone technology. The application for the determination of methamphetamine was installed onto the mobile phone and the relationship profile between RGB intensity, including other calculated values, and the colorimetric product, respectively. The proposed method provided a wide linear range (0.1–2.5 mg mL^{-1}) and a low detection limit (0.0110±0.0001– 0.044±0.002 mg mL^{-1}). The results obtained from the analysis of illicit methamphetamine tablets were comparable to values obtained from gas chromatograph-flame ionization detector (GC-FID) analysis. Method validation indicated good intra- and inter-day precision (2.27–4.49 %RSD and 2.65–5.62 %RSD, respectively). The results shows that this is a powerful real-time mobile method with the potential to be applied in field tests.

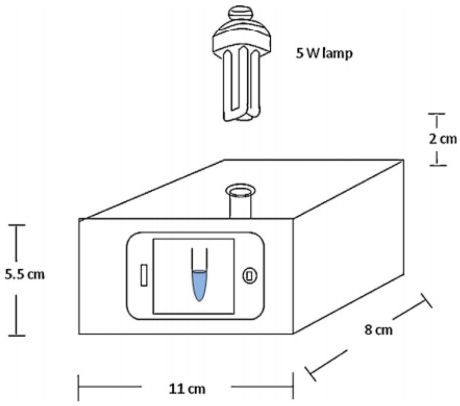

Fig. 2.3 Real time on-mobile color analysis system for methamphetamine detection [30]**.**

Table 2.1 Comparison of the sensing performance of reported unmodified AgNPs for Hg(II) detection

Types of unmodified AgNPs	**Characteristics of the sensor**	**Enhancer**	**Linear range/LOD (mg L^{-1})**	**Analysis time (min)**	**Interferences**	**Real samples**	**Ref.**
Soap-root plant-capped AgNPs	Use of freshly prepared biological extract for stabilization^{b}	–	2.01 - 20.06, (0.44)	5	Tolerance of Hg(II) to 13 cation species (1-fold)	Lake water	[16]
Yogurt-derived compounds-capped AgNPs	Use of biomolecule for stabilization^{b}	–	No report/(0.002)	–	Tolerance of Hg(II) to 8 cation species (1-fold)	Tap water and groundwater	[17]
Bioreductant-capped AgNPs	Use of freshly prepared biological extract for stabilization^{b}	–	1.0 - 20.06, (0.17)	instant measurement	Tolerance of Hg(II) to 11cation species (4-fold)	Tap and lake water	[18]
L-Tyrosine-capped AgNPs	Use of biological compound (L-Tyrosine) as reducing agent^{b}	–	0.0032 - 0.13, (0.0032)	5	NA.	Drinking and tap water	[19]
Citrate-capped AgNPs	Use of Strong reducing agent ($NaBH_4$)	Cu(II)	0.5 - 7.0, (0.008)	instant measurement	Tolerance of Hg(II) to 7 cations species (3-fold)	Tap and drinking water	[20]
Citrate-capped AgNPs	Use of strong reducing agent ($NaBH_4$)^{b}	AChE, ACTh	0.002 - 0.01, (0.00024)	5	Tolerance of Hg(II) to 11 cation species (1-fold)	Lake water, groundwater and sea water	[21]

Table 2.1 Comparison of the sensing performance of reported unmodified AgNPs for Hg(II) detection (continued)

Types of unmodified AgNPs	Characteristics of the sensor	Enhancer	Linear range/LOD (mg L^{-1})	Analysis time (min)	Interferences	Real samples	Ref.
Citrate-capped AgNPs	Use of strong reducing agent ($NaBH_4$)$^{b\ (48\ h)}$	H_2O_2	No report/(2.0 mg L^{-1})	–	Tolerance ratio of Hg(II) to cations (1-fold)	NA.	[22]
PVP-capped AgNPs	Use of strong reducing agent ($NaBH_4$)^b	Lysine	0.0002 - 6.0, (0.0002)	1.5	Tolerance of Hg(II) to 14 cation species	Tap water	[23]
TPDT^a-SiO_2-capped Ag NPs	Use of toxic reducing agent (hydrazine)^b	–	1.0 - 15.0, (1.0)	2	Tolerance of Hg(II) to 10 cation species (5-fold)	NA.	[24]

[a] N-[-3-(trimethoxysilyl) propyl] diethylenetriamine

[b] These synthesized sensors require a complicated and time-consuming process.

[C] Polyvinylpyrrolidone

[d] Based on UV-Vis spectrophotometry system

[e] Based on smartphone as a colorimetric analyzer

NA. Defined as "Not Analysis

CHAPTER 3
EXPERIMENTAL

3.1 Instrumentation

The instrumentations used in this thesis were shown in Table 3.1

Table 3.1 The instrumentations

Instruments	Model	Company
UV-Vis spectrophotometer	UV-2600	Shimadzu, Japan
Transmission Electron Microscope, TEM	JEM-2010	JEOL, Japan
Scanning Electron Microscopy with Energy Dispersive Spectroscopy, SEM-EDS	JSM-6335F	JEOL, Japan
Zetasizer nanoZ	nanoZs	Malvel, UK
Scanner	9000F Mark ll	Canon
Smartphone	Galaxy J7	Samsung
Microtiter plate	Brand plates	Wertheim, DE

3.2 Chemicals and materials

All chemicals used in this thesis were of analytical grade which were shown in Table 3.2

Table 3.2 Chemicals and materials

Chemical	Formula	Supplier
Formic acid (98%)	CH_2O_2	Fisher Scientific, UK
Polyvinylpyrrolidone (PVP)	$(C_6H_9NO)_n$	Sigma-Aldrich, US
Silver nitrate	$AgNO_3$	Bendosen, Malaysia
Mercury(II) chloride	$HgCl_2$	Carlo Erba, IT
Calcium nitrate	$Ca(NO_3)_2$	Carlo Erba, IT
Sodium chloride	$NaCl$	Carlo Erba, IT
Potassium fluoride	KF	Carlo Erba, IT
Sodium nitrate	$NaNO_3$	Carlo Erba, IT
Copper(II) sulfate pentahydrate	$CuSO_4{\cdot}5H_2O$	Carlo Erba, IT
Manganese sulfate monohydrate	$MnSO_4{\cdot}H_2O$	Carlo Erba, IT
Sodium sulfate heptahydrate	$Na_2SO_4{\cdot}7H_2O$	Carlo Erba, IT
Sodium hydrogen sulfide	$NaHS$	Carlo Erba, IT
Iron(II) sulfate heptahydrate	$FeSO_4{\cdot}7H_2O$	Carlo Erba, IT
Zinc sulfate heptahydrate	$ZnSO_4{\cdot}7H_2O$	Carlo Erba, IT
Magnesium sulfate heptahydrate	$MgSO_4.7H_2O$	Carlo Erba, IT
Nickel(II) sulfate	$NiSO_4$	Carlo Erba, IT
Cadmium nitrate tetrahydrate	$Cd(NO_3)_2{\cdot}4H_2O$	Carlo Erba, IT
Barium nitrate	$Ba(NO_3)_2$	Carlo Erba, IT
Lead nitrate	$Pb(NO_3)_2$	Carlo Erba, IT
Methylene blue (MB)	$C_{16}H_{18}ClN_3S$	SUVCHEM, India
Methyl orange (MO)	$C_{14}H_{14}N_3NaO_3S$	SUVCHEM, India
Neutral red (NR)	$C_{15}H_{17}ClN_4$	SUVCHEM, India

Table 3.2 Chemicals and materials (continued)

Material	Details	Supplier
Standard reference material (SRM) of mercury in water (1641d)	Certified value of mercury 1.56 ± 0.02 mg kg^{-1}	National institute of standards and technology, NIST, US
The plasma from human blood	Contained 4% tri-sodium citrate	Sigma-Aldrich, USA

3.3 Synthesis of PVP-stabilized AgNPs

AgNPs were synthesized using the methods developed by our collaboration (Muniandy, Sasidharan & Lee, 2019) [36]. AgNPs were easily synthesized based on the hydrothermal method in the presence of PVP, used as a reducing and stabilizing agent. Briefly, a preparation of one molar ratio, R= 1 was done by mixing 0.612 g of $AgNO_3$ and 0.4 g of PVP in 20 mL of distilled water separately at room temperature. The molar ratio, R between the repeating unit of PVP and $AgNO_3$ in this study however was fixed at R = 5. The solutions were then added dropwise into another 50 mL of distilled water. The total solution (90 mL) was stirred for 15 min and the entire mixture was transferred into a Teflon vessel (capacity = 100 mL). The reaction vessel was then put in a stainless steel hydrothermal reactor and placed in the oven at 160 °C for 24 h. Finally, a yellowish-brown color solution of AgNPs stabilized by PVP was obtained as shown in Figure 3.1. The absorption spectrum was observed with a UV-Vis spectrophotometer. The particle size characterization of AgNPs was also confirmed by TEM.

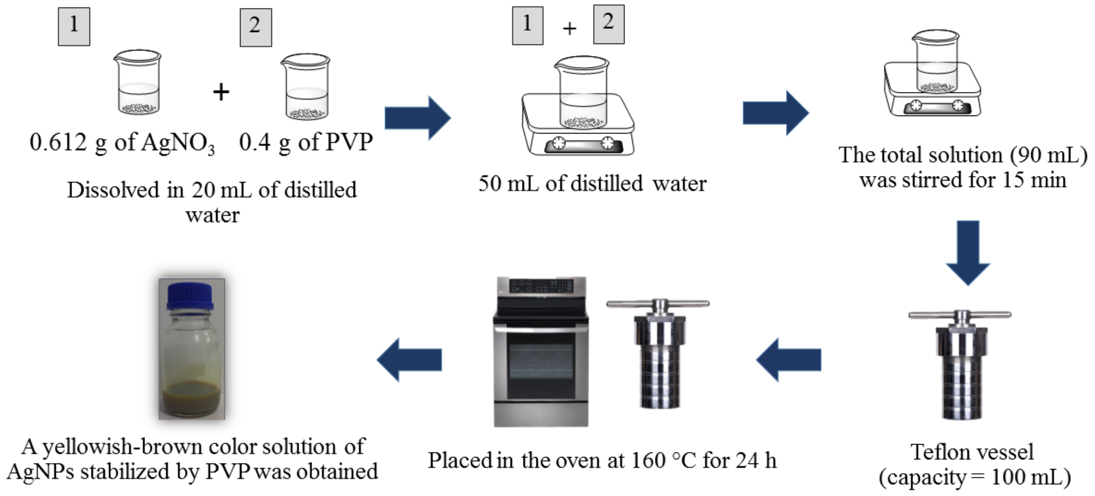

Figure 3.1 The process of unmodified AgNPs synthesis [36]**.**

3.4 Characterizations of PVP-stabilized AgNPs

The absorbance spectrum of the AgNPs was collected using a double beam, UV- 2600 UV-Vis spectrophotometer (Shimadzu, Japan) in the spectral range of 200-800 nm. The morphology and size of the AgNPs were examined by a JEM-2010 transmission electron microscope (TEM; JEOL, Japan) at 200 kV using 200-mesh Cu grids coated with carbon film. Energy dispersive X-ray spectroscopy (EDS) analysis of the formation of various amalgam particles (Hg-Ag) was carried out using a JSM-6335F scanning electron microscope (SEM; JEOL, Japan) equipped with INCA energy dispersive X-ray spectroscopy detector (EDS; JEOL, Japan), operated at an acceleration voltage of 15 kV. The zetasizer nanoZS (Malvern, UK) was used to observe the effect of different concentrations of Hg(II) on the hydrodynamic size and zeta potential of the synthesized AgNPs in the presence and absence of formic acid. All pictures were recorded by a smart phone camera (Samsung Galaxy J7) and microtiter plate (Brand plates® made in Germany).

Table 3.3 The operating conditions of UV-Vis spectrophotometer, TEM, SEM-EDS and Zetasizer parameter

UV-Vis spectrophotometer operating conditions	
Slit width (nm)	1.0
Scan range (nm)	200-800
Scan speed	medium
Sample interval (nm)	0.5
TEM operating conditions	
Acceleration voltage (kV)	200
Working distance (nm)	10
Time scan (s)	300
Temperature (ºC)	25
Zetasizer operating conditions	
Temperature (ºC)	25
Refractive Index	1.4969
Viscosity	0.5580
Dielectric Constant	2.4
SEM-EDS operating conditions	
Acceleration voltage (kV)	15
Acquisition time (s)	60
Process time (s)	5

Table 3.4 The specification of the smartphone camera

Specification of the smartphone		**Details**
Display	Type	Super AMOLED capacitive touchscreen, 16 M colors
	Size	5.5 inches, 83.4 cm^2 (~69.6% screen-to-body ratio)

Table 3.4 The specification of the smartphone camera (continued)

Specification of the smartphone		**Details**
Display	Resolution	720 x 1280 pixels, 16:9 ratio (~267 ppi density)
Main camera	Single	13 MP, f/1.9, 28mm (wide), AF
Platform	OS	Android 5.1 (Lollipop), upgradable to 6.0.1 (Marshmallow)
	Chipset	Qualcomm MSM8939 Snapdragon 615 (28 nm)
	CPU	Octa-core (4x1.4 GHz Cortex-A53 & 4x1.0 GHz Cortex-A53) Octa-core 1.5 GHz Cortex-A53

3.5 Optimization of experimental conditions for colorimetric detection of Hg(II) (based on UV-Vis spectrophotometry system) using unmodified silver nanoparticles (AgNPs) as colorimetric probe

3.5.1 Optimization of the volume of AgNPs

To investigate the optimized conditions in which AgNPs-based colorimetric sensor can effectively detect Hg(II), it was essential to study the various parameters affecting Hg(II) detection. The volume of AgNPs was first optimized without Hg(II) by studying the UV-Vis spectra of AgNPs at volumes of 50, 75 and 100 µL, respectively. Briefly, 50, 75 and 100 µL of freshly prepared AgNPs were transferred to a volumetric flask and the final volume of 5 mL was adjusted by DI water as shown in Figure 3.2. Subsequently, the absorption spectra were investigated by UV-Vis spectrophotometer.

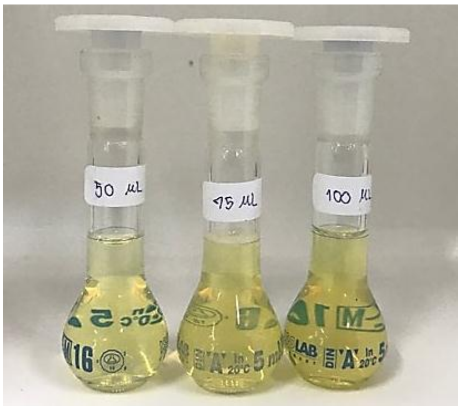

Figure 3.2 The volume of AgNPs solution at 50, 75 and 100 µL.

3.5.2 Study the effect of enchancer on the reduction of mercury

To study the effect of enchancer on the reduction of mercury, formic acid was dropped into the AgNP solution. The different concentrations of formic acid and pH values were investigated in this study. The concentration range of 0.0 to 2.0 M and pH range of 1.0 to 6.0 were optimized. Firstly, 50 µL of the AgNPs was added into a volumetric flask. Then, Hg(II) at different volumes of 50 mg L^{-1} Hg(II) stock was added to a solution containing AgNPs. In addition, formic acid solution was added and the final volume of 5 mL was adjusted by DI water after which the solution was subjected to vigorous shake. Finally, the color of the solution changed from yellowish brown to light yellow. The surface plasmon resonance (SPR) was monitored by UV-Vis spectrophotometer at wavelengths of around 424-433 nm.

3.6 Optimization of experimental conditions for colorimetric detection of Hg(II) (based on smartphone as a colorimetric analyzer) using unmodified silver nanoparticles (AgNPs) as colorimetric probe

3.6.1 Optimization of the volume of AgNPs

Volume optimizing of the AgNPs was firstly performed in the well plate-based system in the presence of Hg(II) at concentrations of 0.10 and 1.0 mg L^{-1}. Based on RGB intensity calculated by ImageJ, performance of the system using the smartphone as an analytical device was compared to that with a scanner. The volume of the AgNP solution was varied from 5.0 to 50 µL. Briefly, the different volume of AgNPs solution was added into a well plate. Then, Hg(II) was added to a solution containing AgNPs to carry out the final concentration of Hg(II) at 0.10 and 1.0 mg L^{-1} in 200 µL of final volume which was adjusted by DI water. The solution was subjected to vigorous shake. Finally, the color of the solution changed from yellowish brown to light yellow. The comparison between smartphone and scanner based colorimetric sensor were performed (Figure 3.3).

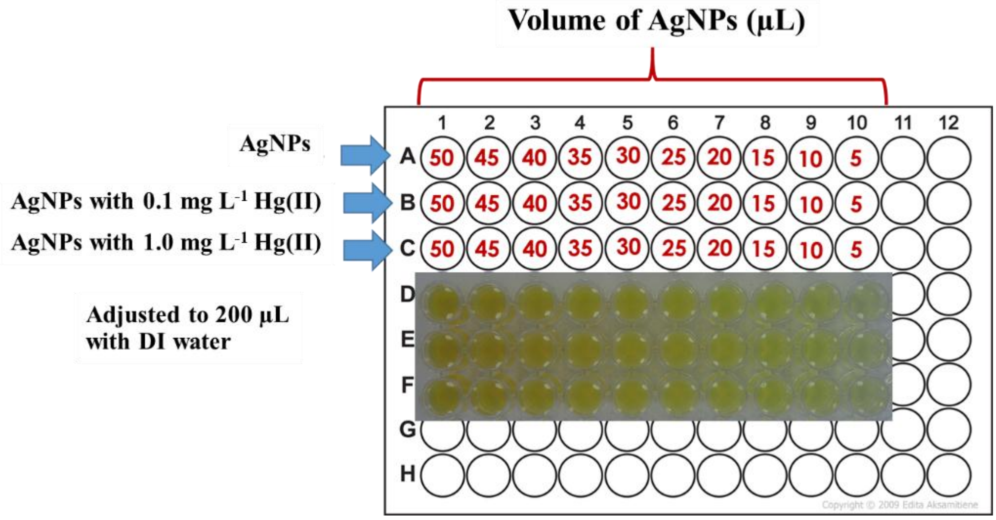

Figure 3.3 The process of the optimization volume of AgNPs solution in the present of Hg(II) concentration at 0.1 and 1.0 mg L^{-1}, respectively.

3.6.2 Optimization of the color intensity in the RGB system

To optimize the color intensity in the RGB system using our developed smartphone-based sensor in the presence of Hg(II). Briefly, 30 µL of the AgNPs was firstly added to a well plate, followed by Hg(II) at different volumes of 50 mg L^{-1} Hg(II) stock, with the final volume in each well of 200 µL achieved by adjustment with DI water. Then, the well plate was covered with black cover before photographing to prevent effect of luminosity from environmental light. The cover of the well plate was modified from a lid that came with the well plate upon purchase. Laser was used to punch holes on the lid in a way that every hole on the lid spatially matched its corresponding hole of the well plate. Then the punctured cover was color-sprayed black to prevent environmental light from disturbing the measurement. The well plate together with its modified lid was placed in a control light box and the smartphone was attached at the lid of the box directly above the well plate as explained in our previous work [37]. The intensity of the color was determined by ImageJ (https:Imagej.net/Downloads) and the calibration curve was plotted in Microsoft Excel; a calibration graph was constructed by measuring the change between the intensity of the color upon the sensor reacting with different concentrations of standard Hg(II) and that of a blank.

3.7 Colorimetric detection of Hg(II) using AgNPs as a probe in the presence of formic acid

3.7.1 UV-Vis spectrophotometry

Colorimetric detection of Hg(II) can be measured using AgNPs as a probe in the presence of 0.5 M formic acid. Firstly, 50 µL of the AgNPs was added into a volumetric flask. Then, Hg(II) at different volumes of 50 mg L^{-1} Hg(II) stock was added to a solution containing AgNPs. In addition, 500 µL of 0.5 M formic acid solution was added and the final volume of 5 mL was adjusted by DI water after which the solution was subjected to vigorous shake. Finally, the color of the solution changed from yellowish brown to light yellow are shown in Figure 3.4a. The surface plasmon resonance (SPR) was monitored by UV-Vis spectrophotometer at wavelengths of around 424-433 nm. The Hg(II) concentration reported in mg L^{-1} unit was determined by establishment of calibration curve (plotted between A_0/A and Hg(II) concentration (mg L^{-1})). The results were compared to those obtained by the condition without formic acid as demonstrated in Figure 3.4b.

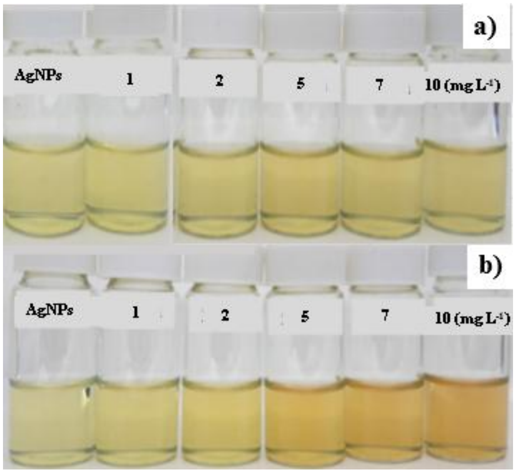

Figure 3.4 The instant change of visible color of unmodified AgNPs in the presence of Hg(II) concentration from 0.005 to 10.0 mg L^{-1}: presence of 0.5 M formic acid a) and absence of 0.5 M formic acid b).

3.7.2 Use of smartphone as a colorimetric analyzer (developed CAnal application) in the absence of formic acid

To measure Hg(II) using our developed smartphone-based sensor, 30 µL of the AgNPs was firstly added to a well plate, followed by Hg(II) at different volumes of 50 mg L^{-1} Hg(II) stock, with the final volume in each well of 200 µL achieved by adjustment with DI water. Then, the well plate was covered with black cover before photographing to prevent effect of luminosity from environmental light. Steps concerning the determination of Hg(II) using a smartphone as a colorimetric analyzer were demonstrated in Figure 3.5. The results were also compared to those obtained by the condition with formic acid.

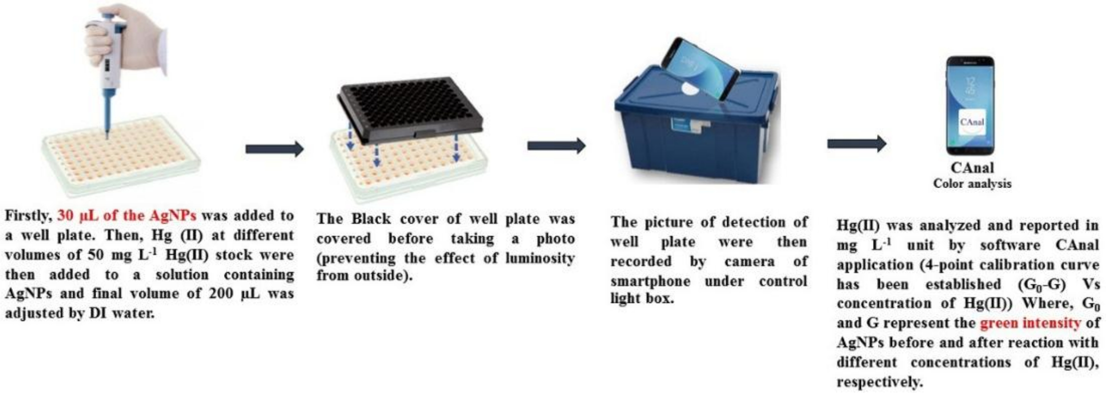

Firstly, 30 µL of the AgNPs was added to a well plate. Then, Hg (II) at different volumes of 50 mg L^{-1} Hg(II) stock were then added to a solution containing AgNPs and final volume of 200 µL was adjusted by DI water.

The Black cover of well plate was covered before taking a photo (preventing the effect of luminosity from outside).

The picture of detection of well plate were then recorded by camera of smartphone under control light box.

Hg(II) was analyzed and reported in mg L^{-1} unit by software CAnal application (4-point calibration curve has been established (G_0-G) Vs concentration of Hg(II)) Where, G_0 and G represent the green intensity of AgNPs before and after reaction with different concentrations of Hg(II), respectively.

Figure 3.5 Determination of Hg(II) using a smartphone equipped with software application CAnal as a colorimetric analyzer on a well plate-based system in the control light box.

The analytical program for Hg(II) analyzer was developed. The application program used for the detection of Hg(II) is called CAnal (version 5.0) developed from [37] which is suitable for solution based analysis. It was developed on an Eclipse code [38] on the Java platform and compiled to run on the Android operating system. To operate the application, a number of steps are followed (Figure 3.6). Prior to each measurement of the samples, a calibration graph was constructed by measuring the change between the intensity of the green color upon the sensor reacting with different concentrations of standard Hg(II) (G) and that of a blank (G_0). The intensity of the color of the reaction was determined by ImageJ (https://Imagej.net/Downloads) and a 4-point calibration curve was plotted in Microsoft Excel; difference in green intensity (G_0-G) was plotted against concentration in mg L^{-1} of Hg(II). After the calibration curve has been established, Hg(II) concentrations can be measured following the steps shown in Figure 3.7. First, open the application, in the setting, choose color “green” and unit “mg L^{-1}”, and then input the calibration curve. After that, import the image of the well plate, or use the application to take an image, then set blank by placing the square pointer at the detection zone of the blank and the program then reads a G_0 value. Finally, move the square pointer to the sample zone and then the value G is given. The difference between the intensity of the green color of the blank and that of the sample is then used to compute the concentration of Hg(II) in the sample, the unit of which is mg L^{-1} as chosen earlier in the setting.

Main display

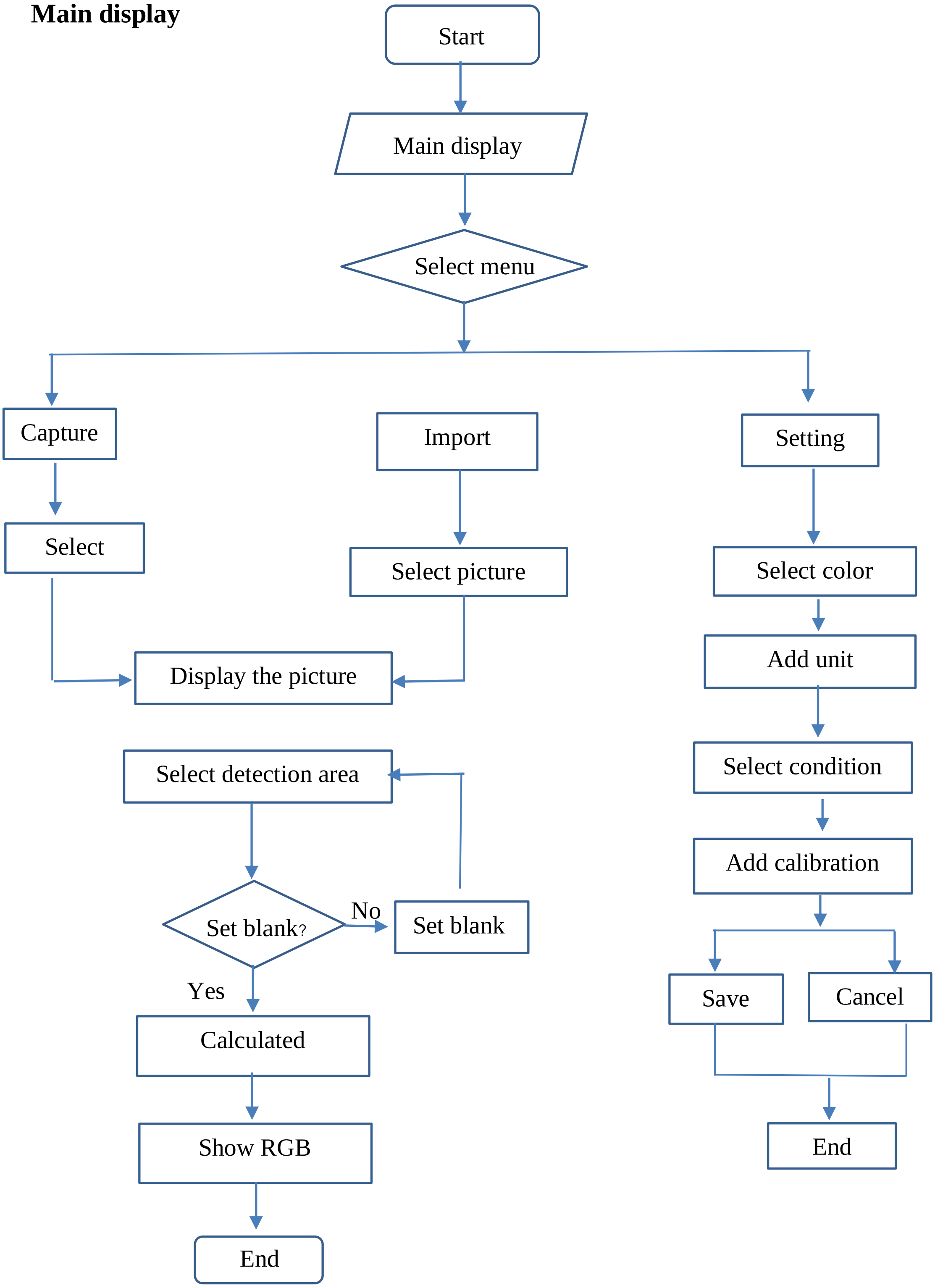

Figure 3.6 Flowchart of CAnal application processing.

Screenshots of smartphone application CAnal detailing the processes of Hg(II) detection

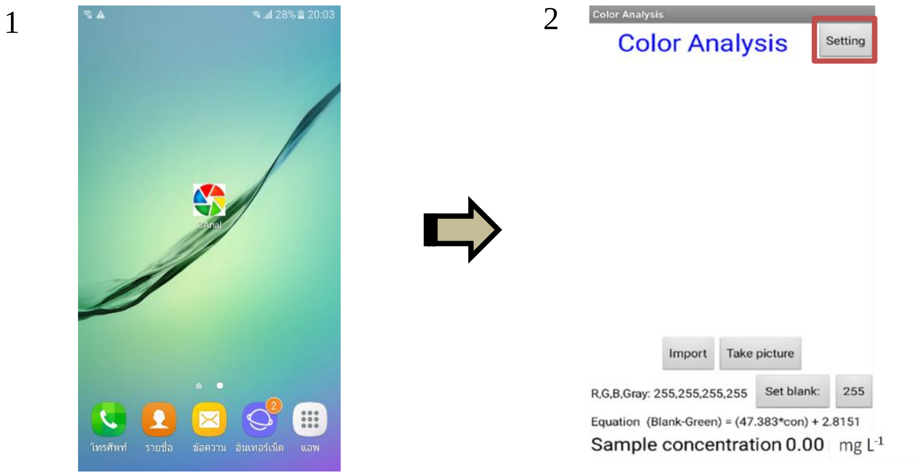

R,G,B,Gray: 255,255,255,255

Set blank: 255

Equation (Blank-Green) = (47.383*con) + 2.8151

Sample concentration 0.00 mg L^{-1}

Icon of CAnal application as appeared on the Android-based smartphone

After starting the application, go to setting

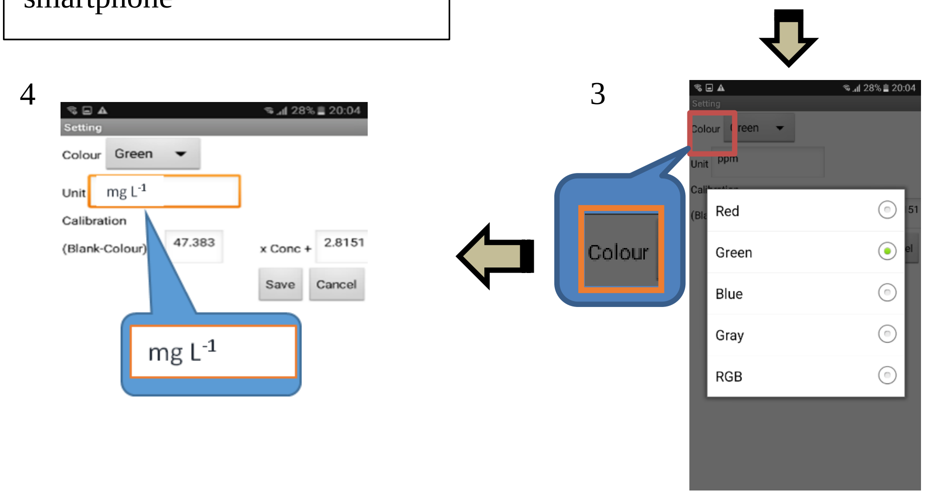

Colour: Green

Unit: mg L^{-1}

Calibration (Blank-Colour) 47.383 x Conc + 2.8151

Choose the unit (for our work mg L^{-1} is chosen)

Choose the color intensity used for the analysis (green)

Figure 3.7 Screenshots of smartphone application CAnal detailing the processes of Hg(II) detection.

Screenshots of smartphone application CAnal detailing the processes of Hg(II) detection (continued)

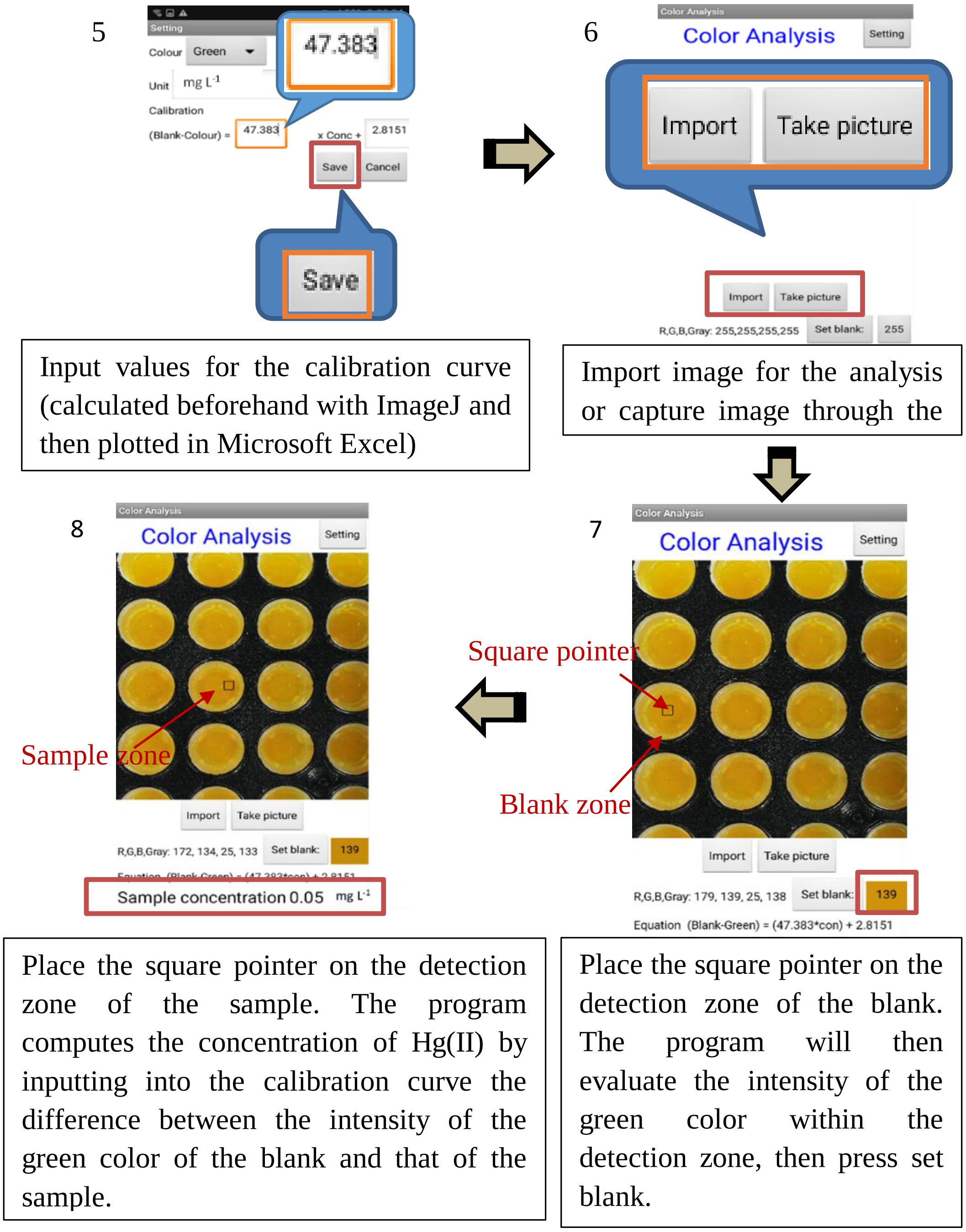

5

Setting

Colour: Green

Unit: mg L^{-1}

Calibration

(Blank-Colour) = 47.383 x Conc + 2.8151

Input values for the calibration curve (calculated beforehand with ImageJ and then plotted in Microsoft Excel)

6

Color Analysis

R,G,B,Gray: 255,255,255,255 Set blank: 255

Import image for the analysis or capture image through the

7

Color Analysis

R,G,B,Gray: 179, 139, 25, 138 Set blank: 139

Equation (Blank-Green) = (47.383*con) + 2.8151

Place the square pointer on the detection zone of the blank. The program will then evaluate the intensity of the green color within the detection zone, then press set blank.

8

Color Analysis

R,G,B,Gray: 172, 134, 25, 133 Set blank: 139

Sample concentration 0.05 mg L^{-1}

Place the square pointer on the detection zone of the sample. The program computes the concentration of Hg(II) by inputting into the calibration curve the difference between the intensity of the green color of the blank and that of the sample.

Figure 3.7 Screenshots of smartphone application CAnal detailing the processes of Hg(II) detection.

3.8 The analytical characteristic of the Hg(II) sensor (based on UV-Vis spectrophotometry and smartphone as a colorimetric analyzer)

The limits of detection (LOD) and quantitation (LOQ) were calculated as $3SD_{blank}$/slope and $10SD_{blank}$/slope, respectively, where SD_{blank} is the standard deviation of the blank signals (n=10) and slope is the slope of calibration curve obtained in each system.

3.9 Study of selectivity of the Hg(II) sensor based on UV-Vis spectrophotometry

To evaluate the selectivity of our developed sensors, Hg(II) ions were determined in the presence of 15 foreign ions, each with a concentration of 10 mg L^{-1}, including 10 cations (Ba(II), Ca(II), Cd(II), Cu(II), Fe(II), Mg(II), Mn(II), Pb(II), Zn(II) and Ni(II)) and 5 anions (chloride, fluoride, nitrate, sulfate and sulfide). Briefly, 50 µL of freshly prepared AgNPs were transferred to a volumetric flask, containing Hg(II) with a fixed final concentration of 0.1 mg L^{-1} in the presence of 0.5 M formic acid. The 15 foreign ions at 10 mg L^{-1} were then added into the volumetric flask and the final volume of 5 mL was adjusted by DI water. Subsequently, the absorption spectra were recorded by UV-Vis spectrophotometer. Moreover, to compare the selectivity of our developed PVP-stabilized AgNP sensor with that of our previous report where the nanoparticles were decorated with citrate molecule [20], the same foreign ions were added into the solution containing the citrate-based AgNPs. Briefly, 1500 µL of freshly prepared AgNPs were transferred to a volumetric flask, containing Hg(II) with a fixed final concentration of 0.1 mg L^{-1}. The 15 foreign ions at 10 mg L^{-1} were then added into the volumetric flask and the final volume of 5 mL was adjusted by DI water. Subsequently, the absorption spectra were recorded by UV-Vis spectrophotometer, respectively.

In waste water, organic dyes constitute a large group of pollutants especially pollutants originated from the textiles industries. Their presence in waste water may interfere with the detection of mercuric ions. The sensitivity of our sensor was therefore evaluated in the presence of these pollutants. Positively charged methylene blue was firstly investigated. The concentration of methylene blue was performed in the range from 1.0 to 6.0 mg L^{-1}. Briefly, 50 µL of freshly prepared AgNPs were transferred to a volumetric flask. After that, the methylene blue solution from

1.0 to 6.0 mg L^{-1}were then added into the volumetric flask and the final volume of 5 mL was adjusted by DI water. Moreover, Methyl orange (MO) and neutral red (NR) are negatively and neutral charged, respectively were also investigated with similar method of MB detection as mentioned above. Subsequently, the absorption spectra were recorded by UV-Vis spectrophotometer.

3.10 Real sample preparation

Drinking and mineral water samples were obtained from a convenience store and a tap water sample was collected from the water supplied to the Faculty of Science, Ubon Ratchathani University. Chlorine in the tap water was removed by letting the water run through the open tap for 30 min at room temperature prior to further procedure. The sample was then heated at 100 °C for 15 min. Pond water samples were obtained from the water supply of Ubon Ratchathani University. The plasma from human blood contained 4% trisodium citrate as anticoagulant was purchased from Sigma-Aldrich, USA. The standard reference material (SRM) 1641d was provided by the National Institute of Standards and Technology. It contained a certified mercury value of 1.56 ± 0.02 mg kg^{-1}. Recovery was determined by spiking aqueous samples with standard Hg(II) at 0.05, 0.10 and 0.25 mg L^{-1}.

3.11 Study of stability of unmodified AgNPs as a probe for the Hg(II) sensor

The stability of unmodified AgNPs is an important parameter for the determination of Hg(II). Briefly, 50 µL of freshly prepared AgNPs were transferred to a volumetric flask and the final volume of 5 mL was adjusted by DI water. Subsequently, the absorption spectra were recorded by UV-Vis spectrophotometer once a week during 3 months by comparison with 4 different batches of unmodified AgNPs.

CHAPTER 4

RESULTS AND DISCUSSION

4.1 Synthesis and their mechanism of PVP-stabilized AgNPs

Silver nanoparticles were synthesized based on a hydrothermal method using polyvinylpyrrolidone (PVP) as a stabilizing and reducing agent. The possible formation of PVP-stabilized AgNPs has been explained in detailed by our collaboration (Muniandy, Sasidharan & Lee, 2019) [36]. PVP is frequently used as a capping agent, which is used as reducing agent for the formation of AgNPs, and also stabilizes the resultant AgNPs via steric repulsion.

According to this thesis, it is suggested that the electron could be strongly partial to the oxygen in the polar carbonyl group (C=O), leaving a negative charge localized at the oxygen atom and a positive charge localized at the nitrogen atom as shown in Figure 4.1a [39]. The interaction between the PVP as the capping agent and the ions (Ag^+) is strong by way of ionic bonds between the Ag ions and the amide group via oxygen in the PVP chain. The PVP stabilized the silver nitrate by means of the amide group steric and electrostatic stabilization [40].

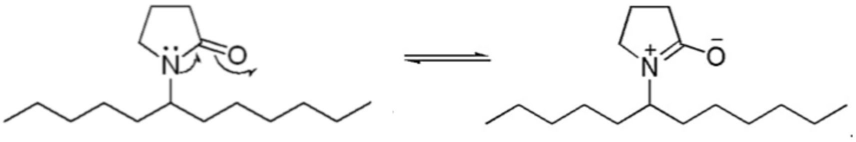

Figure 4.1a Partial electron donation of nitrogen to oxygen [36]**.**

Therefore, the formation of PVP-stabilized AgNPs by chemical reduction may occur between the PVP and metal ions by a process in which metal ions could receive electrons from C=O and form atomic metal as demonstrated in Figure 4.1b. After this reduction occurs, the bonding between the oxygen in the carbonyl group and the silver remained stable. Both factors would provide an ability to generate active reducing and binding sites and the polymer will promote the formation of nanoparticles [40].

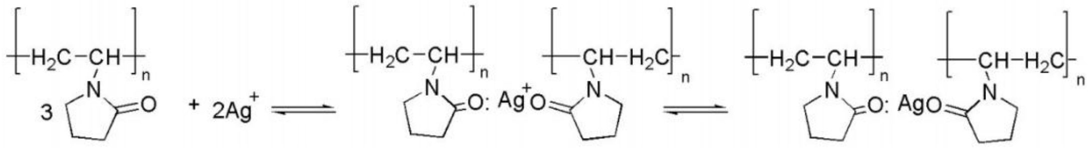

Figure 4.1b Reduction and bond between Ag$^+$ ions and PVP molecules [40].

This could be easily prepared and the resulted sensor was highly stable. Moreover, the mass concentration and number concentration of AgNPs were 3.81 mg mL^{-1} and 1.27×10^{14} NPs mL^{-1}, respectively. The calculation of the number of atoms and number of AgNPs/mL was demonstrated as follows;

Number of atoms

For example, the estimated diameter of a single silver nanoparticle is 21.76 ± 0.22 nm nanoparticle (approximately 22 nm based on our synthesis of the AgNP sensor). Assume that each silver atom occupies the volume of cube with an edge of 0.3 nm (Volume of a sphere = $4/3\pi r^3$).

-Radius of AgNPs = 11 nm

-Diameter of Ag atom = 0.288 nm ≈ 0.3 nm

-Volume of Ag atom = (Diameter of Ag atom)^3 = 0.027 nm^3 ≈ 0.03 nm^3

$$\text{Therefore; Number of atoms} = \frac{\frac{4}{3}\pi r^3 nm^3}{(Volume_{Ag\ atom})nm^3}$$

$$= \frac{\frac{4}{3}\pi(11)^3 nm^3}{0.03\ nm^3} \sim 185{,}843\ atoms$$

- Number of AgNPs/mL

For example, assume that all the silver ions are reduced for the estimation of the number of 22-nm AgNPs produced in this method using fixed mass concentration of Ag (0.0392 M Ag in 90 mL (Ag 3.81 mg mL^{-1}) prepared from 0.6 g $AgNO_3$ in 100 mL

- Number of AgNPs

$$= \frac{Conc.mol\ Ag^+}{1\ L} \times 0.090L \times \frac{6.02\times10^{23}\ Ag^+}{1\ mol\ Ag^+} \times \frac{1\ Ag^0}{1\ Ag^+} \times \frac{1\ AgNP}{No.of\ atom}$$

$$= \frac{0.0392\ Ag^{+}}{1\ L} \times 0.090L\ \times \frac{6.02\times10^{23}\ Ag^{+}}{1\ mol\ Ag^{+}} \times \frac{1\ Ag^{0}}{1\ Ag^{+}} \times \frac{1\ AgNP}{185{,}843\ atom}$$

$$= 1.14 \times 10^{16} NPs/90mL$$

$$= 1.27 \times 10^{14} NPs/mL$$

Note; for the other sizes, calculation of the number of AgNPs/mL can be done in the same manner as the above estimation.

4.2 Characterizations and their mechanism of PVP-stabilized AgNPs as a probe for colorimetric detection of Hg(II) ions

The color of the aqueous solution of the PVP-based nanoparticles was yellowish-brown (insert of Figure 4.2) and also provided a good reproducibility of synthesis. The maximum absorbance of these AgNPs occurred at roughly 424-433 nm (Figure 4.2) due to its surface plasmon resonance (SPR) of AgNPs [12].

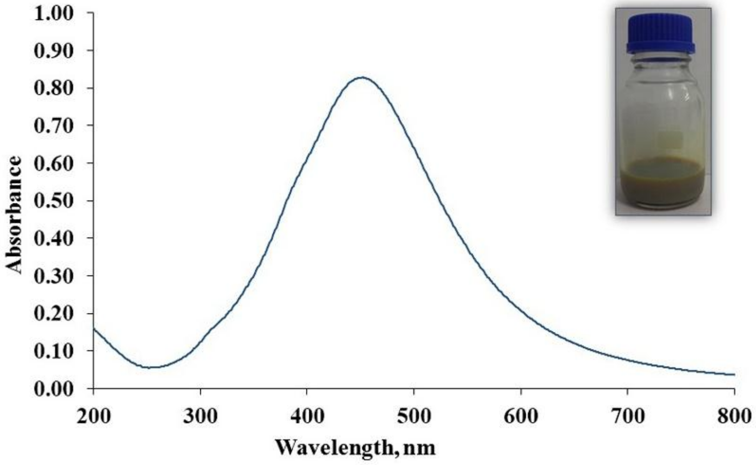

Figure 4.2 UV-Vis absorption spectrum of unmodified AgNPs stabilized with PVP solution was recorded by adding of 50 µL of AgNPs into 5 mL of volumetric flask and final volume was adjusted at 5 mL by DI water. Inset: Photograph of unmodified AgNPs stabilized with PVP solution.

The morphology of PVP-stabilized AgNPs, PVP-stabilized AgNPs after addition of 5 mg L^{-1} Hg(II) and PVP-stabilized AgNPs after addition of 5 mg L^{-1} Hg(II) in the presence of 0.5 M formic acid were studied by recording the TEM coupled EDS. According to TEM study, the average diameter of AgNPs was 21.76 ± 0.22 nm shown in Figure 4.3b. The TEM result was clearly shown that unmodified AgNPs were well dispersed in aqueous solution. Furthermore, the particle sizes after the addition of Hg(II) to an unmodified AgNPs was found to be increased when compared with the TEM image of an original of unmodified AgNPs, resulting that the amalgam particles gradually became larger upon adding Hg(II) (Figure 4.3c). Due to the AgNPs being oxidized by Hg(II), resulting in the disintegration of the AgNPs into smaller particles and Hg(0). Deposition of Hg(0) on the surface of AgNPs also occurred, resulting in amalgam particles of mercury (Hg-Ag) [41]. Strong interaction between the Hg(II) and AgNPs is related to the lower redox potential of Ag(I)/Ag (0.799V) than that of Hg(II)/Hg (0.851V) [42-43]. In addition, the TEM image (Figure 4.3d) also indicated that after adding 0.5 M formic acid, the better amalgamation was observed. These phenomenon could be ascribed that formic acid is small molecules that can be easily adsorbed onto the surface of AgNPs, the acid [44], indicating that increase in the reduction efficiency and fast reduction from Hg(II) to Hg(0), and that molecules of the acid were easily adsorbed onto the surface of AgNPs enabling better reaction between Hg and AgNPs, which resulted in better Hg-Ag amalgamation.

In addition, the EDS spectra of the control stub (substrate) and stub doped with PVP-stabilized AgNPs were shown in Figure 4.3a and b, respectively. The Ag and N elements (%weight) only were observed in the Figure 4.3b when compared to Figure 4.3a due to its composition of PVP-stabilized AgNPs. After that, the solution containing 5.0 mg L^{-1} of Hg(II) solution was doped into the PVP-stabilized AgNPs and PVP-stabilized AgNPs after addition of 5 mg L^{-1} Hg(II) in the presence of 0.5 M formic acid were shown in Figure 4.3c and d, respectively. The results showed that the Ag element (%weight) were decreased whereas the Hg element (%weight) were increased when compared to Figure 4.3b.

In addition, hydrodynamic size and zeta potential of the PVP-stabilized AgNPs, PVP-stabilized AgNPs in the presence of 0.5 mg L^{-1} Hg(II) and PVP-stabilized AgNPs in the presence of 0.5 mg L^{-1} Hg(II) and 0.5 M formic acid were investigated and shown in Table 4.1. The results also confirmed these phenomena, in good agreement in the results obtained from TEM coupled EDS. Moreover, zeta potential of the synthesized AgNPs with various conditions (Table 4.1.) indicates no charge surrounding the AgNPs, suggesting strong stabilization of AgNPs by PVP.

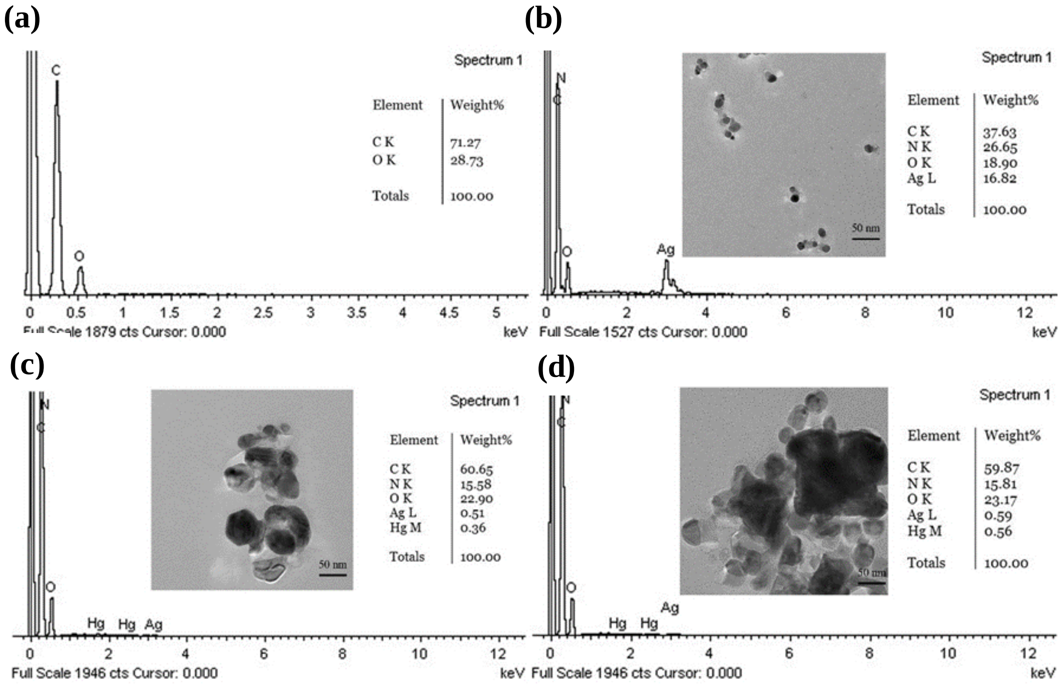

Figure 4.3 EDS spectrum of the sample stub (a), TEM images and EDS spectra of the dispersion of PVP-stabilized AgNPs (b), PVP-stabilized AgNPs after addition of 5 mg L^{-1} Hg(II) (c), and PVP-stabilized AgNPs after addition of 5 mg L^{-1} Hg(II) and 0.5 M formic acid (d).

Table 4.1 Effect of hydrodynamic size and zeta potential of the PVP-stabilized AgNPs, PVP-stabilized AgNPs in the presence of 0.5 mg L^{-1} Hg(II) and PVP-stabilized AgNPs in the presence of 0.5 mg L^{-1} Hg(II) and 0.5 M formic acid

Name	Particles size (nm) ± SD (n=3)	Zeta potential (mV) ± SD (n=3)
AgNPs	188.00 ± 0.42	0.50 ± 23.28
AgNPs+ Hg (II) 0.5 mg L^{-1}	403.20 ± 16.05	-0.20 ± 31.20
AgNPs+ Hg (II) 0.5 mg L^{-1} + 0.5 M formic acid	440.30 ± 81.81	-0.30 ± 27.90

4.3 Optimization of experimental conditions for colorimetric detection of Hg(II) (based on UV-Vis spectrophotometry system)

4.3.1 Optimization of the volume of AgNPs

To investigate the optimized conditions in which AgNPs-based colorimetric sensor can effectively detect Hg(II), it was essential to study the various parameters affecting Hg(II) detection. The volume of AgNPs was firstly optimized without Hg(II) by studying the UV-Vis spectra of AgNPs at volumes of 50, 75 and 100 µL (Figure 4.4a). The optimum condition was achieved with 50 µL of AgNPs, which was the volume to be used for the following experiments. At this volume, the absorbance value of AgNPs was lower than 1.0 following the Beer-Lambert law, whereas volumes of 75 and 100 µL showed the absorbance value of over 1.0, indicating deviation from the Beer-Lambert law. Moreover, we studied the volume of AgNPs in the presence of Hg(II) ions in the linear range of 0.1 to 5.0 mg L^{-1} (Figure 4.4b). The results showed that the AgNPs volume of 50 µL demonstrated a good linear correlation between the different concentrations of Hg(II) and absorbance ratio (A_0/A), where A_0 is the absorbance of bare AgNPs at 424 nm and A is the absorbance of AgNPs at the same wavelength after reaction with Hg(II). The volume used in this work was a fraction that needed for the sensor of our previous work [20]. For detailed comparison between the PVP-based AgNPs developed in this work and the citrate-based AgNPs in the previous work [20] see also in Table 4.2.

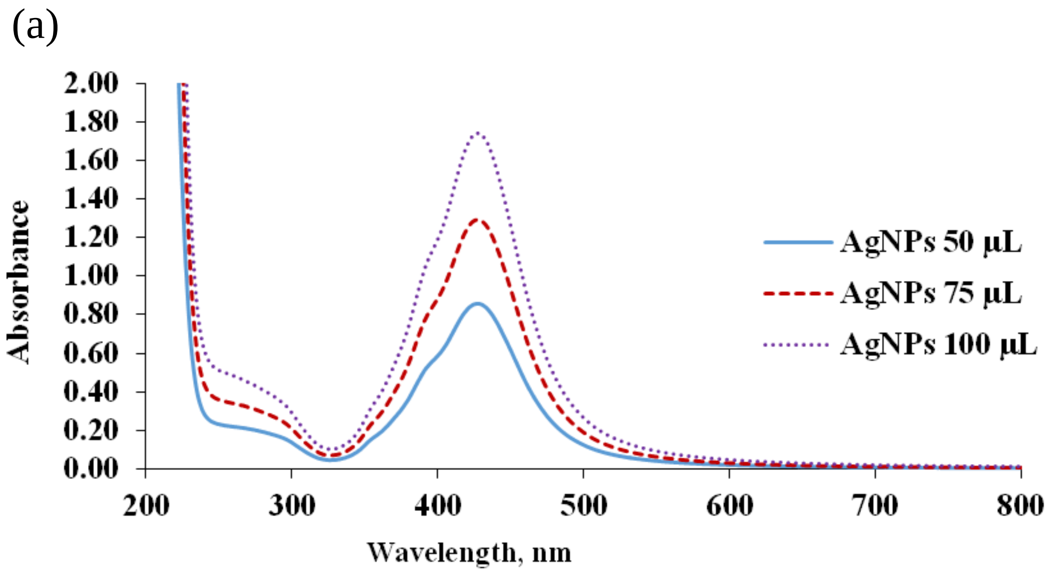

Figure 4.4 Optimization of the volume of AgNPs (50, 75 and 100 µL) using UV-Vis spectrophotometer: (a) spectra of AgNPs at different volumes.

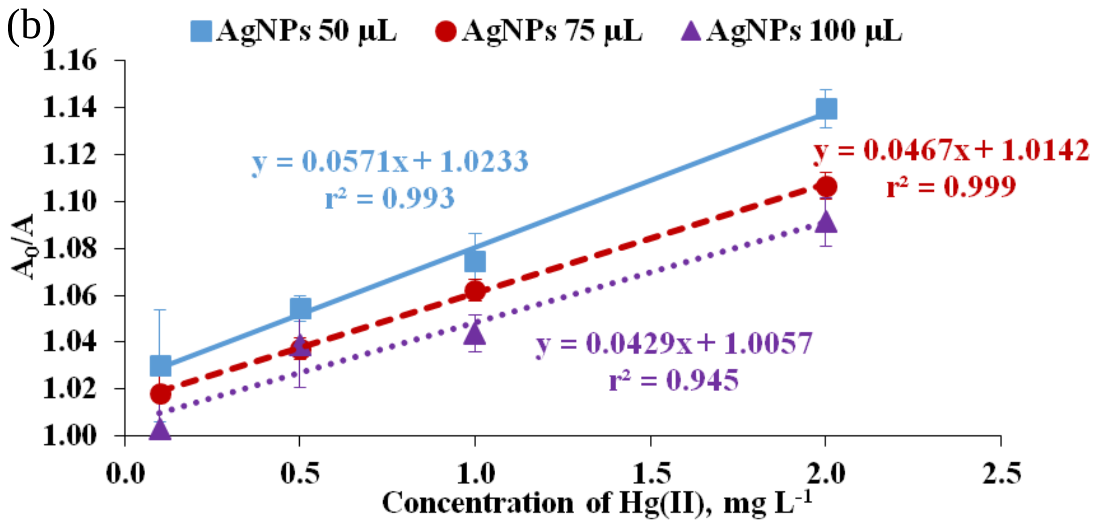

Figure 4.4 Optimization of the volume of AgNPs (50, 75 and 100 µL) using UV-Vis spectrophotometer: (b) comparison of the calibration curves comparing different volumes of AgNPs (50, 75 and 100 µL) with A_0/A plotted against the different concentrations of Hg(II) ions.

Table 4.2 Comparison between the performance of the current sensor for Hg(II) detection and that of our previous work

No	Parameters	Our previous work	Present study	
			UV-Vis spectrophotometer	Portable colorimetry by smartphone detection
1	The volume of AgNPs (µL) in total volume of 5 mL	1500	50	30 (total volume of 200 µL)
2	Enhancer	Cu(II)	Formic acid	No
3	Reducing agent /Stabilizing agent	Using strong $NaBH_4$ as reducing agent and citrate as stabilizing agent	PVP (reducing and stabilizing agent)	
4	Sample matrix	Tolerance of Hg(II) to 7 cation species	Tolerance of Hg(II) to 10 cations and 5 anions (100 fold by fixing Hg(II) concentration at 0.1 mg L^{-1})	
5	Working pH	>4	>1	>1
6	Linearity range/LOD (mg L^{-1})	0.5-2.5/0.008	0.01-10/0.007	0.05-0.5/0.011
7	Detection system	UV-Vis spectrophotometer	UV-Vis spectrophotometer	Portable colorimetry by smartphone detection/green synthesis
8	Application	Tap and drinking water	Water, blood and dye organic samples	
9	Sample throughput	No report	No report	128 sample h^{-1}, ~15 min for eight samples analysis (n=4)

4.3.2 Study the effect of enhancer on the reduction of mercury

To study the effect of enhancer on the reduction of mercury, organic formic acid was dropped into the AgNP solution. Having small molecules that can be easily adsorbed onto the surface of AgNPs, the acid has been shown to significantly enhance Hg(II) analytical sensitivity [44]. The efficiency for the reduction of Hg(II) however depended on its concentration. Hence, different concentrations of formic acid and pH values were investigated in this study. The concentration range of 0.0 to 2.0 M and pH range of 1.0 to 6.0 were optimized. The results presented in Figure 4.5 and Table 4.3 showed that Hg(II) analytical sensitivity progressively increased with increasing concentration of formic acid in the Hg(II) concentration range of 0.01 to 2.0 mg L^{-1}. The optimal value for the concentration of formic acid was 0.5 M (with wide working pH range of >1 Table 4.2), indicating an increase in reduction efficiency and fast reduction from Hg(II) to Hg(0), and that molecules of the acid were easily adsorbed onto the surface of AgNPs enabling better reaction between Hg and AgNPs, which resulted in better amalgamation (Figure 4.3d and Table 4.1). However, higher concentrations of the acid (pH 1; at concentrations of 1.0-2.0 M) led to a decrease in Hg(II) analytical sensitivity.

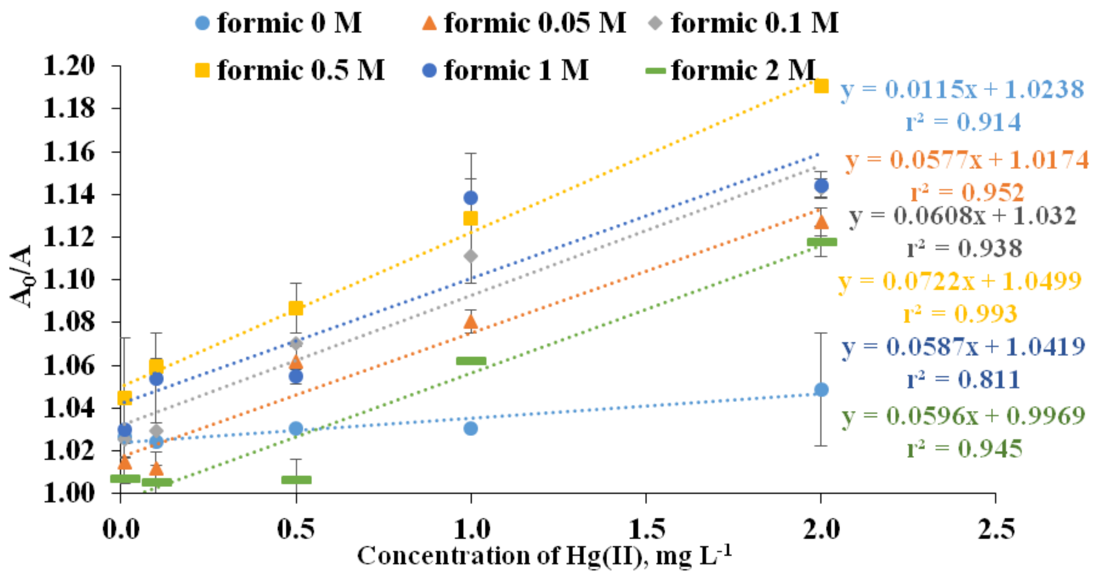

Figure 4.5 Calibration curves showing the effect of different concentrations (0-2.0 M) of formic acid used as a enhancer reagent for reduction of mercury. Absorbance ratios are plotted against various concentrations of Hg(II) (0.01-2.0 mg L^{-1}).

Table 4.3 pH values of the solution containing various concentrations of formic acid and their corresponding maximum wavelength values of in the presence of Hg(II) in the range 0.05 to 2.0 mg L^{-1}

Concentration of Hg (II) mg L^{-1}	λ_{max} (nm); pH											
	Formic acid 0 M		Formic acid 0.05 M		Formic acid 0.1 M		Formic acid 0.5 M		Formic acid 1 M		Formic acid 2 M	
0.0	426.0	6	423.8	3	423.5	2	424.0	2	425.3	1	428.8	1
0.0	425.0	6	423.5	3	423.5	2	424.3	2	426.3	1	429.3	1
0.1	425.0	6	424.0	3	423.5	2	422.8	2	425.0	1	429.0	1
0.5	424.5	6	422.5	3	421.8	2	422.8	2	422.8	1	427.8	1
1.0	424.5	6	422.3	3	421.8	2	422.0	2	422.5	1	425.3	1
2.0	425.8	6	422.5	3	422.5	2	420.8	2	424.3	1	428.3	1

4.4 Optimization of experimental conditions for colorimetric detection of Hg(II) (based on smartphone as a colorimetric analyzer)

4.4.1 Optimization of the volume of AgNPs

Volume optimizing of the AgNPs was firstly performed in the well plate-based system in the presence of Hg(II) at concentrations of 0.10 and 1.0 mg L^{-1}. Based on RGB intensity calculated by ImageJ, performance of the system using the smartphone as an analytical device was compared to that with a scanner. The volume of the AgNP solution was varied from 5.0 to 50 µL and the optimal volume of AgNPs was found to be 30 µL (Figure 4.6), an excellent 50-fold reduction in volume of the sensor compared to the previous work [20] and a significant reduction in comparison to the UV-Vis spectrophotometric system based on the same PVP-stabilized AgNP sensor (Table 4.2). We found that the smartphone was more sensitive to color change, sensing better gray intensity, than the scanner, which perceived the detected solution as being too white than it actually was. Prior to this experiment, the effect of formic acid on the sensitivity of our colorimetric detection of Hg(II) was evaluated.

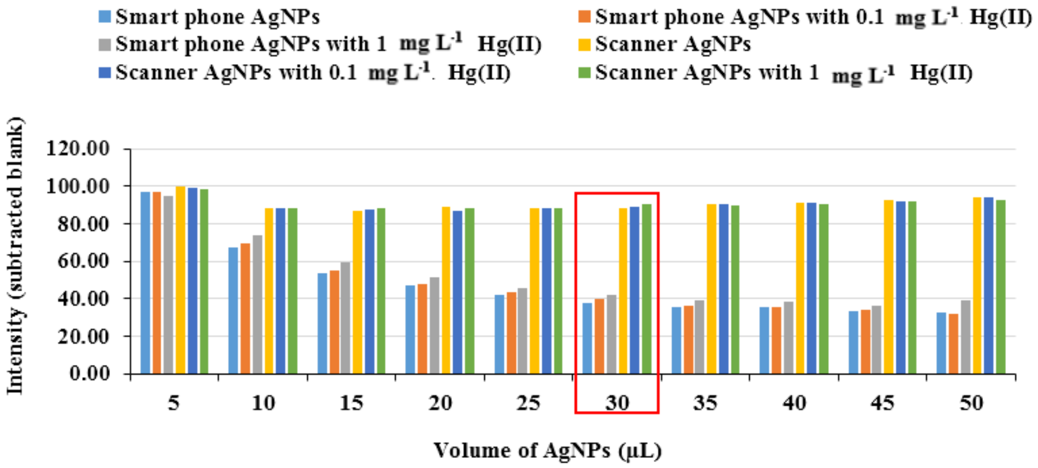

Figure 4.6 Optimal volume of AgNPs studied in the range of 5-50 µL for detecting Hg(II) under different devices (smart phone and scanner) in the presence of Hg(II) in the range of 0.10 to 1.0 mg L^{-1}.

4.4.2 Optimization of the color intensity in the RGB system

To measure the concentration of Hg(II) ions, we first had to determine which color intensity in the RGB system was the most sensitive to change occurring upon interaction of the PVP-stabilized AgNPs with Hg(II). Among the five components in the RGB system (R (red), G (green), B (blue), average gray calculated from (R + G + B)/3, and gray with a luminosity which is equal to 0.299R + 0.587G + 0.114B), it was found that green was the most sensitive to the color change from yellowish-brown in samples without Hg(II) to progressively paler yellow with a tint of orange with increasing concentrations of Hg (II) (Figure 4.7) [37]; hence, intensity of the green color is used in the determination of Hg(II). Prior to each measurement of the samples, a calibration graph was constructed by measuring the change between the intensity of the green color upon the sensor reacting with different concentrations of standard Hg(II) (G) and that of a blank (G_0). The intensity of the color of the reaction was determined by ImageJ (https://Imagej.net/Downloads) and a 4-point calibration curve was plotted in Microsoft Excel; difference in green intensity (G_0-G) was plotted against concentration in mg L^{-1} of Hg(II). After the calibration curve has been established, Hg(II) concentrations can be measured following the steps shown in Figure 3.7.

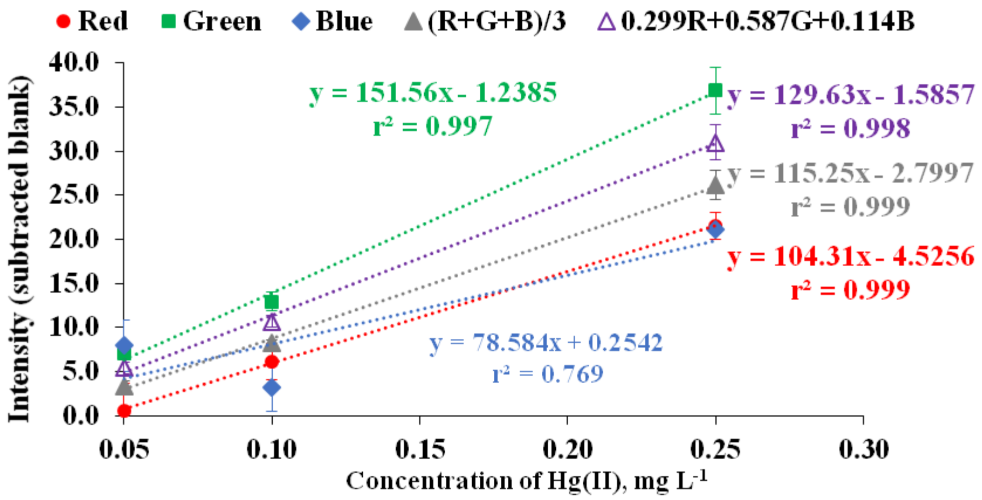

Figure 4.7 Calibration curve showing optimization of different colors based on the RGB system, ●R (red), ■G (green), ◆B (blue), ▲(R + G + B)/3 for average gray and △(0.299R + 0.587G + 0.114B) for gray with luminosity.

4.5 Using optimized condition for colorimetric detection of Hg(II) using AgNPs as a probe

4.5.1 UV-Vis spectrophotometry (in the presence of formic acid)

The colorimetric sensing for Hg(II) was performed. After addition of Hg(II) solution to freshly prepared AgNPs, instant color change from brownish yellow to orange was observed and it changed gradually with increasing concentration of Hg(II) ions, corresponding to the absorption spectra in Figure 4.8a which show a slight blue shift of the maximum absorption wavelength. The absorption intensity of the UV-Vis spectra progressively decreased with increasing concentrations of Hg(II). Such phenomena were also described previously [45-46]. The decrease in the absorption intensity of the SPR band with a blue shift could be due to the AgNPs being oxidized by Hg(II), resulting in the disintegration of the AgNPs into smaller particles and Hg(0). Deposition of Hg(0) on the surface of AgNPs also occurred, resulting in amalgam particles of mercury (Hg-Ag) [41]. Strong interaction between the Hg(II) and AgNPs is related to the lower redox potential of Ag(I)/Ag (0.799V) than that of Hg(II)/Hg (0.851V) [42-43]. Our result indicated that the PVP-stabilized AgNPs can be used as a promising colorimetric sensor for the detection of Hg(II).

Sensitivity of the sensor to detect Hg(II) was also investigated. Figure 4.8a shows the UV-Vis spectra upon adding various concentrations of Hg(II). When the concentration of Hg(II) was increased from 0.005 to 10 mg L^{-1}, the absorption intensity progressively decreased correlating well with the observed color change**,** which indicated gradually increasing aggregation of AgNPs **(**Figure 4.8a, inset). The result showed a linear correlation (r^2 = 0.988) was observed between the different concentrations of Hg(II) and absorbance ratio (A_0/A), where A_0 is the absorbance of AgNPs at 424 nm for control and A is the absorbance of AgNPs at 424 nm after reaction with Hg(II). It was found that the calibration curve, with the measurements carried out in triplicates, was in the range of 1.0 to 10.0 mg L^{-1} (r^2 = 0.988) with the limit of detection (LOD) of 0.03 mg L^{-1}. Generally, when the concentration of Hg(II) is increased to higher than 2.0 mg L^{-1}, it is expected that the characteristic peak will red shift and broaden. However, blue shift in the absorption wavelength was observed in this experiment due to the use of 0.5 M formic acid as a catalytic organic compound.

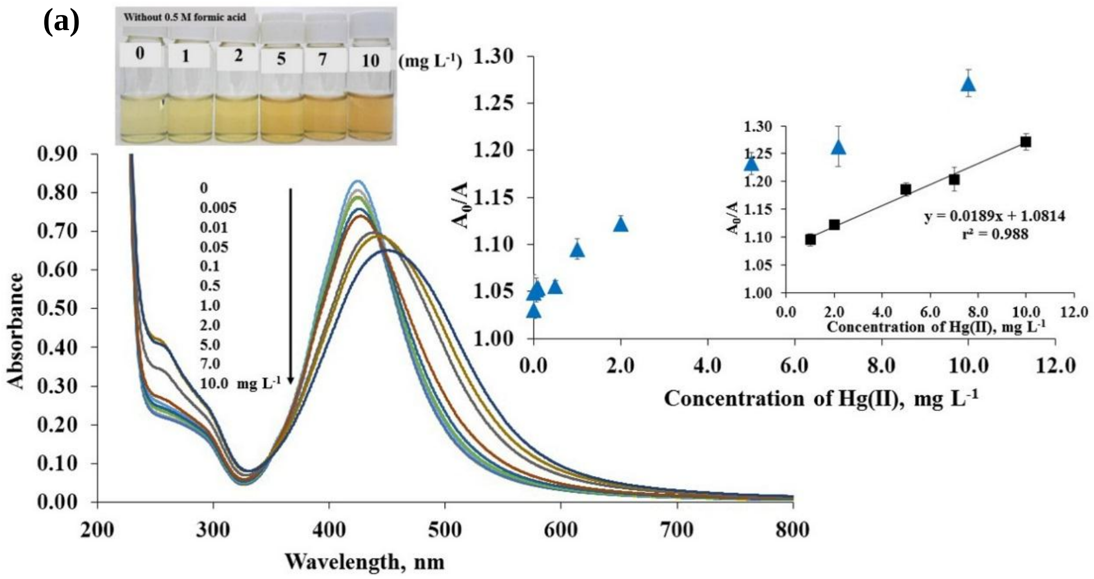

Figure 4.8a UV-Vis absorption spectra of the unmodified AgNPs solution upon addition of different concentrations of Hg(II) in the absence of 0.5 M formic acid, inset: the calibration curve of the A_0/A versus the concentration of Hg(II). Where, A_0 and A represent the absorption intensity of AgNPs roughly occurred at 424-433 nm before and after reaction with different concentrations of Hg(II), respectively.

Interestingly, addition of 0.5 M formic acid is necessary to enhance the reduction efficiency of mercury, indicating that the re-oxidation of Hg(II) to Hg(0) occurs easily under strong acidic conditions. Under optimized detection conditions, 500 µL (0.5 M) of formic acid was added to a mixture of AgNPs (50 µL) and Hg(II) at different concentrations before final adjustment to a volume of 5 mL was achieved using DI water. When the concentration of Hg(II) was increased from 0.005 to 10 mg L^{-1}, the absorbance value at 424 nm progressively decreased, correlating well with the observed color change of the solution (brownish yellow becoming paler, Figure 4.8b), and the absorption spectra exhibited a blue shift with decreasing absorbance indicating gradually increasing amalgamation of the AgNPs (Figure 4.8b) [12,20,41-43,45-46]. The absorbance of the AgNPs progressively decreased and slightly shifted to the blue wavelength with increasing concentrations of Hg(II) ions (in the range 0.01-10 mg L^{-1}). The absorption peak of the detection in the presence of 0.5 M formic acid occurred at a different wavelength when the enhancer was absent. In addition, the analytical sensitivity of the method was improved in the presence of 0.5 M formic acid (Figure 4.8b, inset). Significant sensitivity enhancement was observed with an addition of the enhancer compared to without formic acid. The calibration curve obtained from the presence of 0.5 M formic acid shows two linearity ranges: a low linearity range between 0.01 and 1.0 mg L^{-1}, and a high linearity range between 1.0 and 10 mg L^{-1}. The calibration curve of A_0/A value versus the concentration of Hg(II) shows significant enhancement in the Hg(II) analytical sensitivity upon addition of 0.5 M formic acid onto the AgNPs, leading to improvement of quantitative detection limit (Figure 4.8c).

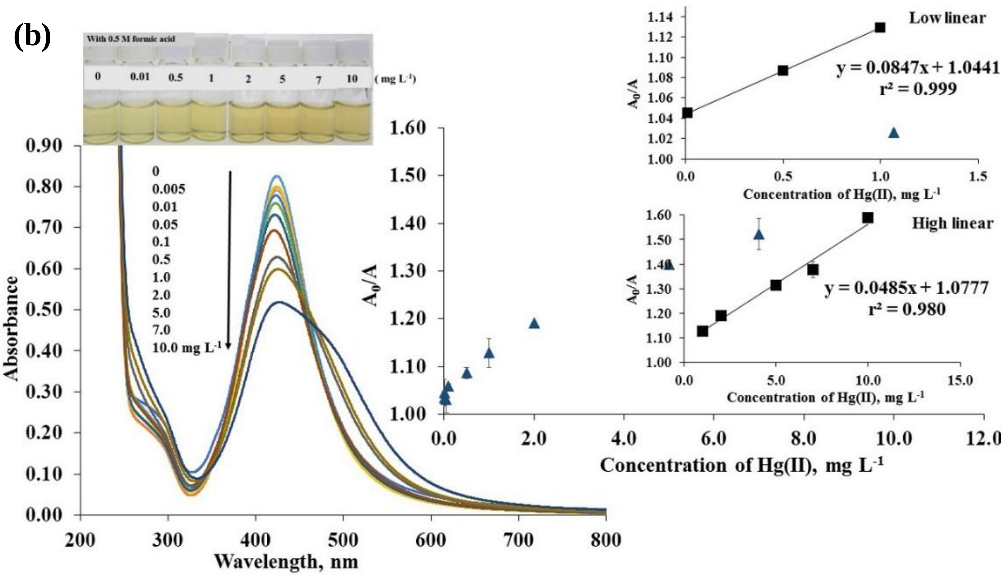

Figure 4.8b UV-Vis absorption spectra of the unmodified AgNPs solution upon addition of different concentrations of Hg(II) in the presence of 0.5 M formic acid, inset: the two calibration curves of the A_0/A versus the concentration of Hg(II) (high and low linearity) (b).

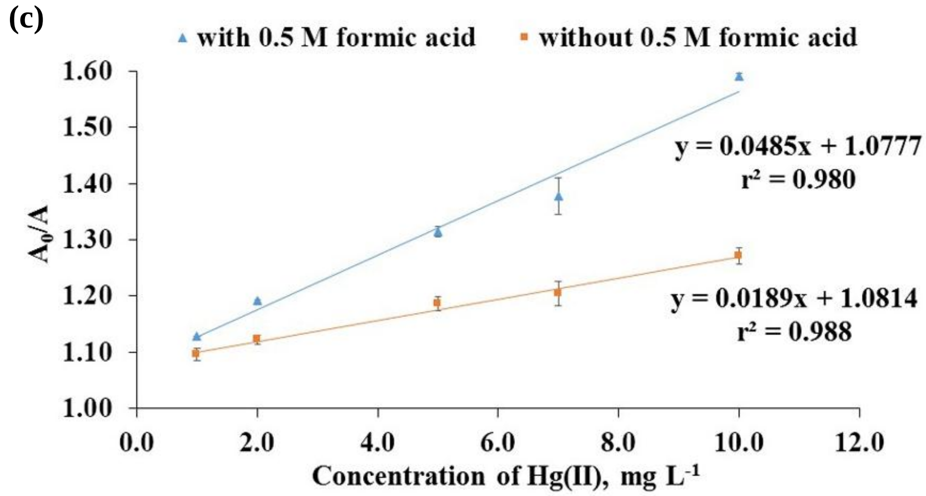

Figure 4.8c UV-Vis absorption spectra of the unmodified AgNPs solution upon addition of different concentrations of Hg(II), and the calibration curve of A_0/A value versus the concentration of Hg(II) before and after the addition 0.5 M formic acid (c) Where, A_0 and A represent the absorption intensity of AgNPs roughly occurred at 424-433 nm before and after reaction with different concentrations of Hg(II), respectively.

The limit of detection (LOD) of the sensor in the presence of 0.5 M formic acid was reduced to 0.007 mg L^{-1} with a good precision (%RSD is less than 4.83) of the calibration curve observed in three different synthesis batches of AgNPs at various concentration of Hg(II) (1.0, 5.0 and 7.0 mg L^{-1}) (Table 4.4).

Table 4.4 Precision (%RSD) of the calibration curve of the developed AgNPs observed in three different synthesis batches of AgNPs at various concentration of Hg(II)

Three different synthesis batches of AgNPs	**Absorption A_0/A value of an unmodified AgNPs at various concentration of Hg(II) ions**		
	Concentration of Hg(II), mg L^{-1} ± SD (n=3)		
	1.0	**5.0**	**7.0**
1	1.11 ± 0.01	1.34 ± 0.01	1.43 ± 0.00
2	1.10 ± 0.00	1.23 ± 0.01	1.30 ± 0.01
3	1.13 ± 0.00	1.31 ± 0.01	1.38 ± 0.03
Average	1.11	1.29	1.37
SD	0.01	0.06	0.07
% RSD	1.12	4.50	4.83

4.5.2 Use of smartphone as a colorimetric analyzer established CAnal application (in the absence of formic acid)

Under the optimum conditions as mentioned above, use of smartphone as a colorimetric analyzer established CAnal application for Hg(II) was evaluated the effect of formic acid on the sensitivity. The results demonstrated that the addition of the formic acid was unnecessary, considering the slope of calibration as shown in Figure 4.9 and comparison of the results as demonstrated in Table 4.5, respectively. Moreover, the addition of 0.5 M formic acid is complicated and time-consuming processes of Hg(II) detection.

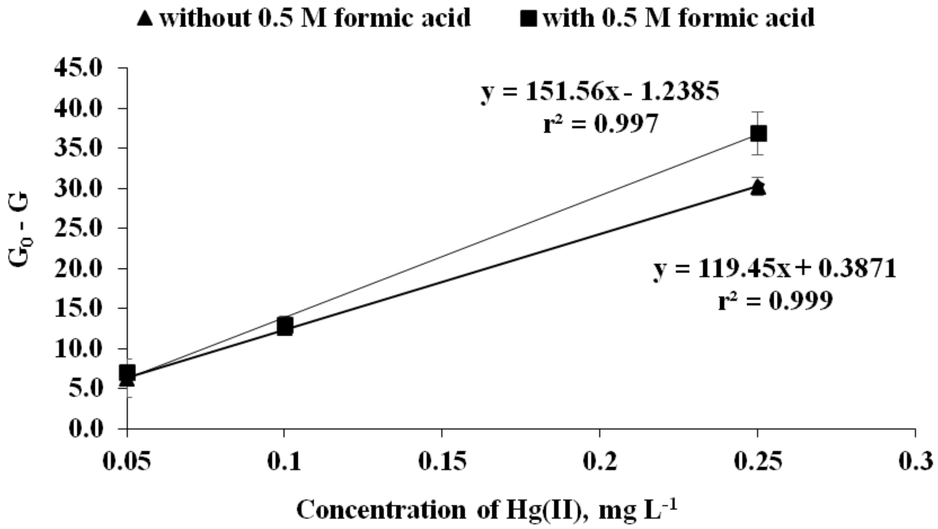

Figure 4.9 Calibration curve of AgNPs-based colorimetric sensor for Hg(II) detection by using green intensity (Image processing, ImageJ) at different conditions (▲ with formic acid and ■without formic acid).

Table 4.5 Comparison of the results of AgNPs-based colorimetric sensor for Hg(II) detection by using green intensity (Image processing, ImageJ) at different conditions (with formic acid and without formic acid)

Concentration of Hg (II) mg L^{-1}	Without 0.5 M formic acid			With 0.5 M formic acid		
	G_0	G_0-G	Found (mg L^{-1}) ± SD (n=3)	G_0	G_0-G	Found (mg L^{-1})± SD (n=3)
0.05	161.14	6.24	0.05 ± 0.02	167.93	7.07	0.05 ± 0.00
0.1	154.89	12.49	0.10 ± 0.00	162.06	12.94	0.09 ± 0.01
0.25	137.17	30.21	0.25 ± 0.01	138.11	36.90	0.25 ± 0.02

Note: Where, G_0 and G represent the green intensity of AgNPs before and after reaction with different concentrations of Hg(II), respectively.

Analytical characteristics of the smartphone-based colorimetric analyzer for Hg(II) was examined. Under the optimized detection condition, the sensor sensitivity was investigated. In three replicates, a series of standard Hg(II) (0.05-0.5 mg L^{-1}) was measured and the calibration curve shows a good linear correlation (r^2 = 0.993) with the linear range from 0.05 to 0.5 mg L^{-1} (4-point calibration curve) existing between the intensity differences (G_0-G) and the concentrations of Hg(II), where G_0 and G represent the green intensity of AgNPs before and after reaction with different concentrations of Hg(II), respectively (Figure 4.10). The calibration equation obtained was retained by the developed program (slope = 47.38, r^2 = 0.993) with a detection limit of 0.011 mg L^{-1}, indicating that the colorimetric sensor holds a promising potential for quantitative determination of Hg(II) ions in real sample application. High sample throughput for the analysis could be achieved through our developed method; approximately eight samples (n=4, totaling 32 wells) could be measured in 15 min corresponding to about 32 samples (128 wells) per hour.

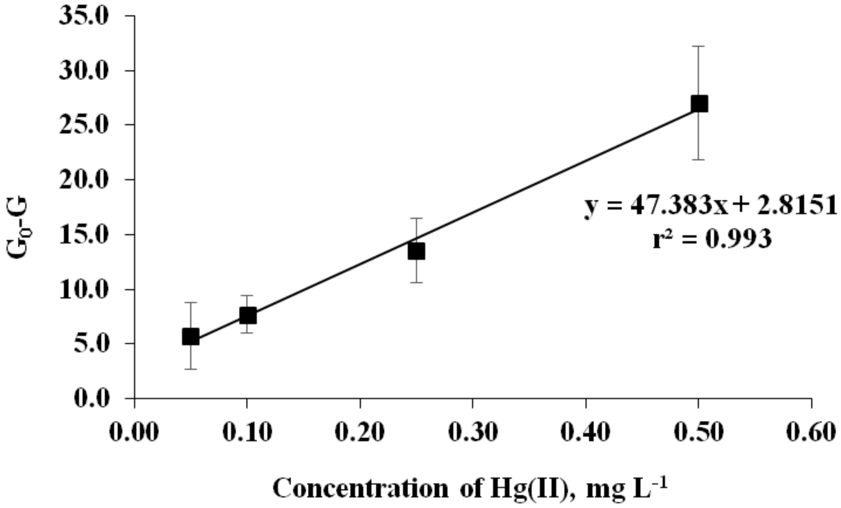

Figure 4.10 Calibration curve of the smartphone-based colorimetric analyzer where differences in the green color intensity (G_0-G) are plotted against difference concentrations of Hg(II) (0.05-0.5 mg L^{-1}).

4.6 Study of selectivity of the Hg(II) sensor based on UV-Vis spectrophotometry

In order to evaluate the selectivity of the colorimetric sensor over commonly known interference species in aqueous samples, Hg(II) ions were examined in the presence of ten cations and five anions, each with a concentration of 10.0 mg L^{-1}. As has already been established, upon adding Hg(II) ions at 0.1 mg L^{-1}, 1.0 mg L^{-1} and 10.0 mg L^{-1} into the unmodified AgNPs solution in the presence of 0.5 M formic acid (without the presence of any foreign ions), the color solution visibly changed from brownish yellow to pale yellow, and the absorption intensity of the unmodified AgNPs roughly occurred at 424 nm. When the foreign ions were present in the solution containing 0.1 mg L^{-1} of Hg(II) in the presence of 0.5 M formic acid, it did not significantly alter the absorbance with less than ±5% change in the absorbance values (Figure 4.11a). To compare the selectivity of our developed PVP-stabilized AgNP sensor with that of our previous one where the nanoparticles were decorated with citrate, the same foreign ions were added into the solution containing the citrate-based AgNPs. It was found that the newly developed sensor fared much better in terms of selectivity compared to the citrate-based AgNPs (Figure 4.11b and Table 4.2), likely a result of better stabilization (by PVP) of the AgNPs.

(a)

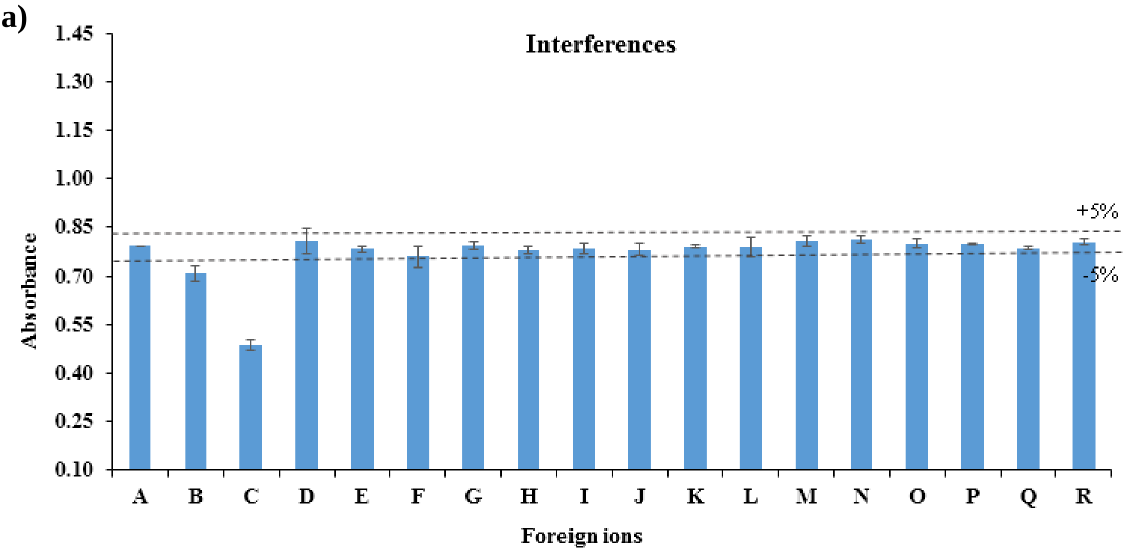

Figure 4.11 Comparison between the selectivity of the newly developed sensor (PVP-stabilized AgNPs) (a) and that of our previous work (citrate-based AgNPs) (b); AgNPs + 0.1 mg L^{-1} Hg(II) (A), AgNPs + 1 mg L^{-1} Hg(II) (B), AgNPs + 10 mg L^{-1} Hg(II) (C), AgNPs + 0.1 mg L^{-1} Hg(II) + 10 mg L^{-1} anions (D-H; chloride, fluoride, nitrate, sulfate, sulfide, respectively) and cations (I-R; Ba(II), Ca(II), Cd(II), Cu(II), Fe(II), Mg(II), Mn(II), Pb(II), Zn(II), Ni(II), respectively).

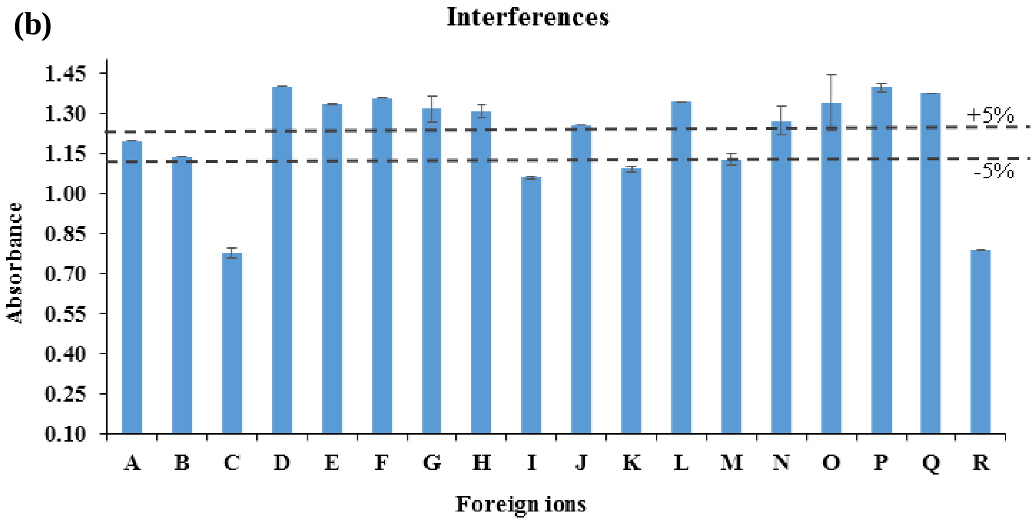

Figure 4.11 Comparison between the selectivity of the newly developed sensor (PVP-stabilized AgNPs) (a) and that of our previous work (citrate-based AgNPs) (b); AgNPs + 0.1 mg L^{-1} Hg(II) (A), AgNPs + 1 mg L^{-1} Hg(II) (B), AgNPs + 10 mg L^{-1} Hg(II) (C), AgNPs + 0.1 mg L^{-1} Hg(II) + 10 mg L^{-1} anions (D-H; chloride, fluoride, nitrate, sulfate, sulfide, respectively) and cations (I-R; Ba(II), Ca(II), Cd(II), Cu(II), Fe(II), Mg(II), Mn(II), Pb(II), Zn(II), Ni(II), respectively).

In waste water, organic dyes constitute a large group of pollutants especially pollutants originated from the textiles industries. Their presence in waste water may interfere with the detection of mercuric ions. The selectivity of our sensor was therefore evaluated in the presence of these pollutants. Positively charged methylene blue was firstly investigated. Figure 4.12a and b showed the evolution of UV-Vis spectra after adding different concentrations of methylene blue (MB). When the concentration of methylene blue was increased from 1.0 to 6.0 mg L^{-1}, the visible wavelength of the maximum absorption of the AgNPs and methylene blue roughly occurred at 424 nm and 665 nm, respectively. The absorbance value of methylene blue at 665 nm increased with increasing concentrations of methylene blue associated with color change of the AgNPs solution from yellowish-brown to blue with constant 424 nm of AgNPs. The result shows that the developed approach provides high selectivity of Hg(II) detection even when there is a presence of methylene blue

(Table 4.6). In addition, the studies with presence of neutral red and methyl orange as neutral and anionic dyes, respectively were also evaluated. The experimental data shown in Figure 4.13a and b indicate that the visible wavelength of the maximum absorption of neutral red and methyl orange occurred where AgNPs absorption took place. As such, their presence show interference occurred with the detection of Hg(II) using our current developed method. The obtained results will serve as good information for our future work.

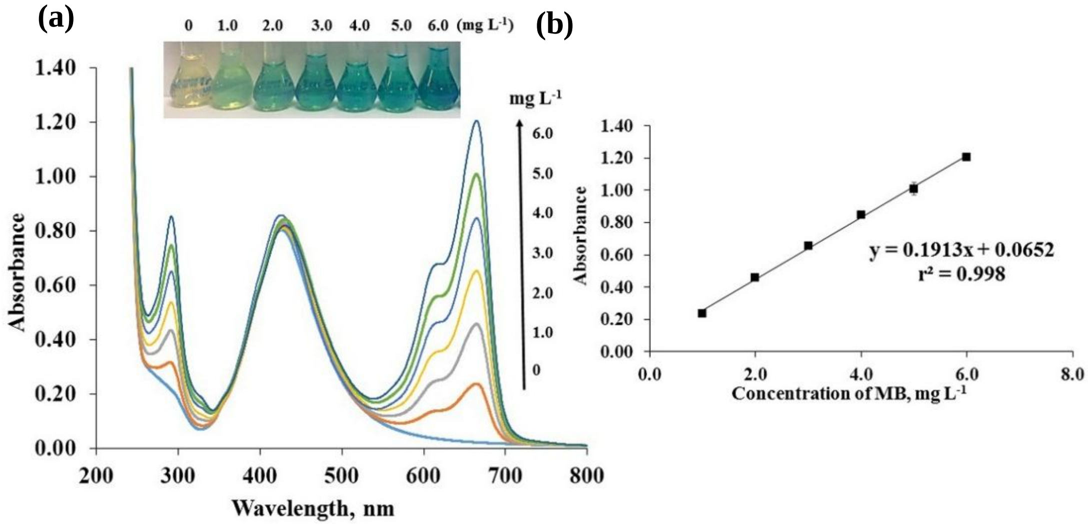

Figure 4.12 UV-Vis absorption spectra (a) showing the effect of organic dye (methylene blue) on the maximum absorption wavelength of AgNPs, the absorbance versus the concentration of MB (mg L^{-1}) (b).

Table 4.6 Percentages of recovery for Hg(II) determination in the presence of methylene blue

Name	Wavelength (nm)	Absorbance	% recovery
AgNPs +Hg(II) 0.1 mg L^{-1}	425.5	0.79876	
AgNPs +Hg(II) 0.1 mg L^{-1} + with MB 6 mg L^{-1}	427.8	0.83624	104.7
AgNPs +Hg(II) 1 mg L^{-1}	423.8	0.72879	
AgNPs +Hg(II) 1 mg L^{-1} + with MB 6 mg L^{-1}	423.5	0.70093	96.2
AgNPs +Hg(II) 2 mg L^{-1}	422.5	0.70203	
AgNPs +Hg(II) 2 mg L^{-1} + with MB 6 mg L^{-1}	423.8	0.69475	99.0

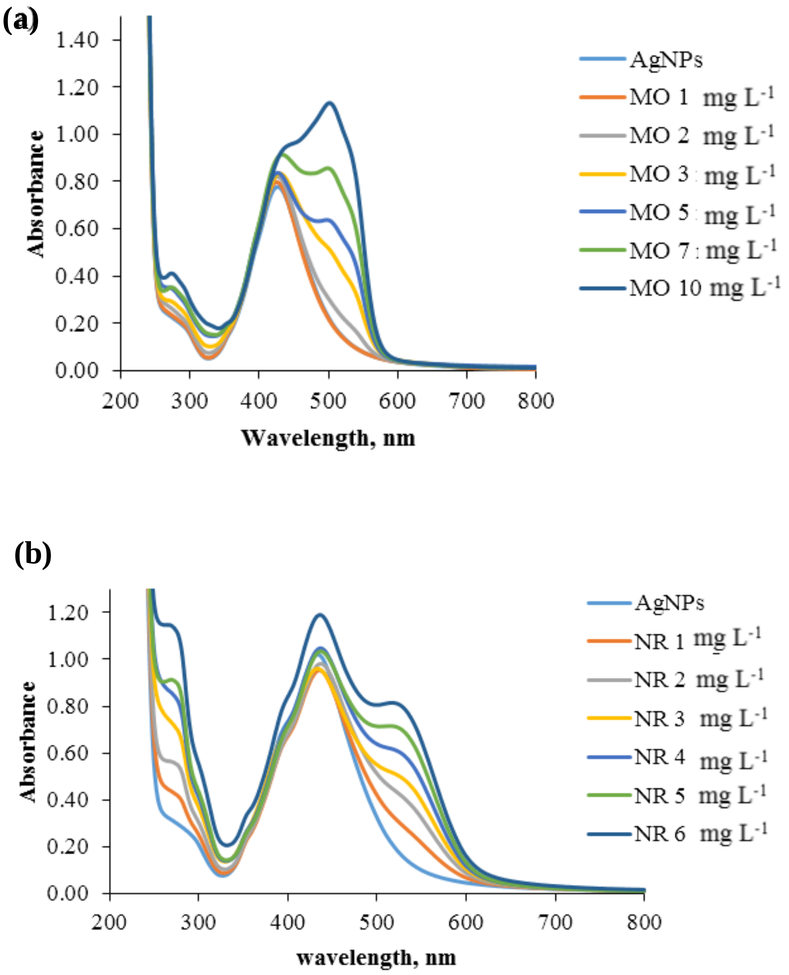

Figure 4.13 UV-Vis spectra showing the effect of organic dyes on the absorption intensity of AgNPs: (a) methyl orange (MO) and (b) neutral red (NR).

4.7 Real sample application

Potential of the developed approach for determination of Hg(II) in various samples was evaluated with a strong emphasis on its efficiency for environmental analysis. The samples included drinking water, mineral water, tap water, pond water, pond water in the presence of methylene blue as a matrix, synthetic human plasma and a standard reference material (SRM) 1641d with the certified value of mercury in water being 1.56 ± 0.02 mg kg^{-1}. The samples were spiked with Hg(II) at three different concentrations of 0.05, 0.10 and 0.25 mg L^{-1}. The recoveries for the three spiked concentrations were found to be satisfactory, 93.6-104.0% for water samples, 97.6-112.0% for blood samples and 98.0% for SRM. The samples were measured for their Hg(II) content using our developed colorimetric analyzer with the results compared with those of the batch spectrophotometric method. Each measurement was repeated three times and the average values were presented in Table 4.7. Statistical analysis (pair t-test) reveals that there was no significant difference between the two methods ($t_{observed}$ = -0.83, $t_{critical}$ =1.67, 95% confidence), confirming the potential use of the smartphone-based colorimetric analyzer in selective Hg(II) determination in the real environmental analysis [47].

Table 4.7 Determination of Hg(II) concentration in real aqueous samples application and Standard Reference Material (SRM) 1641d using the UV-Vis spectrophotometry system and smartphone as colorimetric sensor (n=3)

Name	UV-Vis spectrophotometry system (n=3)		Smartphone as colorimetric sensor (n=3)	
	Hg(II), mg L^{-1}	**% recovery**	**Hg(II), mg L^{-1}**	**% recovery**
D	ND*		ND*	
D + 0.05 mg L^{-1}	0.05 ± 0.00	96.0	0.05 ± 0.01	96.0
D + 0.10 mg L^{-1}	0.10 ± 0.00	104.7	0.11 ± 0.02	108.0
D + 0.25 mg L^{-1}	0.27 ± 0.01	106.6	0.26 ± 0.01	102.4
M	ND*		ND*	
M + 0.05 mg L^{-1}	0.05 ± 0.02	108.1	0.05 ± 0.01	104.0
M + 0.10 mg L^{-1}	0.10 ± 0.02	97.7	0.09 ± 0.01	94.0
M + 0.25 mg L^{-1}	0.24 ± 0.01	95.1	0.23 ± 0.01	93.6
T	ND*		ND*	
T + 0.05 mg L^{-1}	0.06 ± 0.03	112.2	0.05 ± 0.01	96.0
T + 0.10 mg L^{-1}	0.12 ± 0.02	116.1	0.10 ± 0.01	102.0
T + 0.25 mg L^{-1}	0.23 ± 0.02	93.4	0.25 ± 0.01	98.4
P	ND*		ND*	
P + 0.05 mg L^{-1}	0.05 ± 0.00	106.3	0.05 ± 0.01	104.0
P + 0.10 mg L^{-1}	0.10 ± 0.00	96.8	0.10 ± 0.01	102.0
P + 0.25 mg L^{-1}	0.24 ±0.02	95.0	0.26 ± 0.01	102.4
P added MB	ND*		ND*	
P added MB + 0.05 mg L^{-1}	0.05 ± 0.01	100.0	0.05 ± 0.01	100.0
P added MB +0.10 mg L^{-1}	0.11 ± 0.03	106.2	0.09 ± 0.01	94.0
SP	ND*		ND*	
SP + 0.05 mg L^{-1}	0.05 ± 0.02	103.8	0.05 ± 0.01	108.0
SP + 0.10 mg L^{-1}	0.09 ± 0.01	93.4	0.10 ± 0.01	100.0
SP + 0.25 mg L^{-1}	0.25 ± 0.06	101.2	0.25 ± 0.01	100.8
Standard Reference Material (1614d)	1.53 ± 0.01	98.1	1.53 ± 0.02	98.1

D = Drinking water, M = Mineral water, T = Tap water, P = Pond water, SP = Synthetic human plasma

ND* Defined as "Not Determined"

The t-test at the 95 % confidence limit level, the experiment *t*-stat value is -0.83, which was less than the critical *t*-values of 1.67.

4.8 The stability of PVP-stabilized AgNPs

The sensor was found to be stable for at least three months without significant changes occurring in the SPR band position and the band intensity are shown in Table 4.8 and considering from precision (%RSD) of the calibration curve of the developed AgNPs observed in three different synthesis batches of AgNPs at various concentration of Hg(II) as demonstrated in Table 4.4.

Table 4.8 Stability of the AgNPs at room temperature observed on three replicates. Four different batches of the nanoparticles were synthesized. The maximum absorption of AgNPs roughly occurred at 424-433 nm for all synthesis batches, suggesting that our synthesis method provided a good reproducibility. The nanoparticles were also stable at room temperature for several months despite being stored in a transparent vial

Week	Absorbance	Wavelength (nm)	Batch
1	0.94900	426.0	Batch 1
2	1.34012	425.5	
3	1.37320	425.7	
4	0.89698	426.0	
5	1.33156	425.5	
6	1.11427	425.3	
7	1.22291	425.5	
1	1.16859	428.0	Batch 2
2	0.85272	428.0	
3	0.85858	427.8	
1	0.82969	424.0	Batch 3
2	0.80813	424.5	
3	0.81417	425.3	
4	0.82817	424.8	
5	0.82091	425.0	
6	0.82025	424.5	
7	0.81619	425.3	
8	0.83807	425.0	
9	0.84075	424.5	
10	0.82599	425.0	

Table 4.8 Stability of the AgNPs at room temperature observed on three replicates. Four different batches of the nanoparticles were synthesized. The maximum absorption of AgNPs roughly occurred at 424-433 nm for all synthesis batches, suggesting that our synthesis method provided a good reproducibility. The nanoparticles were also stable at room temperature for several months despite being stored in a transparent vial (continued)

Week	Absorbance	Wavelength (nm)	Batch
1	1.03554	433.5	Batch 4
2	1.01684	433.5	
3	1.00415	433.5	
4	0.98284	433.3	
5	1.01641	433.0	
6	0.96791	433.5	
7	1.02905	434.1	
8	0.98196	433.9	
9	1.06848	433.4	

CHAPTER 5

CONCLUSION

The proposed method using smartphone as colorimetric sensor based on unmodified AgNPs stabilized by PVP has been successfully applied for determination of Hg(II) in various aqueous samples including water, blood and organic dye samples. The present study reports a use of unmodified AgNPs stabilized by PVP that was synthesized by simple and green approach based on a hydrothermal method. The PVP-stabilized AgNPs were successfully characterized by UV-Vis absorption spectra, TEM coupled with EDS, DLS and zeta potential analyses. Under the optimal condition, the developed colorimetric sensor shows magnificent sensitivity and greater selectivity towards Hg(II) over potential ions and a color dye matrix. Moreover, our sensor could be used in a wide pH range due to strong stabilizing effect of PVP in the AgNPs making the sensor resistant to the influence of ionic suppression which in turn would reduce failure upon their application on real samples. The results have demonstrated that our proposed colorimetric sensor provides a simple, rapid (with high sample throughput of 128 h^{-1}), sensitive, selective and cost-effective Hg(II) determination. Its successful application in real samples has also been established. These advantages allow it to be used by relatively unskilled end users for effective analysis of Hg(II) at resource-limited setting. The comparison between our developed method and others techniques used in Hg(II) detection as detailed in Table 5.1 and Table 4.2 clearly demonstrates the advantages of our sensor. In comparison to other existing sensors, ours, synthesized by a simple hydrothermal method, provides a fast and reliable detection of mercuric ions using only a small amount of AgNP solution for each measurement without any enhancer needed. The AgNP solution was also found to be stable for at least three months. In addition, by not using any toxic reducing agents like sodium borohydride ($NaBH_4$) or adding weak stabilizing agents like trisodium citrate ($Na_3C_6H_5O_7$), the synthesis of proposed PVP-based AgNPs poses no risk arising from exposure to toxic and hazardous chemicals, providing a greener and safer alternative in the determination of mercuric ions in aqueous samples.

Table 5.1 Comparison of the sensing performance of reported unmodified AgNPs for Hg(II) detection

Types of unmodified AgNPs	Characteristics of the sensor	Enhancer	Linear range/LOD (mg L^{-1})	Analysis time (min)	Interferences	Real samples	Ref.
Soap-root plant-capped AgNPs	Use of freshly prepared biological extract for stabilization[b]	–	2.01 - 20.06, (0.44)	5	Tolerance of Hg(II) to 13 cation species (1-fold)	Lake water	[16]
Yogurt-derived compounds-capped AgNPs	Use of biomolecule for stabilization[b]	–	No report/(0.002)	–	Tolerance of Hg(II) to 8 cation species (1-fold)	Tap water and groundwater	[17]
Bioreductant-capped AgNPs	Use of freshly prepared biological extract for stabilization[b]	–	1.0 - 20.06, (0.17)	instant measurement	Tolerance of Hg(II) to 11cation species (4-fold)	Tap and lake water	[18]
L-Tyrosine-capped AgNPs	Use of biological compound (L-Tyrosine) as reducing agent[b]	–	0.0032 - 0.13, (0.0032)	5	NA.	Drinking and tap water	[19]
Citrate-capped AgNPs	Use of Strong reducing agent ($NaBH_4$)	Cu(II)	0.5 - 7.0, (0.008)	instant measurement	Tolerance of Hg(II) to 7 cations species (3-fold)	Tap and drinking water	[20]
Citrate-capped AgNPs	Use of strong reducing agent ($NaBH_4$)[b]	AChE, ACTh	0.002 - 0.01, (0.00024)	5	Tolerance of Hg(II) to 11 cation species (1-fold)	Lake water, groundwater and sea water	[21]

Table 5.1 Comparison of the sensing performance of reported unmodified AgNPs for Hg(II) detection (continued)

Types of unmodified AgNPs	Characteristics of the sensor	Enhancer	Linear range/LOD (mg L^{-1})	Analysis time (min)	Interferences	Real samples	Ref.
Citrate-capped AgNPs	Use of strong reducing agent ($NaBH_4$)[b] (48 h)	H_2O_2	No report/(2.0 mg L^{-1})	–	Tolerance ratio of Hg(II) to cations (1-fold)	NA.	[22]
PVP-capped AgNPs	Use of strong reducing agent ($NaBH_4$)[b]	Lysine	0.0002 - 6.0, (0.0002)	1.5	Tolerance of Hg(II) to 14 cation species	Tap water	[23]
TPDT[a]-SiO_2-capped Ag NPs	Use of toxic reducing agent (hydrazine)[b]	–	1.0 - 15.0, (1.0)	2	Tolerance of Hg(II) to 10 cation species (5-fold)	NA.	[24]
PVP [c]-capped AgNPs	**Green and facile synthesis without using of strong reducing agent, only use PVP as reducing and stabilizing agent**	**Formic acid[d], no enhancer[e]**	**0.01–10 (0.007)[d] 0.05–0.50, (0.011)[e]**	**instant measurement**	**Tolerance ratio of Hg(II) to 10 cations and 5 anions (100-fold)**	**Water, blood and dye organic samples**	**This thesis**

[a] N-[-3-(trimethoxysilyl) propyl] diethylenetriamine

[b] These synthesized sensors require a complicated and time-consuming process.

[c] Polyvinylpyrrolidone

[d] Based on UV-Vis spectrophotometry system

[e] Based on smartphone as a colorimetric analyzer

NA. Defined as "Not Analysis

REFERENCES

REFERENCES

[1] Cui B and et al. “Analyzing trophic transfer of heavy metals for food webs in the newly-formed wetlands of the Yellow River Delta, China”, **Environmental Pollution**. 159(5): 1297–1306; March, 2011.

[2] Du J and et al. “Colorimetric detection of mercury ions based on plasmonic nanoparticles”, **Small**. 9(9-10): 1467–1481; April, 2012

[3] Clarkson T and et al. “The toxicology of mercury current exposures and clinical manifestations”, **New England Journal of Medicine**. 349(18): 1731–1737; May, 2003.

[4] Hatch W and et al. “Determination of submicrogram quantities of mercury by atomic absorption spectrophotometry”, **Analytical Chemistry**. 40(14): 2085–2087; December, 1968.

[5] Olesik JW. “Elemental analysis using ICP-OES and ICP/MS”, **Analytical Chemistry**. 63(1): 12A–21A; January, 1991.

[6] Sabela M and et al. “A review of gold and silver nanoparticle-based colorimetric sensing assays”, **Advanced Engineering Materials**. 19(12): 1700270; July, 2017.

[7] Apilux A and et al. “Simple and rapid colorimetric detection of Hg(II) by a paper-based device using silver nanoplates”, **Talanta**. 97: 388–394; May, 2012.

[8] Liu X and et al. “Visual detection of Hg^{2+} with high selectivity using thymine modified gold nanoparticles”, **Analytical Sciences**. 26(11): 1169–1172; November, 2010.

[9] Wang Y and et al. “Colorimetric detection of mercury (II) ion using atomic unmodified silver nanoparticles and mercury-specific oligonucleotides”, **ACS Applied Materials & Interfaces**. 2(2): 339–342; February, 2010.

[10] Chai F and et al. “L-cysteine functionalized gold nanoparticles for the colorimetric detection of Hg^{2+}induced by ultraviolet light”, **Nanotechnology**. 21(2): 025501; December, 2009.

REFERENCES (CONTINUED)

[11] Chen PC and et al. “Gold and silver nanomaterial-based optical sensing systems”, **Particle & Particle Systems Characterization**. 31(9): 917–942; March, 2014.

[12] Botasini S and et al. “Toward decentralized analysis of mercury (II) in real samples. A critical review on nanotechnology-based methodologies”, **Analytica Chimica Acta**. 800: 1–11; August, 2013.

[13] Huang NM and et al. “Amalgamation based optical and colorimetric sensing of mercury (II) ions with silver@graphene oxide nanocomposite materials”, **Microchimica Acta**. 183(1): 369–377; October, 2015.

[14] Noor AM and et al. “Visual and spectrophotometric determination of mercury(II) using silver nanoparticles modified with graphene oxide”, **Microchimica Acta**. 183(2): 597–603; November, 2015.

[15] Mehdinia A and et al. “A novel label-free method for determination of inorganic mercury in environmental aqueous media using BSA-modified silver nanoparticles”, **International Journal of Environmental Science and Technology**. 13(11): 2663–2674; September, 2016.

[16] Farhadi K and et al. “Highly selective Hg^{2+} colorimetric sensor using green synthesized and unmodified silver nanoparticles”, **Sensors and Actuators B: Chemical**. 161(1): 880–885; December, 2012.

[17] Gao S and et al. “Old tree with new shoots: silver nanoparticles for label-free and colorimetric mercury ions detection”, **Journal of Nanoparticle Research**. 15(1): 1385; December, 2013.

[18] Firdaus M and et al. “Colorimetric detection of mercury (II) ion in aqueous solution using silver nanoparticles”, **Analytical Sciences**. 33(7): 831-837; July, 2017.

[19] Annadhasan M and et al. “Green synthesized silver and gold nanoparticles for colorimetric detection of Hg^{2+}, Pb^{2+}, and Mn^{2+} in aqueous medium”, **ACS Sustainable Chemistry & Engineering**. 2(4): 887–896; January, 2014.

REFERENCES (CONTINUED)

[20] Jarujamrus P and et al. “Selective colorimetric sensors based on the monitoring of an unmodified silver nanoparticles (AgNPs) reduction for a simple and rapid determination of mercury”, **Spectrochimica Acta Part A: Molecular and Biomolecular Spectroscopy**. 142: 86–93; February, 2015.

[21] Nanda K and et al. “Acetylcholinesterase inhibition-based colorimetric determination of Hg^{2+} using unmodified silver nanoparticles”, **New Journal of Chemistry**. 39(2): 1172–1178; November, 2015.

[22] Wang GL and et al. “Ultrasensitive and dual functional colorimetric sensors for mercury (II) ions and hydrogen peroxide based on catalytic reduction property of silver nanoparticles”, **Biosensors and Bioelectronics**. 31(1): 337–342; October, 2012.

[23] Li L and et al. “A colorimetric silver nanoparticle-based assay for Hg(II) using lysine as a particle-linking reagent”, **Microchimica Acta**. 182(11-12): 1977–1981; June, 2015.

[24] Rameshkumar P and et al. “Silicate sol–gel stabilized silver nanoparticles for sensor applications toward mercuric ions, hydrogen peroxide and nitrobenzene”, **Sensors and Actuators B: Chemical**. 202: 1070–1077; June, 2014.

[25] Choodum A and Daeid NN. “Rapid and semi-quantitative presumptive tests for opiate drugs”, **Talanta**. 86: 284–292; October, 2011.

[26] Sharma, G. **Digital color imaging handbook: color fundamentals for digital imaging**. New York: CRC Press, 2002.

[27] Burger W and MJ Burge. **Principles of digital image processing: fundamental techniques**. Springer Science & Business Media, 2010.

[28] Birch NC and Stickle DF. “Example of use of a desktop scanner for data acquisition in a colorimetric assay”, **Clinica Chimica Acta**. 333: 95–96; July, 2003.

REFERENCES (CONTINUED)

[29] Choodum A and et al. "Rapid quantitative colourimetric tests for trinitrotoluene (TNT) in soil", **Forensic Science International**. 222: 340–345; October, 2011.

[30] Choodum A and et al. "Using the iPhone as a device for a rapid quantitative analysis of trinitrotoluene in soil", **Talanta**. 115: 143–149; October, 2013.

[31] Epperson PM and et al. "Applications of charge transfer devices in spectroscopy", **Analytical Chemistry**. 60: 327A–335A; March, 1998.

[32] Suziki Y and et al. "Tristimulus colorimetry using a digital still camera and its application to determination of iron and residual chlorine in water samples", **Analytical Science**. 22: 411–414; March, 2006.

[33] Cantrell K and et al. "Use of the hue parameter of the hue, saturation, value color space as a quantitative analytical parameter for bitonal optical sensors", **Analytical Chemistry**. 82: 531–542; December, 2010.

[34] Byrne L, Barker J, Thomas G P, Diamond D, Edwards S. "Digital imaging as a detector for generic analytical measurements", **TrAC Trends in Analytical Chemistry**. 19: 517–522; August, 2000.

[35] Meelapsom R and et al. "Chromatic analysis by monitoring unmodified silve nanoparticles reduction on double layer microfluidic paper-based analytical devices for selective and sensitive determination of mercury (II)", **Talanta**. 155: 193-201; August, 2016.

[36] Muniandy SS and et al. Sains Malaysiana, Penerbit UKM, (2019). (Accepted).

[37] Jarujamrus P and et al. "Use of a smartphone as a colorimetric analyzer in paper-based devices for sensitive and selective determination of mercury in water samples", **Analytical Sciences**. 34(1): 75–81; January, 2018.

[38] Pecharee, S. "CAnal application", **Google play store**. https://play.google.com/store/.apps/detailsMid=appinventor.ai somkid p.CAnal. July, 2018.

REFERENCES (CONTINUED)

[39] Gharibshahi L and et al. "Structural and optical properties of Ag nanoparticles synthesized by thermal treatment method", **Materials**. 10: 402; April, 2017.

[40] Oku T and et al. "Chemical synthesis of silver nanoparticles encapsulated in boron nitride nanocages", **Journal of Materials Chemistry**. 10(2): 255-257; January, 2000.

[41] FAN Y and et al. "Synthesis of starch-stabilized Ag nanoparticles and Hg^{2+} recognition in aqueous media", **Nanoscale research letters**. 4(10): 1230; October, 2009.

[42] Henglein A and Chris B. "Absorption spectra and reactions of colloidal bimetallic nanoparticles containing mercury", **Chemistry of materials**. 9(10): 2164-2167; October, 1997.

[43] Morris T and et al. "The effects of mercury adsorption on the optical response of size-selected gold and silver nanoparticles", **Langmuir**. 18(20): 7261-7264; August, 2002.

[44] Matusiewicz H and Ewa Stanisz. "Evaluation of the catalyzed photo-cold vapour generation for determination of mercury by AAS", **Journal of the Brazilian Chemical Society**. 23(2): 247-257; February, 2012.

[45] Katsikas L and et al. "Bimetallic colloids: silver and mercury", **The Journal of Physical Chemistry**. 100(27): 11203-11206; July, 1996.

[46] Bothra S and et al. "Functionalized silver nanoparticles as chemosensor for pH, Hg^{2+} and Fe^{3+} in aqueous medium", **Sensors and Actuators B: Chemical**. 188: 937-943; November, 2013.

[47] Miller JN and Miller JC. **Statistics and chemometrics for analytical chemistry**. Essex: Pearson Education Limited, 2010.

APPENDIX

LIST OF PUBLICATIONS AND CONFERENCE PRESENTATIONS

LISTS OF PUBLICATIONS

1. S. Puchum, R. Meelapsom, S. S. Muniandy, HL. Lee, S. Pencharee, M. Amatatongchai, K. Suttisintong and P. Jarujamrus*. "Use of unmodified silver nanoparticles (AgNPs) as colorimetric Hg(II) sensor: A new approach to sensitive and high sample throughput determination of Hg(II) under high influence of ionic suppression" **International Journal of Environmental Analytical Chemistry (2019).** 99(2), 139-156.
2. P. Jarujamrus*, N. Malahom, S. Puchum, R. Meelapsom, A. Siripinyanond, M. Amatatongchai , S. Chairam and C. Kulsing "Complexometric and argentometric titrations using thread-based analytical devices" **Talanta**. **(2018).** 183, 228-236.

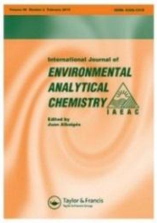

Taylor & Francis
Taylor & Francis Group

International Journal of Environmental Analytical Chemistry

ISSN: 0306-7319 (Print) 1029-0397 (Online) Journal homepage: https://www.tandfonline.com/loi/geac20

Use of unmodified silver nanoparticles (AgNPs) as colorimetric Hg(II) sensor: A new approach to sensitive and high sample throughput determination of Hg(II) under high influence of ionic suppression

Sodsai Puchum, Rattapol Meelapsom, Sunderishwary S. Muniandy, Hooi Ling Lee, Somkid Pencharee, Maliwan Amatatongchai, Khomson Suttisintong & Purim Jarujamrus

To cite this article: Sodsai Puchum, Rattapol Meelapsom, Sunderishwary S. Muniandy, Hooi Ling Lee, Somkid Pencharee, Maliwan Amatatongchai, Khomson Suttisintong & Purim Jarujamrus (2019) Use of unmodified silver nanoparticles (AgNPs) as colorimetric Hg(II) sensor: A new approach to sensitive and high sample throughput determination of Hg(II) under high influence of ionic suppression, International Journal of Environmental Analytical Chemistry, 99:2, 139-156, DOI: 10.1080/03067319.2019.1580703

To link to this article: https://doi.org/10.1080/03067319.2019.1580703

INTERNATIONAL JOURNAL OF ENVIRONMENTAL ANALYTICAL CHEMISTRY
2019, VOL. 99, NO. 2, 139–156
https://doi.org/10.1080/03067319.2019.1580703

Taylor & Francis
Taylor & Francis Group

ARTICLE

Use of unmodified silver nanoparticles (AgNPs) as colorimetric Hg(II) sensor: A new approach to sensitive and high sample throughput determination of Hg(II) under high influence of ionic suppression

Sodsai Puchum[a,b], Rattapol Meelapsom[b,c], Sunderishwary S. Muniandy[d], Hooi Ling Lee[d], Somkid Pencharee[e], Maliwan Amatatongchai[a,b], Khomson Suttisintong[f] and Purim Jarujamrus[a,b]

[a]Department of Chemistry and Center of Excellence for Innovation in Chemistry, Faculty of Science, Ubon Ratchathani University, Ubon Ratchathani, Thailand; [b]Nanomaterials Science, Sensors & Catalysis for Problem-Based Projects, Faculty of Science, Ubon Ratchathani University, Ubon Ratchathani, Thailand; [c]Department of Science and Mathematics, Faculty of Science and Health Technology, Kalasin University, Kalasin, Thailand; [d]Nanomaterials Research Group, School of Chemical Sciences, Universiti Sains Malaysia, Penang, Malaysia; [e]Department of Physics, Faculty of Science, Ubon Ratchathani University, Ubon Ratchathani, Thailand; [f]National Nanotechnology Center (NANOTEC), National Science and Technology Development Agency (NSTDA), Pathum Thani Thailand

ABSTRACT

Facile unmodified silver nanoparticles (AgNPs) as colorimetric sensor for determination of Hg(II) ions in aqueous samples were developed using UV-Vis spectrophotometry. Abrupt change in absorbance of the AgNPs was observed, which progressively decreased and slightly shifted to the blue wavelength as the concentration of Hg(II) increased. It appears that the AgNPs were oxidized by Hg(II), resulting in disintegration of the AgNPs and Hg(0). Deposition of Hg(0) on the surface of AgNPs also occurred, resulting in amalgam particles of mercury (Hg-Ag). Interestingly, the developed approach showed a significant enhancement in the Hg(II) analytical sensitivity when formic acid was doped onto the AgNPs, with the linearity range of 0.01–10 mg L^{-1} ($r^2 = 0.999$) providing the quantitative detection limit of 0.007 mg L^{-1} (3SD blank/slope of the calibration curve). Greater selectivity toward Hg(II) over other ions and colour dyes was also observed, likely a result of stabilization by polyvinylpyrrolidone (PVP), which kept the AgNPs well-stabilized and dispersed in the bulk aqueous environment making them resistant to ionic suppression. Under using a 96-well microplate and a smartphone equipped with homemade application as a colorimetric analyzer under controlled lighting, high sample throughput (128 sample h^{-1}, n = 4) was achieved, establishing its potential for practical analysis. The percentage recoveries of spiked aqueous samples obtained from the microplate-based system were in acceptable range, in agreement with the values obtained from the UV-Vis spectrophotometry-based system. The proposed colorimetric sensor has been shown to provide a rapid, simple, sensitive and selective detection of Hg(II) ions in various aqueous samples.

ARTICLE HISTORY
Received 9 December 2018
Accepted 4 February 2019

KEYWORDS
Silver nanoparticles (AgNPs); mercury (Hg(II)); colorimetric sensors; formic acid; smartphone

CONTACT Purim Jarujamrus purim.j@ubu.ac.th

Supplemental data for this article can be accessed here.

1. Introduction

Environmental pollution caused by heavy metals, especially mercury, is a cause for concern around the world. Mercury has been shown to pollute soil, food and even water, originating from diverse sources including increasing human activities, rapid industrialization of cosmetics as well as pharmaceutical and battery manufacturing [1,2]. The toxic effects of Hg(II) greatly harm the digestive, nervous and immune systems as well as organs like kidneys, skin and eyes, and lungs [3]. Mercury exists in various forms which are all toxic to the environment and human beings. Inorganic mercury is one of the most stable and commonly used forms due to its high solubility, existing mostly in water and living systems (mercuric ion, Hg(II)). The World Health Organization (WHO) and US Environmental Protection Agency (USEPA) guidelines recommend that the total maximum mercury content in drinking water should be less than 0.006 mg L^{-1} and 0.002 mg L^{-1}, respectively [2]. Therefore, it is of necessity to have a highly selective and rapid method to monitor Hg(II) levels in various samples under aqueous conditions.

There are various conventional analytical approaches to estimate Hg(II) concentration in aqueous samples including cold vapour atomic absorption spectrometry (CVAAS) and inductively coupled plasma mass spectrometry (ICP-MS) [4,5]. Despite having high selectivity, these methods are costly and time-consuming, and require advanced instruments. Recently, portable instrumentation has attracted considerable research attention whereby detection of an analyte can be done with high simplicity, rapidity, reliability and precision. One of the most simple methods successfully applied to the detection of Hg(II) takes advantage of the colour change upon the interaction of nanoparticles and the target analytes. Gold nanoparticles (AuNPs) and silver nanoparticles (AgNPs) have been developed as colorimetric sensors for Hg(II) determination due to their optical and high extinction coefficients of their surface plasmon resonance (SPR) absorption band [6]. AgNPs, in particular, are more favourable because of their low cost and higher extinction coefficients of their surface plasmon resonance (SPR) absorption band (approximately 100-fold) compared to those of gold nanoparticles (AuNPs) of the same size [7].

Up to now, most nanoparticles-based colorimetric sensors for analyte ions detection rely on the interaction between surface modification of AuNPs or AgNPs and the analyte ions inducing 'non-cross linking aggregation' or 'interparticles crosslinking aggregation' of nanoparticles giving characteristic colorimetric responses [6]. Although these sensors can be used to successfully detect metal ions with high sensitivity, Hg(II) included, their syntheses involve expensive and complicated procedures to modify the surface with recognition molecules such as thymine [8], oligonucleotides [9], L-cysteine [10], protein and DNA [11]. Despite their high sensitivity, the modified NPs lose their superior optical properties through surface modification due to the effects of adsorbed species or capping on the wavelength position and intensity of the SPR band [12].

Successful use of modified silver nanoparticles (AgNPs)-based sensors for monitoring the level of mercury has been reported [13–15]. A research group led by Huang reported a colorimetric detection method for mercury ions in aqueous medium using graphene oxide (GO)-modified AgNPs [13]. GO was found to be an excellent stabilizer for AgNPs and the invented sensors provided a LOD for Hg(II) of 0.068 mg L^{-1}. However, their synthesis involved the use of sodium borohydride ($NaBH_4$), a toxic agent to reduce GO and Ag(I). In their other publication, they proposed a greener method whereby (GO)-modified AgNPs were prepared by the horn sonication method [14]. Through this method, the LOD for Hg(II) was 0.12 mg L^{-1}. Although no hazardous agents were involved, the green method was time-consuming and complicated. In another study, Mehdinia et al. used AgNPs modified with a biomolecule for determination of inorganic mercury in environmental aqueous media and the LOD of the developed sensor was found to be 0.54 mg L^{-1} [15]. Although highly sensitive, the synthesized biomolecule-linked nanoparticles needed to be freshly prepared and the preparation of these biomolecules was often a complicated and expensive process. Despite their high stability and sensitivity, in general, the modified AgNPs were difficult to prepare as their synthesis usually involved a complicated process. The goal, therefore, has been to develop a colorimetric sensor based on 'unmodified AgNPs' for Hg(II) detection through a simple and cost-effective method.

Recently, a few works have reported the use of unmodified AgNPs as a colorimetric sensor for Hg(II) detection [16–18]. Farhadi et al. used soap-root plant as a stabilizing agent for AgNPs to achieve a LOD of 0.44 mg L^{-1} [16]. Gao et al. reported the use of a yoghurt-mediated silver nanostructure for label-free and colorimetric mercury ions detection with a LOD as low as 0.002 mg L^{-1} [17]. Although both works achieved low LODs, their synthesized methods were complicated. In 2015, our recent work reported a selective colorimetric sensor based on unmodified AgNPs to detect Hg(II) using trisodium citrate as a stabilizing agent, which achieved a LOD of 0.008 mg L^{-1} using Cu(II) as sensitivity enhancer [19]. However, our previous method involved the use of sodium borohydride ($NaBH_4$), a toxic reducing agent. There is also another drawback associated with the aforementioned work in that the unmodified AgNPs may fail in their application on real samples because of the negative incidence of the ionic strength and the presence of exchangeable ligands [12].

Herein, we reported a green and novel facile unmodified silver nanoparticles (AgNPs) as colorimetric sensor for sensitive and high sample throughput determination of Hg(II) ions in aqueous samples. The AgNPs were stabilized with polyvinylpyrrolidone (PVP) leading to good stabilization and dispersion of the nanoparticles in the bulk aqueous environment making them resistant to the influence of ionic suppression, without any need for toxic and hazardous reducing agents like sodium borohydride ($NaBH_4$). Moreover, the effect of formic acid as a catalytic enhancer was investigated with a first view to enhancing Hg(II) detection sensitivity based on UV-Vis spectrophotometry. In addition, high sample throughput of Hg(II) determination based on 96-well microplate using a smartphone as a colorimetric analyzer with our homemade application under a housing light controlling system was successfully applied to analyzing Hg(II) ions in various real samples.

2. Experimental

2.1. *Chemicals and materials*

All chemicals used in this study were of analytical grade. All solutions were prepared in deionized water with 18 MΩ resistance (obtained from a Millipore Milli-Q purification system, Bedford, MA, USA). Chemical reagents, such as formic acid (98%) were purchased from Fisher Scientific, UK. The following chemicals were used as received: polyvinylpyrrolidone (PVP) and silver nitrate ($AgNO_3$), purchased from Sigma-Aldrich (US) and Bendosen (Malaysia) respectively; mercury(II) chloride ($HgCl_2$), calcium nitrate ($Ca(NO_3)_2$), sodium chloride (NaCl), potassium fluoride (KF), sodium nitrate ($NaNO_3$), copper(II) sulfate pentahydrate ($CuSO_4$ $5H_2O$), manganese sulfate monohydrate ($MnSO_4 \cdot H_2O$), sodium sulfate heptahydrate (Na_2SO_4 $7H_2O$), sodium hydrogen sulfide (NaHS), iron(II) sulfate heptahydrate ($FeSO_4$ $7H_2O$), zinc sulfate heptahydrate ($ZnSO_4$ $7H_2O$), magnesium sulfate heptahydrate ($MgSO_4.7H_2O$), nickel(II) sulfate ($NiSO_4$), cadmium nitrate tetrahydrate ($Cd(NO_3)_2$ $4H_2O$), barium nitrate ($Ba(NO_3)_2$), lead nitrate ($Pb(NO_3)_2$), all from Carlo Erba, IT, methylene blue (MB), methyl orange (MO) and neutral red (NR) used in the interference study, all from SUVCHEM, India. Standard reference material (SRM) of mercury in water (1641d) with certified value of mercury 1.56 ± 0.02 mg kg^{-1} was purchased from National institute of standards and technology (NIST, US).

2.2. *Synthesis of PVP-stabilized AgNPs*

AgNPs were synthesized using our methods explained by Muniandy et al. [20]. AgNPs were easily prepared based on the hydrothermal method in the presence of PVP, used as a reducing and stabilizing agent. Briefly, a preparation of one molar ratio, $R = 1$ was done by mixing 0.612 g of $AgNO_3$ and 0.4 g of PVP in 20 mL of distilled water separately at room temperature. The molar ratio, R between the repeating unit of PVP and $AgNO_3$ in this study, however, was fixed at $R = 5$. The solutions were then added dropwise into another 50 mL of distilled water. The total solution (90 mL) was stirred for 15 min and the entire mixture was transferred into a Teflon vessel (capacity = 100 mL). The reaction vessel was then put in a stainless steel hydrothermal reactor and placed in the oven at 160°C for 24 h. Finally, a yellowish-brown colour solution of AgNPs stabilized by PVP was obtained. The absorption spectrum was observed with a UV-Vis spectrophotometer. The particle size characterization of AgNPs was also confirmed by TEM.

2.3. *Characterizations*

The absorbance spectrum of the AgNPs was collected using a double beam, UV- 2600 UV-Vis spectrophotometer (Shimadzu, Japan) in the spectral range of 200–800 nm. The morphology and size of the AgNPs were examined by a JEM-2010 transmission electron microscope (TEM; JEOL, Japan) at 200 kV using 200-mesh Cu grids coated with carbon film. Energy dispersive X-ray spectroscopy (EDS) analysis of the formation of various amalgam particles (Hg-Ag) was carried out using a JSM-6335F scanning electron microscope (SEM; JEOL, Japan) equipped with INCA energy dispersive X-ray spectroscopy detector (EDS; JEOL, Japan), operated at an acceleration voltage of 15 kV. The zetasizer nanoZS (Malvern, UK) was used to observe the effect of different concentrations of Hg(II) on the hydrodynamic size and zeta potential of the synthesized AgNPs in the presence and absence of formic acid. All pictures were recorded by a smartphone camera (Samsung Galaxy J7) and microtiter plate (Brand plates® made in Germany).

2.4. Colorimetric detection of Hg(II) using AgNPs as a probe in the presence of formic acid

2.4.1. UV-Vis spectrophotometry

Colorimetric detection of Hg(II) can be measured using AgNPs as a probe in the presence of 0.5 M formic acid. Firstly, 50 µL of the AgNPs was added into a volumetric flask. Then, Hg(II) at different volumes of 50 mg L^{-1} Hg(II) stock was added to a solution containing AgNPs. In addition, 500 µL of 0.5 M formic acid solution was added and the final volume of 5 mL was adjusted by DI water after which the solution was subjected to vigorous shake. Finally, the colour of the solution changed from yellowish brown to light yellow. The surface plasmon resonance (SPR) was monitored by UV-Vis spectrophotometer at wavelengths of around 424–433 nm. The Hg(II) concentration reported in mg L^{-1} unit was determined by establishment of calibration curve (plotted between A_0/A and Hg(II) concentration (mg L^{-1})).

To evaluate the selectivity of our developed sensors, Hg(II) ions were determined in the presence of 15 foreign ions, each with a concentration of 10 mg L^{-1}, including 10 cations (Ba(II), Ca(II), Cd(II), Cu(II), Fe(II), Mg(II), Mn(II), Pb(II), Zn(II) and Ni(II)) and five anions (chloride, fluoride, nitrate, sulfate and sulfide). Briefly, 50 µL of freshly prepared AgNPs were transferred to a volumetric flask, containing Hg(II) with a fixed final concentration of 0.1 mg L^{-1}. The 15 foreign ions at 10 mg L^{-1} were then added into the volumetric flask and the final volume of 5 mL was adjusted by DI water. Subsequently, the absorption spectra were recorded by UV-Vis spectrophotometer.

2.4.2. Use of smartphone as a colorimetric analyzer (CAnal application)

To measure Hg(II) using our developed smartphone-based sensor, 30 µL of the AgNPs was first added to a well plate, followed by Hg(II) at different volumes of 50 mg L^{-1} Hg(II) stock, with the final volume in each well of 200 µL achieved by adjustment with DI water. Then, the well plate was covered with its cover before photographing to prevent effect of luminosity from environmental light. The cover of the well plate was modified from a lid that came with the well plate upon purchase. Laser was used to punch holes on the lid in a way that every hole on the lid spatially matched its corresponding hole of the well plate. Then the punctured cover was colour-sprayed black to prevent environmental light from disturbing the measurement. The well plate together with its modified lid was placed in a control light box, and the smartphone was attached at the lid of the box directly above the well plate as explained in our previous work [21]. Steps concerning the determination of Hg(II) using a smartphone as a colorimetric analyzer were demonstrated in Scheme 1.

2.4.3. The analytical program for Hg(II) analyzer

The application program used for the detection of Hg(II) is called CAnal (version 5.0) modified from [22] for solution-based analysis. It was developed on an Eclipse code [23] on the Java platform and compiled to run on the Android operating system. To operate the application, a number of steps are followed (Figure S1). However, prior to the measurement of Hg(II), we first had to determine which colour intensity in the RGB system was the most sensitive to changes occurring upon interaction of the PVP-stabilized AgNPs with Hg(II). Among the five components in the RGB system (R (red), G (green), B (blue), average gray calculated from (R + G + B)/3, and gray with a luminosity which is equal to

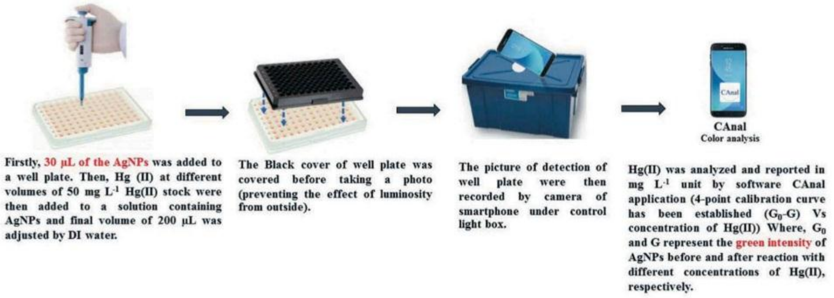

Firstly, 30 µL of the AgNPs was added to a well plate. Then, Hg (II) at different volumes of 50 mg L^{-1} Hg(II) stock were then added to a solution containing AgNPs and final volume of 200 µL was adjusted by DI water.

The Black cover of well plate was covered before taking a photo (preventing the effect of luminosity from outside).

The picture of detection of well plate were then recorded by camera of smartphone under control light box.

Hg(II) was analyzed and reported in mg L^{-1} unit by software CAnal application (4-point calibration curve has been established (G_0-G) Vs concentration of Hg(II)) Where, G_0 and G represent the green intensity of AgNPs before and after reaction with different concentrations of Hg(II), respectively.

Scheme 1. Determination of Hg(II) using a smartphone equipped with software application CAnal as a colorimetric analyzer on a well plate-based system in the control light box.

0.299R + 0.587G + 0.114B), it was found that green was the most sensitive to the colour change from yellowish-brown in samples without Hg(II) to progressively paler yellow with a tint of orange with increasing concentrations of Hg (II) (Figure S2) [21]; hence, intensity of the green colour is used in the determination of Hg(II). Prior to each measurement of the samples, a calibration graph was constructed by measuring the change between the intensity of the green colour upon the sensor reacting with different concentrations of standard Hg(II) (G) and that of a blank (G_0). The intensity of the colour of the reaction was determined by imageJ (https://imagej.net/Downloads) and a four-point calibration curve was plotted in Microsoft Excel; difference in green intensity (G_0-G) was plotted against concentration in mg L^{-1} of Hg(II). After the calibration curve has been established, Hg(II) concentrations can be measured following the steps shown in Figure S3. First, open the application, in the setting, choose colour 'green' and unit 'mg L^{-1}', and then input the calibration curve. After that, import the image of the well plate, or use the application to take an image, then set blank by placing the square pointer at the detection zone of the blank and the program then reads a G_0 value. Finally, move the square pointer to the sample zone and then the value G is given. The difference between the intensity of the green colour of the blank and that of the sample is then used to compute the concentration of Hg(II) in the sample, the unit of which is mg L^{-1} as chosen earlier in the setting.

2.5. *Real sample preparation*

Drinking and mineral water samples were obtained from a convenience store, and a tap water sample was collected from the water supplied to the Faculty of Science, Ubon Ratchathani University. Chlorine in the tap water was removed by letting the water run through the open tap for 30 min at room temperature prior to further procedure. The sample was then heated at 100°C for 15 min. Pond water samples were obtained from the water supply of Ubon Ratchathani University. The plasma from human blood contained 4% trisodium citrate as anticoagulant was purchased from Sigma-Aldrich, USA. The standard reference material (SRM) 1641d was provided by the National Institute of Standards and Technology. It contained a certified mercury value of 1.56 ± 0.02 mg kg^{-1}. Recovery was determined by spiking aqueous samples with standard Hg(II) at 0.05, 0.10 and 0.25 mg L^{-1}.

3. Results and discussion

3.1. *Synthesis and characterization of PVP-stabilized AgNPs*

Silver nanoparticles were synthesized based on a hydrothermal method using polyvinylpyrrolidone (PVP) as a stabilizing and reducing agent. The possible formation of PVP-stabilized AgNPs has been explained in detailed by Muniandy, Sasidharan & Lee, 2019 [20]. This could be easily prepared and the resulted sensor was highly stable. The colour of the aqueous solution of the PVP-based nanoparticles was yellowish-brown (insert of Figure 1). The sensor was found to be stable for at least three months without significant changes occurring in the SPR band position and the band intensity (Table S1). The maximum absorbance of these AgNPs occurred at roughly 424–433 nm (Figure 1). According to the TEM study, the average diameter of AgNPs was 21.76 ± 0.22 nm (Figure 2(b)). Dynamic light scattering was used to measure the particle size of the AgNPs (Table S2), showing good agreement with the TEM result. Zeta potential of the synthesized AgNPs indicates no charges surrounding the AgNPs, suggesting strong stabilization of AgNPs by PVP. Moreover, the mass concentration and number concentration of AgNPs were 3.81 mg mL^{-1} and 1.27 × 10^{14} NPs mL^{-1}, respectively, as shown in **S1**.

3.2. *Optimization of experimental conditions for colorimetric detection of Hg(II) and their mechanism by using AgNPs as a probe (based on UV-Vis spectrophotometry system)*

To investigate the optimized conditions in which AgNPs-based colorimetric sensor can effectively detect Hg(II), it was essential to study the various parameters affecting Hg(II) detection. The volume of AgNPs was first optimized without Hg(II) by studying the UV-Vis spectra of AgNPs at volumes of 50 µL, 75 µL and 100 µL (Figure S4a). The optimum condition was achieved with 50 µL of AgNPs, which was the volume to be used for the

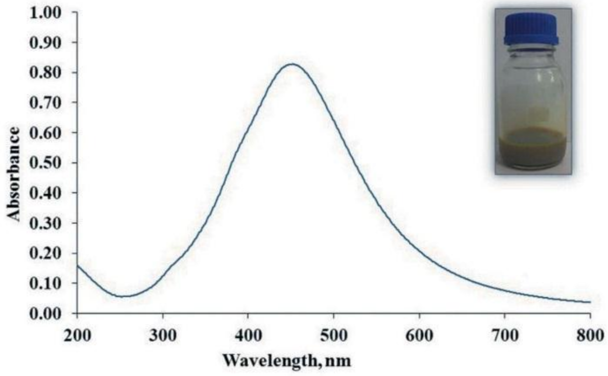

Figure 1. UV-Vis absorption spectrum of unmodified AgNPs stabilized with PVP solution was recorded by adding of 50 µL of AgNPs into 5 mL of volumetric flask and final volume was adjusted at 5 mL by DI water. Inset: Photograph of unmodified AgNPs stabilized with PVP solution.

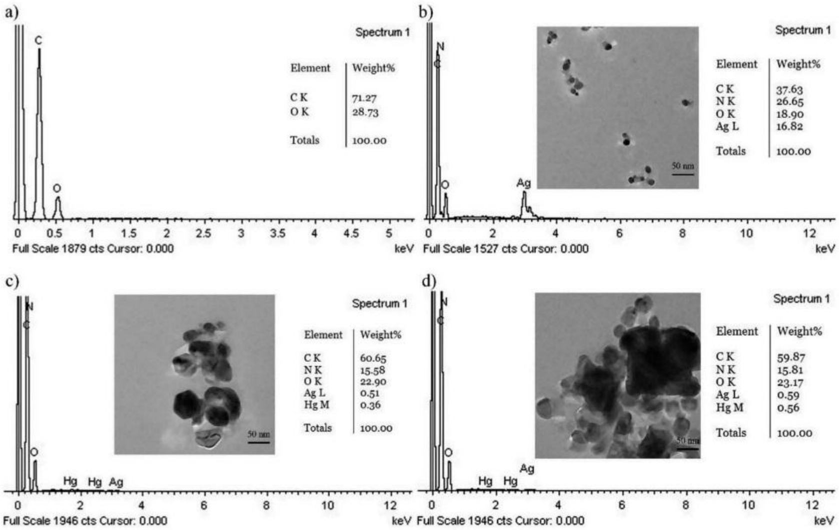

Figure 2. EDS spectrum of the sample stub (a), TEM images and EDS spectra of the dispersion of PVP-stabilized AgNPs (b), PVP-stabilized AgNPs after addition of 5 mg L^{-1} Hg(II) (c), and PVP-stabilized AgNPs after addition of 5 mg L^{-1} Hg(II) and 0.5 M formic acid (d).

following experiments. At this volume, the absorbance value of AgNPs was lower than 1.0 following the Beer-Lambert law, whereas volumes of 75 and 100 µL showed the absorbance value of over 1.0, indicating deviation from the Beer–Lambert law. Moreover, we studied the volume of AgNPs in the presence of Hg(II) ions in the linear range of 0.1–5.0 mg L^{-1} (Figure S4b). The results showed that the AgNPs volume of 50 µL demonstrated a good linear correlation between the different concentrations of Hg(II) and absorbance ratio (A_0/A), where A_0 is the absorbance of bare AgNPs at 424 nm and A is the absorbance of AgNPs at the same wavelength after reaction with Hg(II). The volume used in this work was a fraction of that needed for the sensor of our previous work [19]. For detailed comparison between the PVP-based AgNPs developed in this work and the citrate-based AgNPs in the previous work [19] see Table S3.

At first, the colorimetric sensing for Hg(II) was performed. After addition of Hg(II) solution to freshly prepared AgNPs, instant colour change from brownish yellow to orange was observed and it changed gradually with increasing concentration of Hg(II) ions, corresponding to the absorption spectra in Figure 3(a) which show a slight blue shift of the maximum absorption wavelength. The absorption intensity of the UV-Vis spectra progressively decreased with increasing concentrations of Hg(II). Such phenomena were also described previously [24,25]. The decrease in the absorption intensity of the SPR band with a blue shift could be due to the AgNPs being oxidized by Hg(II), resulting in the disintegration of the AgNPs into smaller particles and Hg(0). Deposition of Hg(0) on the surface of AgNPs also occurred, resulting in amalgam particles of mercury (Hg-Ag) [26]. Strong interaction between the Hg(II) and AgNPs is related to the lower redox potential of Ag(I)/Ag (0.799 V)

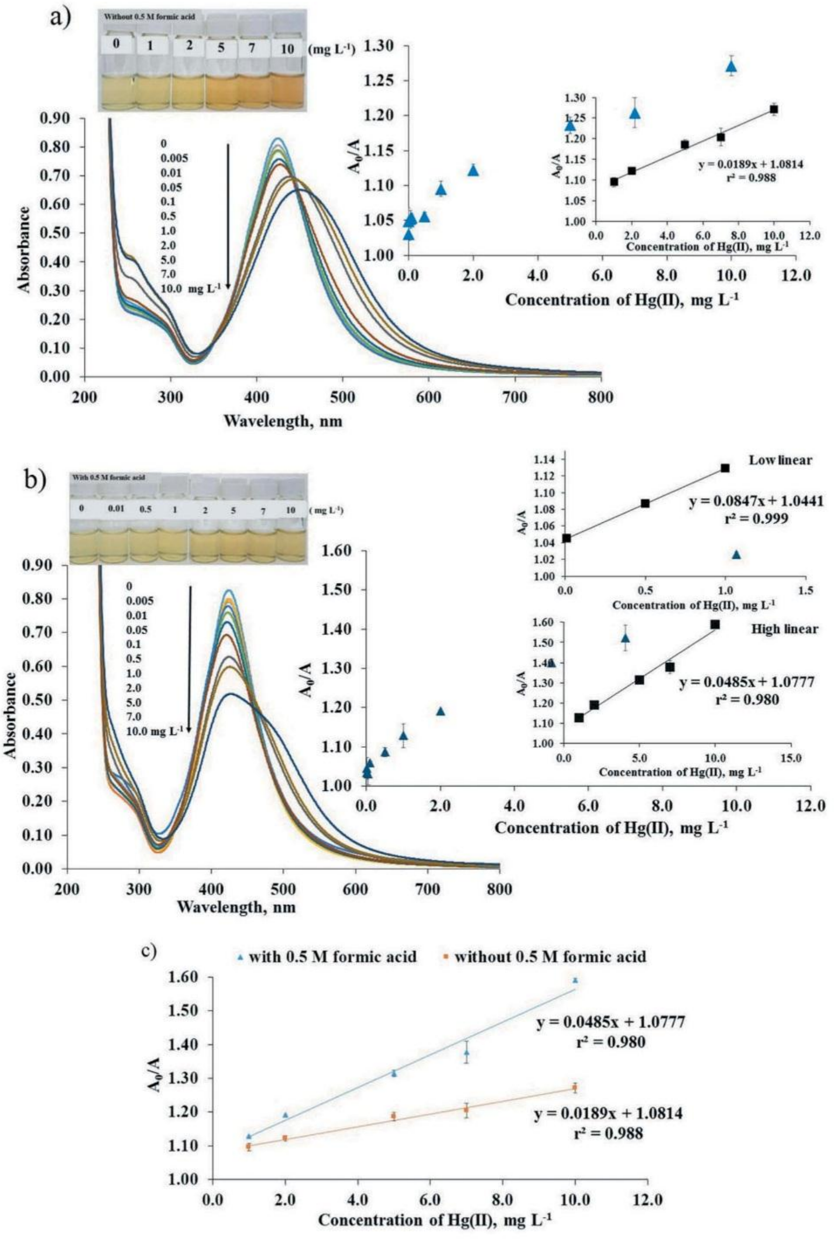

Figure 3. UV-Vis absorption spectra of the unmodified AgNPs solution upon addition of different concentrations of Hg(II) in the absence, inset: the calibration curve of the A_0/A versus the concentration of Hg(II) (a) and presence of 0.5 M formic acid, inset: the two calibration curves of the A_0/A versus the concentration of Hg(II) (high and low linearity) (b) and the calibration curve of A_0/A value versus the concentration of Hg(II) before and after the addition 0.5 M formic acid (c) Where A_0 and A represent the absorption intensity of AgNPs roughly occurred at 424–433 nm before and after reaction with different concentrations of Hg(II), respectively.

than that of Hg(II)/Hg (0.851 V) [27,28]. Our result indicated that the PVP-stabilized AgNPs can be used as a promising colorimetric sensor for the detection of Hg(II). To confirm the formation of amalgam, TEM coupled with EDS was carried out (Figure 2). The result showed that the amalgam particles gradually became larger upon adding Hg(II) (Figure 2(c)). The hydrodynamic size and zeta potential of AgNPs shown in Table S2 also confirmed these phenomena, in good agreement in the results obtained from TEM coupled with EDS.

To study the effect of catalyst on the reduction of mercury, organic formic acid was dropped into the AgNP solution. Having small molecules that can be easily adsorbed onto the surface of AgNPs, the acid has been shown to significantly enhance Hg(II) analytical sensitivity [29]. The efficiency for the reduction of Hg(II) however depended on its concentration. Hence, different concentrations of formic acid and pH values were investigated in this study. The concentration range of 0.0–2.0 M and pH range of 1.0–6.0 were optimized. The results presented in Figure S5 and Table S4 show that Hg(II) analytical sensitivity progressively increased with increasing concentration of formic acid in the Hg(II) concentration range of 0.01–2.0 mg L^{-1}. The optimal value for the concentration of formic acid was 0.5 M (with wide working pH range of >1, Table S3), indicating an increase in reduction efficiency and fast reduction from Hg(II) to Hg(0), and that molecules of the acid were easily adsorbed onto the surface of AgNPs enabling better reaction between Hg and AgNPs, which resulted in better amalgamation (Figure 2(d) and Table S2). However, higher concentrations of the acid (pH 1; at concentrations of 1.0–2.0 M) led to a decrease in Hg(II) analytical sensitivity.

Sensitivity of the sensor to detect Hg(II) was also investigated. Figure 3(a) shows the UV-Vis spectra upon adding various concentrations of Hg(II). When the concentration of Hg(II) was increased from 0.005 to 10 mg L^{-1}, the absorption intensity progressively decreased correlating well with the observed color change, which indicated gradually increasing aggregation of AgNPs (Figure 3(a), inset). The result showed a linear correlation ($r^2 = 0.988$) was observed between the different concentrations of Hg(II) and absorbance ratio (A_0/A), where A_0 is the absorbance of AgNPs at 424 nm for control and A is the absorbance of AgNPs at 424 nm after reaction with Hg(II). It was found that the calibration curve, with the measurements carried out in triplicates, was in the range of 1.0–10.0 mg L^{-1} ($r^2 = 0.988$) with the limit of detection (LOD) of 0.03 mg L^{-1}. Generally, when the concentration of Hg(II) is increased to higher than 2.0 mg L^{-1}, it is expected that the characteristic peak will redshift and broaden. However, blue shift in the absorption wavelength was observed in this experiment due to the use of 0.5 M formic acid as a catalytic organic compound.

Interestingly, addition of 0.5 M formic acid is necessary to enhance the reduction efficiency of mercury, indicating that the re-oxidation of Hg(II) to Hg(0) occurs easily under strong acidic conditions. Under optimized detection conditions, 500 µL (0.5 M) of formic acid was added to a mixture of AgNPs (50 µL) and Hg(II) at different concentrations before final adjustment to a volume of 5 mL was achieved using DI water. When the concentration of Hg(II) was increased from 0.005 to 10 mg L^{-1}, the absorbance value at 424 nm progressively decreased, correlating well with the observed colour change of the solution (brownish yellow becoming paler, Figure 3(b)), and the absorption spectra exhibited a blue shift with decreasing absorbance indicating gradually increasing amalgamation of the AgNPs (Figure 3(b)). The absorbance of the AgNPs progressively decreased and slightly shifted to the blue wavelength with increasing concentrations of Hg(II) ions (in the range 0.01–10 mg L^{-1}). The absorption peak of the detection in the presence of 0.5 M formic acid occurred at a different wavelength when the catalyst was absent. In addition, the analytical sensitivity of the method was improved in the presence of 0.5 M formic acid (Figure 3(b), inset). Significant sensitivity enhancement was observed with an addition of the catalyst compared to without formic acid. The calibration curve obtained from the presence of 0.5 M formic acid shows two linearity ranges: a low linearity range between 0.01 and 1.0 mg L^{-1}, and a high linearity range between 1.0 and 10 mg L^{-1}. The calibration curve of A_0/A value versus the concentration of Hg(II) shows significant enhancement in the Hg(II) analytical sensitivity upon addition of 0.5 M formic acid onto the AgNPs, leading to improvement of quantitative detection limit (Figure 3(c)).

The limit of detection (LOD) of the sensor in the presence of 0.5 M formic acid was reduced to 0.007 mg L^{-1} with a good precision (%RSD is less than 4.83) of the calibration curve observed in three different synthesis batches of AgNPs at various concentrations of Hg(II) (1.0, 5.0 and 7.0 mg L^{-1}) (Table S5).

3.3. *Selectivity of the Hg(II) sensor*

In order to evaluate the selectivity of the colorimetric sensor over commonly known interference species in aqueous samples, Hg(II) ions were examined in the presence of 10 cations and five anions, each with a concentration of 10.0 mg L^{-1}. As has already been established, upon adding Hg(II) ions at 0.1 mg L^{-1}, 1.0 mg L^{-1} and 10.0 mg L^{-1} into the unmodified AgNPs solution in the presence of 0.5 M formic acid (without the presence of any foreign ions), the colour solution visibly changed from brownish yellow to pale yellow, and the absorption intensity of the unmodified AgNPs roughly occurred at 424 nm. When the foreign ions were present in the solution containing 0.1 mg L^{-1} of Hg(II), it did not significantly alter the absorbance with less than ±5% change in the absorbance values (Figure 4(a)). To compare the selectivity of our developed PVP-stabilized AgNP sensor with that of our previous one where the nanoparticles were decorated with citrate, the same foreign ions were added into the solution containing the citrate-based AgNPs. It was found that the newly developed sensor fared much better in terms of selectivity compared to the citrate-based AgNPs (Figure 4(b) and Table S3), likely a result of better stabilization (by PVP) of the AgNPs.

In waste water, organic dyes constitute a large group of pollutants especially pollutants originated from the textiles industries. Their presence in waste water may interfere with the detection of mercuric ions. The sensitivity of our sensor was therefore evaluated in the presence of these pollutants. Positively charged methylene blue was first investigated. Figure 5(a,b) shows the evolution of UV-Vis spectra after adding different concentrations of methylene blue (MB). When the concentration of methylene blue was increased from 1.0 to 6.0 mg L^{-1}, the visible wavelength of the maximum absorption of the AgNPs and methylene blue roughly occurred at 424 nm and 665 nm, respectively. The absorbance value of methylene blue at 665 nm increased with increasing concentrations of methylene blue associated with colour change of the AgNPs solution from yellowish-brown to blue with constant 424 nm of AgNPs. The result

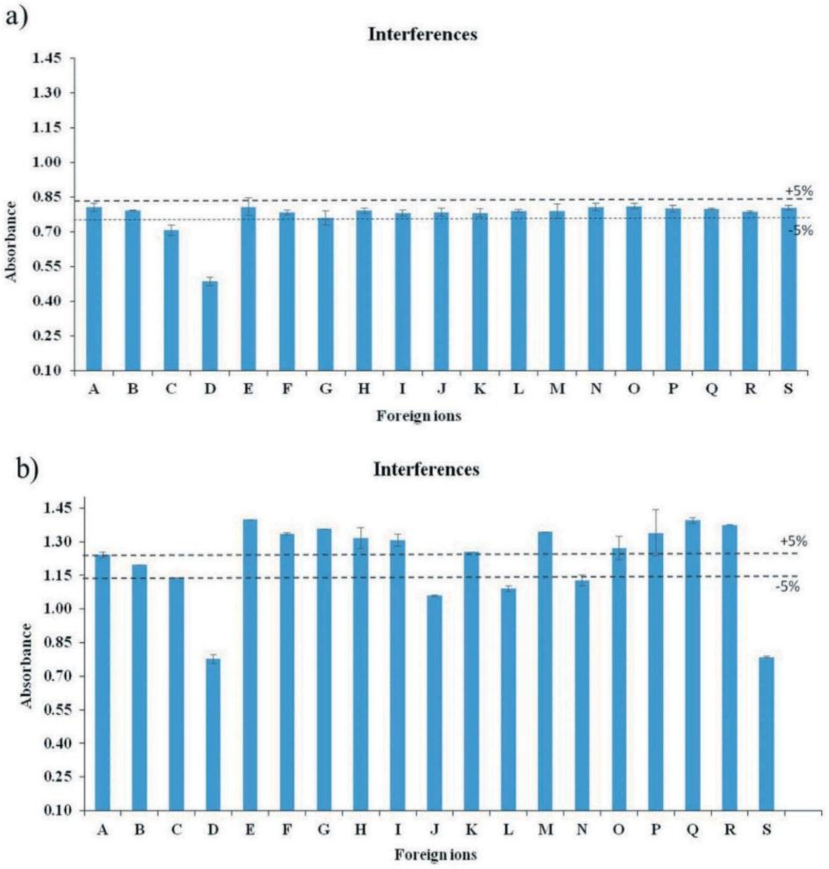

Figure 4. Comparison between the selectivity of the newly developed sensor (PVP-stabilized AgNPs) a) and that of our previous work (citrate-based AgNPs) b); AgNPs without Hg(II) (A), AgNPs + 0.1 mg L^{-1} Hg(II) (B), AgNPs + 1 mg L^{-1} Hg(II) (C), AgNPs + 10 mg L^{-1} Hg(II) (D), AgNPs + 0.1 mg L^{-1} Hg(II) + 10 mg L^{-1} anions (E-I; chloride, fluoride, nitrate, sulfate, sulfide, respectively) and cations (J-S; Ba(II), Ca(II), Cd(II), Cu(II), Fe(II), Mg(II), Mn(II), Pb(II), Zn(II), Ni(II), respectively).

shows that the developed approach provides high selectivity of Hg(II) detection even when there is a presence of methylene blue (Table S6). In addition, the studies with presence of neutral red and methyl orange as neutral and anionic dyes, respectively, were also evaluated. The experimental data shown in Figure S6a and b indicate that the visible wavelength of the maximum absorption of neutral red and methyl orange occurred where AgNPs absorption took place. As such, their presence show interference occurred with the detection of Hg(II) using our current developed method. The obtained results will serve as good information for our future work.

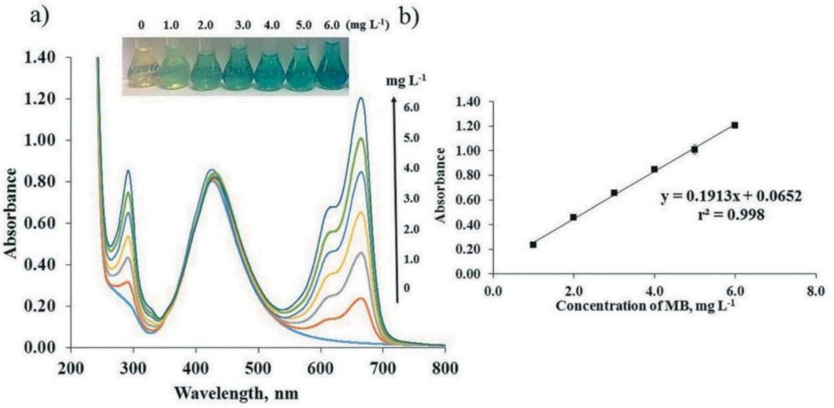

Figure 5. UV-Vis absorption spectra a) showing the effect of organic dye methylene blue on the maximum absorption wavelength of AgNPs, the absorbance versus the concentration of methylene blue (mg L^{-1}) b).

3.4. *Use of smartphone as a colorimetric analyzer*

Volume optimizing of the AgNPs was firstly performed in the well plate-based system in the presence of Hg(II) at concentrations of 0.10 and 1.0 mg L^{-1}. Based on RGB intensity calculated by imageJ, performance of the system using the smartphone as an analytical device was compared to that with a scanner. The volume of the AgNP solution was varied from 5.0 to 50 µL, and the optimal volume of AgNPs was found to be 30 µL (Figure S7), an excellent 50-fold reduction in volume of the sensor compared to the previous work [19] and a significant reduction in comparison to the UV-Vis spectrophotometric system based on the same PVP-stabilized AgNP sensor (Table S3). We found that the smartphone was more sensitive to colour change, sensing better grey intensity in the green channel, than the scanner, which perceived the detected solution as being too white than it actually was. Prior to this experiment, the effect of formic acid on the sensitivity of our colorimetric detection of Hg(II) was evaluated. The result of the colorimetric analysis (Figure S8 and Table S7) demonstrated that the addition of the formic acid was unnecessary.

3.5. *Analytical characteristics of the smartphone-based colorimetric analyzer*

Under the optimized detection condition, the sensor sensitivity was investigated. In three replicates, a series of standard Hg(II) (0.05–0.5 mg L^{-1}) was measured and the calibration curve shows a good linear correlation ($r^2 = 0.993$) with the linear range from 0.05 to 0.5 mg L^{-1} (four-point calibration curve) existing between the intensity differences (G_0-G) and the concentrations of Hg(II), where G_0 and G represent the green intensity of AgNPs before and after reaction with different concentrations of Hg(II), respectively (Figure S9). The calibration equation obtained was retained by the developed program (slope = 47.38, $r^2 = 0.993$) with a detection limit of 0.011 mg L^{-1}, indicating that the colorimetric sensor holds a promising potential for quantitative determination of Hg(II) ions in real sample application. High sample throughput for the analysis could be achieved through our developed method; approximately eight samples (n = 4, totalling 32 wells) could be measured in 15 min corresponding to about 32 samples (128 wells) per hour.

3.6. *Real samples application*

Potential of the developed approach for determination of Hg(II) in various samples was evaluated with a strong emphasis on its efficiency for environmental analysis. The samples included drinking water, mineral water, tap water, pond water, pond water in the presence of methylene blue as a matrix, synthetic human plasma and a standard reference material (SRM) 1641d with the certified value of mercury in water being 1.56 ± 0.02 mg kg^{-1}. The samples were spiked with Hg(II) at three different concentrations of 0.05 mg L^{-1}, 0.10 mg L^{-1} and 0.25 mg L^{-1}. The recoveries for the three spiked concentrations were found to be satisfactory, 93.6–104.0% for water samples, 97.6–112.0% for blood samples and 98.0% for SRM. The samples were measured for their Hg(II) content using our developed colorimetric analyzer with the results compared with those of the batch spectrophotometric method. Each measurement was repeated three times and the average values were presented in Table 1. The

Table 1. Determination of Hg(II) concentration in real aqueous samples application and Standard reference material (SRM) 1641d using the UV-Vis spectrophotometry system and smartphone as colorimetric sensor (n = 3).

	UV-Vis spectrophotometry system (n = 3)		Smartphone as colorimetric sensor (n = 3)	
Name	Hg(II) (mg L^{-1})	% recovery	Hg(II) (mg L^{-1})	%recovery
D	N.D.*		N.D.*	
D + 0.05 mg L^{-1}	0.05 ± 0.00	96.0	0.05 ± 0.01	96.0
D + 0.10 mg L^{-1}	0.10 ± 0.00	104.7	0.11 ± 0.02	108.0
D + 0.25 mg L^{-1}	0.27 ± 0.01	106.6	0.26 ± 0.01	102.4
M	N.D.*		N.D.*	
M + 0.05 mg L^{-1}	0.05 ± 0.02	108.1	0.05 ± 0.01	104.0
M + 0.10 mg L^{-1}	0.10 ± 0.02	97.7	0.09 ± 0.01	94.0
M + 0.25 mg L^{-1}	0.24 ± 0.01	95.1	0.23 ± 0.01	93.6
T	N.D.*		N.D.*	
T + 0.05 mg L^{-1}	0.06 ± 0.03	112.2	0.05 ± 0.01	96.0
T + 0.10 mg L^{-1}	0.12 ± 0.02	116.1	0.10 ± 0.01	102.0
T + 0.25 mg L^{-1}	0.23 ± 0.02	93.4	0.25 ± 0.01	98.4
P	N.D.*		N.D.*	
P + 0.05 mg L^{-1}	0.05 ± 0.00	106.3	0.05 ± 0.01	104.0
P + 0.10 mg L^{-1}	0.10 ± 0.00	96.8	0.10 ± 0.01	102.0
P + 0.25 mg L^{-1}	0.24 ± 0.02	95.0	0.26 ± 0.01	102.4
P added MB	N.D.*		N.D.*	
P added MB + 0.05 mg L^{-1}	0.05 ± 0.01	100.0	0.05 ± 0.01	100.0
P added MB + 0.10 mg L^{-1}	0.11 ± 0.03	106.2	0.09 ± 0.01	94.0
P added MB + 0.25 mg L^{-1}	0.23 ± 0.01	92.6	0.24 ± 0.01	97.6
SP	N.D.*		N.D.*	
SP + 0.05 mg L^{-1}	0.05 ± 0.02	103.8	0.05 ± 0.01	108.0
SP + 0.10 mg L^{-1}	0.09 ± 0.01	93.4	0.10 ± 0.01	100.0
SP + 0.25 mg L^{-1}	0.25 ± 0.06	101.2	0.25 ± 0.01	100.8
Standard Reference Material (1614d)	0.15 ± 0.01	98.1	1.53 ± 0.02	98.0

D = Drinking water, M = Mineral water, T = Tap water, P = Pond water, SP = Synthetic human plasma

ND* Defined as 'Not Determined'

SRM 1641d = Certified Hg(II) content in SRM was 1.56 ± 0.02 mg kg^{-1}

The t-test at the 95% confidence limit level, the experiment *t*-stat value is −0.83, which was less than the critical *t*-values of 1.67.

Table 2. Comparison of the sensing performance of reported unmodified AgNPs for Hg(II) detection.

Types of unmodified AgNPs	Characteristics of the sensor	Enhancer	Linear range/ LOD (mg L^{-1})	Analysis time (min)	Interferences	Real samples	Ref.
TPDT[a]-SiO_2-capped Ag NPs	Use of toxic reducing agent (hydrazine)[b]	–	1.0–15.0, (1.0)	2	Tolerance of Hg(II) to 10 cation species (5-fold)	NA.	[30]
L-Tyrosine-capped AgNPs	Use of biological compound (L-Tyrosine) as reducing agent[b]	–	0.0032–0.13, (0.0032)	5	NA.	Drinking and tap water	[31]
Bioreductant-capped AgNPs	Use of freshly prepared biological extract for stabilization[b]	–	1.0–20.06, (0.17)	instant measurement	Tolerance of Hg(II) to 11cation species (4-fold)	Tap and lake water	[32]
PVP-capped AgNPs	Use of strong reducing agent ($NaBH_4$)[b]	Lysine	0.0002–6.0, (0.0002)	1.5	Tolerance of Hg(II) to 14 cation species	Tap water	[33]
Citrate-capped AgNPs	Use of strong reducing agent ($NaBH_4$)[b]	AChE, ACTh	0.002–0.01, (0.00024)	5	Tolerance of Hg(II) to 11 cation species (1-fold)	Lake water, groundwater and sea water	[17]
Soap-root plant-capped AgNPs	Use of freshly prepared biological extract for stabilization[b]	–	2.01–20.06, (0.44)	5	Tolerance of Hg(II) to 13 cation species (1-fold)	Lake water	[16]
Citrate-capped AgNPs	Use of strong reducing agent ($NaBH_4$)[b] $^{(48\ h)}$	H_2O_2	No report/ (2.0 mg L^{-1})	–	Tolerance ratio of Hg(II) to cations (1-fold)	NA.	[34]
Yogurt-derived compounds-capped AgNPs	Use of biomolecule for stabilization[b]	–	No report/ (0.002)	–	Tolerance of Hg(II) to 8 cation species (1-fold)	Tap water and groundwater	[18]
Citrate-capped AgNPs	Use of Strong reducing agent ($NaBH_4$)	Cu(II)	0.5–7.0, (0.008)	instant measurement	Tolerance of Hg(II) to 7 cations species (3-fold)	Tap and drinking water	[19]
PVP [c]-capped AgNPs	Green and facile synthesis without using of strong reducing agent, only use PVP as reducing and stabilizing agent	Formic acid[d], no enhancer[e]	0.01–10 (0.007)[d] 0.05–0.50, (0.011)[e]	instant measurement	Tolerance ratio of Hg(II) to 10 cations and 5 anions (100-fold)	Water, blood and dye organic samples	This work

[a] N-[–3-(trimethoxysilyl) propyl] diethylenetriamine

[b] These synthesized sensors require a complicated and time-consuming process.

[c] Polyvinylpyrrolidone

[d] Based on UV-Vis spectrophotometry system

[e] Based on smartphone as a colorimetric analyzer

NA. Defined as 'Not Analysis'

expected values were obtained and there was no significant difference between the two methods; at 95% confidence, the *t*-stat value of −0.83 was lower than the critical *t*-value of 1.67, confirming the potential use of the smartphone-based colorimetric analyzer in selective Hg(II) determination in the real environmental analysis.

4. Conclusion

The proposed method using smartphone as colorimetric sensor based on unmodified AgNPs stabilized by PVP has been successfully applied for determination of Hg(II) in various aqueous samples including water, blood and dye organic samples. The present study reports a simple and green approach for the synthesis of unmodified AgNPs stabilized by PVP using a hydrothermal method. The unmodified AgNPs were successfully characterized by UV-Vis absorption spectra, TEM coupled with EDS, DLS and zeta potential analyses. Under the optimal condition, the developed colorimetric sensor shows magnificent sensitivity and greater selectivity towards Hg(II) over potential ions and a colour dye matrix. Moreover, our sensor could be used in a wide pH range due to strong stabilizing effect of PVP in the AgNPs making the sensor resistant to the influence of ionic suppression which in turn would reduce failure upon their application on real samples. The results have demonstrated that our proposed colorimetric sensor provides a simple, rapid (with high sample throughput of 128 h^{-1}), sensitive, selective and cost-effective Hg(II) determination. Its successful application in real samples has also been established. These advantages allow it to be used by relatively unskilled end users for effective analysis of Hg(II) at resource-limited setting. The comparison between our developed method and other techniques used in Hg(II) detection as detailed in Table 2 and Table S3 clearly demonstrates the advantages of our sensor. In comparison to other existing sensors, ours, synthesized by a simple hydrothermal method, provides a fast and reliable detection of mercuric ions using only a small amount of AgNP solution for each measurement without any enhancer needed. The AgNP solution was also found to be stable for at least four months. In addition, by not using any toxic reducing agents like sodium borohydride ($NaBH_4$) or adding weak stabilizing agents like trisodium citrate ($Na_3C_6H_5O_7$), the synthesis of our PVP-based AgNPs poses no risk arising from exposure to toxic and hazardous chemicals, providing a greener and safer alternative in the determination of mercuric ions in aqueous samples.

Acknowledgments

This work is supported by research grants from the Center of Excellence for Innovation in Chemistry (PERCH-CIC), Office of the Higher Education Commission (OHEC), Ministry of Education. The research scholarships and instrumental facilities of the Department of Chemistry, Faculty of Science, Ubon Ratchathani University are also gratefully acknowledged. H.L. Lee would like to thank Universiti Sains Malaysia (USM) Research University Individual Grant (1001/PKimia/8011086) as part of the funding in this project. The authors would like to thank Central Science laboratory, Chiang Mai University, for technical expertise in SEM-EDS analysis and Dr. Sukhum Ruangchai for proof of reading.

Disclosure statement

No potential conflict of interest was reported by the authors.

Funding

This work is supported by research grants from the Center of Excellence for Innovation in Chemistry (PERCH-CIC), Office of the Higher Education Commission (OHEC), Ministry of Education. And H.L. Lee would like to thank Universiti Sains Malaysia (USM) Research University Individual Grant (1001/PKimia/8011086) as part of the funding in this project; Office of the Higher Education Commission.

ORCID

Hooi Ling Lee http://orcid.org/0000-0002-9637-0617
Purim Jarujamrus http://orcid.org/0000-0002-0666-150X

References

[1] B. Cui, Q. Zhang, K. Zhang, X. Liu and H. Zhang, Environ. Pollut. **159**, 1297 (2011). doi:10.1016/j.envpol.2011.01.024.

[2] J. Du, L. Jiang, Q. Shao, X. Liu, R.S. Marks, J. Ma and X. Chen, Small **9**, 1467 (2013). doi:10.1002/smll.201200811.

[3] T.W. Clarkson, L. Magos and G.J. Myers, N. Engl. J. Med. **349**, 1731 (2003). doi:10.1056/NEJMra022471.

[4] W.R. Hatch and W.L. Ott, Anal. Chem. **40**, 2085 (1968). doi:10.1021/ac50158a025.

[5] J.W. Olesik, Anal. Chem. **63**, 12A (1991). doi:10.1021/ac00001a001.

[6] M. Sabela, S. Balme, M. Bechelany, J.M. Janot and K. Bisetty, Adv. Eng. Mater. **19**, 1700270 (2017). doi:10.1002/adem.201700270.

[7] A. Apilux, W. Siangproh, N. Praphairaksit and O. Chailapakul, Talanta **97**, 388 (2012). doi:10.1016/j.talanta.2012.04.050.

[8] X. Liu, X. Cheng, T. Bing, C. Fang and D. Shangguan, Anal. Sci. **26**, 1169 (2010). doi:10.2116/analsci.26.1169.

[9] Y. Wang, F. Yang and X. Yang, ACS Appl. Mater. Interfaces **2**, 339 (2010). doi:10.1021/am9007243.

[10] F. Chai, C. Wang, T. Wang, Z. Ma and Z. Su, Nanotechnology **21**, 025501 (2009). doi:10.1088/0957-4484/21/2/025501.

[11] P.C. Chen, P. Roy, L.Y. Chen, R. Ravindranath and H.T. Chang, Part. Part. Syst. Char. **3**, 917 (2014). doi:10.1002/ppsc.201400043.

[12] S. Botasini, G. Heijo and E. Méndez, Anal. Chim. Acta **800**, 1 (2013). doi:10.1016/j.aca.2013.07.067.

[13] K.Z. Kamali, A. Pandikumar, S. Jayabal, R. Ramaraj, H.N. Lim, B.H. Ong and N.M. Huang, Microchim. Acta. **183**, 369 (2016). doi:10.1007/s00604-015-1658-6.

[14] P. Rameshkumar, N.M. Huang and L.S. Wei, Microchim. Acta. **183**, 597 (2016). doi:10.1007/s00604-015-1680-8.

[15] A. Mehdinia, S. Basiri and A. Jabbari, Int. J. Environ. Sci. Technol. **13**, 2663 (2016). doi:10.1007/s13762-016-1093-1.

[16] K. Farhadi, M. Forough, R. Molaei, S. Hajizadeh and A. Rafipour, Sens. Actuators. B. Chem. **161**, 880 (2012). doi:10.1016/j.snb.2011.11.052.

[17] S. Gao, X. Jia and Y. Chen, J. Nanoparticle. Res. **15**, 1385 (2013). doi:10.1007/s11051-012-1385-4.

[18] D.N. Kumar, A. Rajeshwari, S.A. Alex, N. Chandrasekaran and A. Mukherjee, New. J. Chem. **39**, 1172 (2015). doi:10.1039/C4NJ01722F.

[19] P. Jarujamrus, M. Amatatongchai, A. Thima, T. Khongrangdee and C. Mongkontong, Spectrochim Acta A **142**, 86 (2015). doi:10.1016/j.saa.2015.01.084.

[20] S.S. Muniandy, S. Sasidharan and H.L. Lee, *Sains Malaysiana* (**48**, 4 (2019).Penerbit UKM, 2019).

[21] R. Meelapsom, P. Jarujamrus, M. Amatatongchai, S. Chairam, C. Kulsing and W. Shen, Talanta **155**, 193 (2016). doi:10.1016/j.talanta.2016.04.037.

[22] P. Jarujamrus, R. Meelapsom, S. Pencharee, A. Obma, M. Amatatongchai, N. Ditcharoen and S. Tamuang, Anal. Sci. **34**, 75 (2018). doi:10.2116/analsci.34.75.

[23] Android developer. https://play.google.com/store/.apps/details?id=appinventor.ai somkid p. CAnal.

[24] L. Katsikas, M. Gutiérrez and A. Henglein, J. Phys. Chem. **100**, 11203 (1996). doi:10.1021/jp960357i.

[25] S. Bothra, J.N. Solanki and S.K. Sahoo, Sens. Actuators. B. Chem. **188**, 937 (2013). doi:10.1016/j.snb.2013.07.111.

[26] Y. Fan, Z. Liu and J. Zhan, Nanoscale. Res. Lett. **4**, 1230 (2009). doi:10.1007/s11671-009-9387-6.

[27] A. Henglein and C. Brancewicz, Chem. Mater. **9**, 2164 (1997). doi:10.1021/cm970258x.

[28] T. Morris, H. Copeland, E. McLinden, S. Wilson and G. Szulczewski, Langmuir **18**, 7261 (2002). doi:10.1021/la020229n.

[29] H. Matusiewicz and E. Stanisz, J. Braz. Chem. Soc. **23**, 247 (2012). doi:10.1590/S0103-50532012000200009.

[30] P. Rameshkumar, P. Viswanathan and R. Ramaraj, Sens. Actuators. B. Chem. **202**, 1070 (2014). doi:10.1016/j.snb.2014.06.069.

[31] M. Annadhasan, T. Muthukumarasamyvel, V.R. Sankar Babu and N. Rajendiran, ACS Sustain. Chem. Eng. **2**, 887 (2014). doi:10.1021/sc400500z.

[32] M.L. Firdaus, I. Fitriani, S. Wyantuti, Y.W. Hartati, R. Khaydarov, J.A. McAlister and T. Gamo, Anal. Sci. **33**, 831 (2017). doi:10.2116/analsci.33.831.

[33] L. Li, L. Gui and W. Li, Microchim. Acta. **182**, 1977 (2015). doi:10.1007/s00604-015-1536-2.

[34] G.L. Wang, X.Y. Zhu, H.J. Jiao, Y.M. Dong and Z.J. Li, Biosens. Bioelectron. **31**, 337 (2012). doi:10.1016/j.bios.2011.10.041.

Talanta 183 (2018) 228–236

Contents lists available at ScienceDirect

Talanta

journal homepage: www.elsevier.com/locate/talanta

Complexometric and argentometric titrations using thread-based analytical devices

Purim Jarujamrus[a,b,*], Nutthaporn Malahom[a,b], Sodsai Puchum[a,b], Rattapol Meelapsom[a,b], Maliwan Amatatongchai[a,b], Atitaya Siripinyanond[c], Sanoe Chairam[a,b], Chadin Kulsing[d,e]

[a] *Department of Chemistry and Center of Excellence for Innovation in Chemistry, Faculty of Science, Ubon Ratchathani University, Ubon Ratchathani 34190, Thailand*
[b] *Nanomaterials Science, Sensors & Catalysis for Problem-Based Projects, Faculty of Science, Ubon Ratchathani University, Warin Chamrap, Ubon Ratchathani 34190, Thailand*
[c] *Department of Chemistry and Center of Excellence for Innovation in Chemistry, Faculty of Science, Mahidol University, Rama VI Road, Bangkok 10400, Thailand*
[d] *Chromatography and Separation Research Unit, Department of Chemistry, Faculty of Science, Chulalongkorn University, 254 Phayathai Road, Patumwan, Bangkok 10330, Thailand*
[e] *Center of Molecular Sensory Science, Faculty of Science, Chulalongkorn University, Bangkok 10330, Thailand*

ARTICLE INFO

Keywords:
Magnesium (Mg(II))
Chloride
Complexometric titration
Argentometric titration
Microfluidic thread-based analytical device (μTAD)

ABSTRACT

This work describes analytical approaches based on simple complexometric and argentometric titrations leading to the color change of a novel microfluidic thread-based analytical device (μTAD). The device was fabricated from a cotton thread (15 cm) treated with indicator solution, providing an easy-to-use platform for rapid measurement of analyte concentration in aqueous solution. The thread was immobilized onto a support, being a polypropylene sheet or box platform, to facilitate loading of liquid samples. Interaction between the deposited reagents and analytes in the samples then occurred within a few minutes. This resulted in zones of color change with different lengths along the thread depending on the analyte concentration. The interaction zones can be analyzed by human eyes based on comparison of the zone lengths with the printed scales which are correlated with the analyte concentrations. Complexometric titration using μTADs was initially investigated for Mg(II) determination in water and rubber latex samples. These devices consisted of two threads which were pretreated with Eriochrome Black T (EBT) and then treated with ethylenediaminetetraacetic acid (EDTA) in N-cyclohexyl-3-aminopropanesulfonic acid (CAPS) buffer at pH 10. Both threads were tied together with a central knot before being attached to the box platform prior to the analysis. Load of sample solution (6 μL) resulted in the length of red-violet color product on the threads being proportional to the concentration of Mg(II) in waters and rubber latex samples with the working concentration range of 25–1000 mg L^{-1}. In addition, μTAD with a supporting polypropylene sheet consisting of several threads treated with $AgNO_3$ and K_2CrO_4 indicators was applied for argentometric titration of chloride ion in water and food seasoning samples. After sample loading (3 μL), the initially red-brown threads turned into white corresponding to formation of AgCl(s) on the threads with a working concentration range of 75–600 mg L^{-1}. Greater selectivity towards Mg(II) and chloride compared with potential interference ions was also observed. All the developed μTADs were applied for analysis of real samples which showed results being in agreement with those obtained by classical titrations.

1. Introduction

Colorimetric method is a common technique monitoring the color change of solutions which can be related to concentration of analytes [1]. The analysis conventionally employs large scale instrumental approaches in a laboratory which consumes resources and time to transfer samples in field to the instruments. This leads to development of portable platform of analytical devices reducing generation of waste, consumption of time and use of resources. Recently, novel thread-based analytical devices (μTADs) have been developed since this platform is capable of transporting aqueous and non-aqueous fluids via capillary action and possesses desirable properties for manufacturing fluid transport pathways inside microfluidic devices [2]. The flow within a strand of thread is effectively confined to one dimension, since the aspect ratio (length: diameter) of the thread is high. The lack of lateral transport, which occurs with alternative approach such as 2D paper-

---

* Corresponding author at: Department of Chemistry and Center of Excellence for Innovation in Chemistry, Faculty of Science, Ubon Ratchathani University, Ubon Ratchathani 34190, Thailand.
E-mail address: purim.j@ubu.ac.th (P. Jarujamrus).

https://doi.org/10.1016/j.talanta.2018.02.058
Received 24 November 2017; Received in revised form 5 February 2018; Accepted 12 February 2018

based assays, reduces the sample volume uptake and provides the ability to store reagents in active form within the fiber network [3]. Moreover, thread structure enables fabrication of 3D thread-based microfluidic devices which encompass several microfluidic channels and can be manipulated by use of simple processes such as sewing, knitting and weaving. These techniques could, in principle, be exploited for mass production of μTADs [3]. Thread can also be sewn onto various supporting materials to form fluid transport channels without the need for the patterned hydrophobic barriers, e.g. as that required in paper-based microfluidic approach [4]. In addition, μTADs are small scale, portable, low-cost and easy-to-use with the potential to be applied in many disciplines such as human health diagnostics, environmental monitoring and food safety analysis [2–5]. Development and application of μTADs are thus considered to be a key target.Li et al. [2] and Reches et al. [3] demonstrated 3D semi-quantitative μTADs platforms for diagnostic assays applying different characteristics of the thread including “woven array”, “branching” and “sewn array” designs. They also performed colorimetric assays on these devices for analysis of protein, nitrite and ketone in artificial urine samples where the thread colors can be indicative of concentration. In 2011, Ballerini et al. [6] reported the use of thread for the rapid blood group analysis providing separation of large particles of agglutinated red blood cells (RBCs) from plasma within narrow capillary channels inside the thread. The blood groups of A, B, O and Rh can be successfully determined using only 2 μL of whole blood from a pricked fingertip within 1 min sampling time without sample pre-treatment. In 2012, the lateral-flow immunochromatographic assays for point-of-care screening of infectious diseases, drugs abuse, and pregnancy were demonstrated by Zhou et al. [7]. The possibility of multiplexing was further demonstrated using three knotted threads coated with antibodies against C-reactive protein (CRP), osteopontin (OPN), and leptin (LEP). Since colorimetric method is a common technique used for analysis without requirement of complex instrumental design and implementation, the approach contributes to the analytical decentralization of application [8].

In 2016, Gonzalez et al. [9] reported a thread-based μTAD for glucose detection based on a colorimetric assay. Design of this platform is customizable and mass production could be performed within only 2–3 h. Other design includes a simple and low cost μTAD to assess the activity of acetylcholinesterase (AChE) [10] with the multiplex design enabling triplicate simple data collection. μTADs have great potential to be employed in a myriad of tests including point-of-care (POC) diagnostic devices for resource-challenged settings. In 2017, simple cotton thread on a paper device with mobile phone detection has been proposed for determination of phenolic content (antioxidant) in green tea samples [11]. Recently, Nilghaz et al. [5] described a simple and semi-quantitative method by measuring the length of color change on indicator treated threads using distance measurement by a ruler. The length of the color zones correlated with the analyte concentration in the samples. This approach can be applied to perform simultaneous assays quantifying the concentrations of different biomarkers present in the samples without use of electronic devices.

In this work, simple and low-cost μTADs were firstly developed for two different analytical tasks: 1) determination of Mg(II) content in waters and rubber latex (RL) with portable μTAD based on titration between Mg(II) and EDTA without use of any masking agent and 2) determination of chloride ion in water (tap and canal waters) and food products (fish sauce and seasoning powder) with μTADs based on argentometric titration (Mohr's approach). The devices were fabricated from untreated cotton threads (15 cm) treated with indicator solution. The threads modified with reagents were immobilized onto a support, being a foam box or polypropylene sheet for tasks 1) and 2), respectively. The resulting length of the color change on the μTADs were correlated with the analyte concentrations and analyzed by human eyes. The analysis mechanism, optimization of reagents, analytical characteristics, selectivity towards Mg(II) and chloride compared with potential interference ions and method validation were examined and discussed.

2. Experimental section

2.1. Chemicals and materials

All chemicals used in this study were analytical grade. All solutions were prepared in deionized water with 18 MΩ resistance (obtained from a Millipore Milli-Q purification system, Bedford, MA, USA). Different types of commercial threads (mm ± S.D., n = 10) including cotton 80% (0.30 ± 0.05), cotton 90% (0.29 ± 0.01), cotton 100% (0.30 ± 0.02) and polyester 100% (0.18 ± 0.01) were obtained from a fabric store in Ubon Ratchathani and used as substrate for fabrication of μTAD. The thread was immobilized onto a support, being a foam box or polypropylene sheet platform, to be ready for loading of liquid samples were obtained from a stationery store in Ubon Ratchathani which were used as holders. All glasswares and plastic bottles were soaked in nitric acid (dilute 10% with deionized water) before use.

For complexometric analysis, magnesium sulphate heptahydrate ($MgSO_4{\cdot}7H_2O$) and CAPS ($C_9H_{19}NO_3S$) buffer solution were purchased from Panreac. Calcium carbonate ($CaCO_3$), ammonium chloride (NH_4Cl) and ammonium hydroxide (NH_4OH) were purchased from Fluka. Ethylenediaminetetraacetic acid disodium salt dihydrate ($C_{10}H_{14}N_2Na_2O_8{\cdot}2H_2O$; EDTA, Fisher Chemical), eriochrome black T ($C_{20}H_{12}N_3O_7SNa$; EBT, LABCONCO), ethanol 99%, v/v (C_2H_5OH, Sigma-Aldrich) were used as reagents in the conventional complexometric titration and our developed μTAD for Mg(II) identification in waters and RL samples. The following chemicals were used as received: calcium nitrate ($Ca(NO_3)_2$), potassium sulphate (K_2SO_4), sodium chloride (NaCl), copper(II) sulphate pentahydrate ($CuSO_4{\cdot}5H_2O$) manganese sulphate monohydrate ($MnSO_4{\cdot}H_2O$), sodium sulphate ($Na_2SO_4{\cdot}7H_2O$), and sodium dihydrogen phosphate dihydrate ($NaH_2PO_4{\cdot}2H_2O$) which were obtained from Carlo Erba. Iron(II) sulphate heptahydrate ($FeSO_4{\cdot}7H_2O$, Unilab), zinc sulphate heptahydrate ($ZnSO_4{\cdot}7H_2O$, Fluka), and sodium hydroxide (NaOH, Merck) were used in interference study.

For argentometric method, silver nitrate ($AgNO_3$) was purchased from Fisher Scientific UK. Potassium chromate (K_2CrO_4) and sodium chloride (NaCl) were purchased from Carlo Erba. All chemicals were used as reagents in the conventional argentometric titration and our developed μTAD for determination of chloride in water samples and food samples. The following chemicals were used as received: potassium fluoride (KF), sodium nitrate ($NaNO_3$), sodium dihydrogen phosphate dihydrate ($NaH_2PO_4{\cdot}2H_2O$), potassium bromide (KBr), potassium iodide (KI), mercury(II) sulphate ($HgSO_4$), copper(II) sulphate pentahydrate ($CuSO_4{\cdot}5H_2O$), nickel(II) sulphate ($NiSO_4$), cadmium nitrate tetrahydrate ($Cd(NO_3)_2{\cdot}4H_2O$), sodium sulphate anhydrous (Na_2SO_4), manganese sulphate monohydrate ($MnSO_4{\cdot}H_2O$), potassium sulphate (K_2SO_4) and calcium nitrate ($Ca(NO_3)_2$) were purchased from Carlo Erba. Lead(II) nitrate ($Pb(NO_3)_2$) and zinc sulphate ($ZnSO_4$) were purchased from Fluka. Sodium hydrogensulphide ($NaHS.xH_2O$, ACROS ORGANICS), iron(II) sulphate heptahydrate ($FeSO_4{\cdot}7H_2O$, Unilab), barium nitrate (($Ba(NO_3)_2$), BAKER ANALYZED), and magnesium sulphate heptahydrate ($MgSO_4{\cdot}7H_2O$, Panreac) were used in interferences study.

2.2. Instruments

Polarized light microscope (Model Axio Scope A1, Zeiss,) was used for investigation of the morphology of μTAD. Camera of smartphone coupled with 20 × microscope lens (CHULA SMARTLENS, LENS AND SMARTCLASSROOM CO., LTD) was used to collect the images of lengths of color distance for complexometric reaction (for low range concentration of Mg(II) (25–100 mg L^{-1}) and argentometric reaction on the μTADs. The images of lengths of the color change for complexometric reaction for high range concentration of Mg(II) (250–1000 mg L^{-1}) were taken by Olympus OMD EM10 mark II digital camera with Olympus M. Zuiko Digital ED 45 mm f1.8 lens. The length

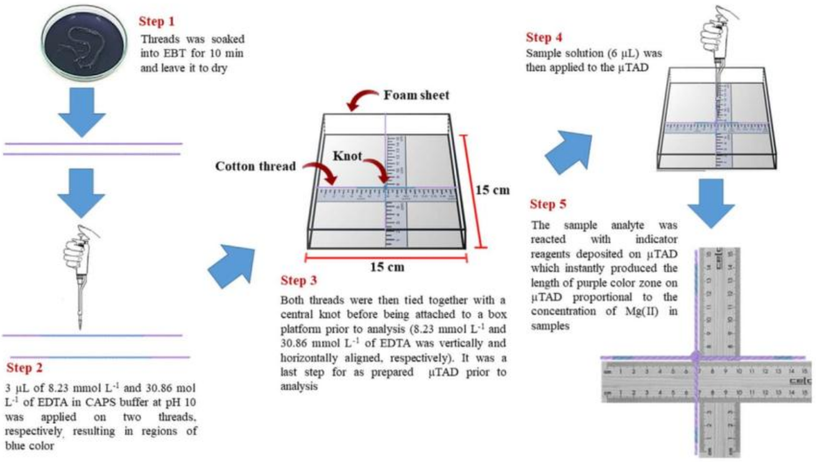

Step 1
Threads was soaked into EBT for 10 min and leave it to dry

Step 2
3 µL of 8.23 mmol L-1 and 30.86 mol L-1 of EDTA in CAPS buffer at pH 10 was applied on two threads, respectively, resulting in regions of blue color

Step 3
Both threads were then tied together with a central knot before being attached to a box platform prior to analysis (8.23 mmol L-1 and 30.86 mmol L-1 of EDTA was vertically and horizontally aligned, respectively). It was a last step for as prepared µTAD prior to analysis

Step 4
Sample solution (6 µL) was then applied to the µTAD

Step 5
The sample analyte was reacted with indicator reagents deposited on µTAD which instantly produced the length of purple color zone on µTAD proportional to the concentration of Mg(II) in samples

Fig. 1. Fabrication of µTAD for complexometric titration.

of color change for complexometric and argentometric titrations on µTAD can be measured with stainless steel metal ruler with 15 cm/0.15. For comparison purposes (method validation), flame atomic absorption spectroscopy; FAAS (PinAAcle 900T; Perkin Elmer, US) equipped with hollow cathode lamps (HCL) of Mg, Ca were exploited to determine Mg (II) and Ca(II) in RL and water samples. Moreover, an ion chromatography; IC (Model DIONEX INTEGRION HPIC, Thermo Scientific) was also used for measurement of chloride ions in water samples and fish sauce samples. The operating conditions of FAAS and IC were demonstrated in Table S1.

2.3. Preparation of reagents

2.3.1. Conventional method

Complexometric titration method without use of masking agent was adapted from ISO 17403: 2014(E) [12] which was applied as a conventional benchmark method based on complexometric titration between Mg(II) and EDTA. Briefly, $CaCO_3$ (0.500 g) was dissolved in 1 L of water (5×10^{-3} mol L^{-1}) as a primary standard. EDTA (1.86 g) was dissolved in 1 L of water (5×10^{-3} mol L^{-1}). The equivalent mole ratio between Mg(II) standard and the EDTA solution is 1:1. pH of the system was adjusted to be 10 by using 0.06 mol L^{-1} NH_4Cl/NH_4OH buffer solution was prepared by dissolving 67.5 g of NH_4Cl in 250 mL of DI water. After that, 25%, w/w NH_4OH (570 mL) was added into NH_4Cl solution and further diluted to 1 L with DI water. An indicator was prepared by dissolving EBT (0.1 g) in 100 mL of 75%, v/v ethanol in water (2.16×10^{-4} mol L^{-1}).

Argentometric titration was performed as a conventional method which was based on titration between chloride ion and $AgNO_3$ using K_2CrO_4 as an indicator solution [13]. Shortly, stock solution of 0.01 mol L^{-1} NaCl (0.1461 g) was dissolved in water of 250 mL. Stock solution of 0.01 M $AgNO_3$ (0.4247 g) was dissolved in water of 250 mL and store the solution in a brown bottle. Indicator solution was prepared by dissolving K_2CrO_4 (5.0 g) in 100 mL of water (5%w/v).

2.3.2. Proposed µTAD based on measurement of the length of color zone

µTAD was developed based on the complexometric titration. The optimized procedure was as follows; an indicator was prepared by dissolving EBT (0.1 g) in 100 mL of 75%, v/v ethanol (2.16×10^{-4} mol L^{-1}) used as pretreated reagents for threads. 0.01 mol L^{-1} of CAPS buffer solution was prepared by dissolving CAPS (2.2100 g) in a mixed solution between 500 mL of DI water and 100 mL of methanol. After that, the solution was adjusted to pH 10 by using 1 mol L^{-1} NaOH and the total volume was made up to 1000 mL with DI water. Each EDTA concentration were prepared by dissolving solid EDTA in 25 mL of CAPS buffer at pH 10 (adjusted by 1 mol L^{-1} NaOH before making up the volume to 25 mL). The solution was further deposited on µTAD, as see also Table S2. Finally, a stock solution of Mg(II) (1000 mg L^{-1}) was prepared by dissolving $MgSO_4 \cdot 7H_2O$ (2.535 g) in 250 mL of DI water. The solution was further diluted to 25, 50, 100, 250, 300, 500, 750 and 1000 mg L^{-1} in 100 mL of DI water. Moreover, argentometric titration based µTAD was developed. The optimized procedure was as follows. A stock solution of $AgNO_3$ (0.1 mol L^{-1}) was prepared by dissolving $AgNO_3$ (1.6987 g) in 100 mL of DI water and further diluted to 0.010, 0.015, 0.025, 0.035 and 0.045 mol L^{-1} with water. Secondly, a stock solution of 10% w/v of K_2CrO_4 (an indicator) was prepared by dissolving K_2CrO_4 (5.0000 g) and made up volume to 50 mL with DI water. The solution was further diluted to 2.5%, 5.0%, 6.5% and 8%w/v in 25 mL water. Finally, a stock solution of chloride ion (1000 mg L^{-1}) was prepared by dissolving NaCl (0.4121 g) in 250 mL of DI water. The solution was diluted to 50, 75, 100, 200, 300, 400, 500, 600, 700, 800, 900 and 1000 mg L^{-1} in 100 mL of DI water. Threads were modified with $AgNO_3$ and K_2CrO_4, respectively.

2.4. Preparation of samples

For complexometric analysis, RL samples were collected in Ubon Ratchathani province. Before analysis with the developed µTAD, a simple sample preparation of RL was developed by modification of ISO 17403:2014, preparation method for concentrated rubber latex (CRL) [12]. RL samples were transferred into microcentrifuge tubes and digested in 25% v/v acetic acid. RL serum was obtained in acidic condition at pH 4–5. The serum (100 µL) was adjusted to pH 7 in a micro centrifuge tube prior to analysis. CAPS buffer solution (500 µL) and 1 mol L^{-1} NaOH (50 µL) were then added, respectively, into the tube as demonstrated in Fig. S1. The developed sample preparation was also validated (Table S3). Before analysis of conventional complexometric titration of RL, the sample preparation step was slightly modified from our developed µTAD. RL (10.0 g) was transferred into a beaker followed by addition of 25% v/v acetic acid (1.0 mL). After separation between

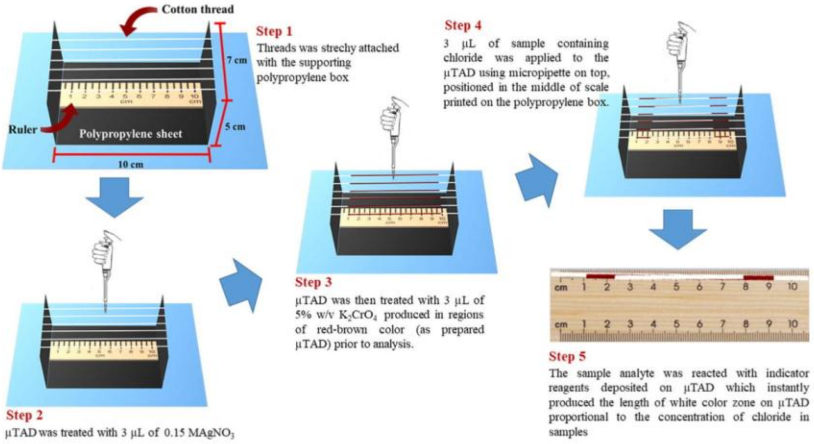

Step 1
Threads was strechy attached with the supporting polypropylene box

Step 2
µTAD was treated with 3 µL of 0.15 MAgNO$_3$

Step 3
µTAD was then treated with 3 µL of 5% w/v K$_2$CrO$_4$ produced in regions of red-brown color (as prepared µTAD) prior to analysis.

Step 4
3 µL of sample containing chloride was applied to the µTAD using micropipette on top, positioned in the middle of scale printed on the polypropylene box.

Step 5
The sample analyte was reacted with indicator reagents deposited on µTAD which instantly produced the length of white color zone on µTAD proportional to the concentration of chloride in samples

Fig. 2. Fabrication of µTAD for argentometric titration.

serum and sludge occurred, clear serum of RL (2.4 mL) was obtained at pH 4–5. Moreover, the sample preparation for FAAS analysis of RL was performed as our previous reported [14] by transferring RL (0.25 g) to a test tube followed by addition of concentrated HNO$_3$ (65% v/v) (4.0 mL). The solution was heated in an oil bath at 165 °C resulting in a transparent solution which was then cooled and diluted with HNO$_3$ (2%, v/v) prior to the FAAS analysis.

The tap sample was collected without pretreatment, and drinking mineral water was obtained from local super market in Ubon Ratchathani, Warin Chamrap, Thailand. In addition, FAAS analysis, all water samples were diluted with HNO$_3$ (2%, v/v) prior to the FAAS analysis.

For argentometric method, all samples were collected at Ubon Ratchathani University. The contaminants in the samples of canal water, tap water, fish sauce (diluted 5000 fold before analysis) and seasoning powder (dissolved in DI water and diluted 2000 fold) were removed by using filter paper no. 4 followed by 0.45 µm PVDF syringe filter membrane. This was performed for conventional methods (titration and IC) and the developed µTAD.

2.5. Fabrication and operating procedures of complexometric and argentometric titration on µTAD

µTADs in all analyses were prepared by using untreated 100% cotton threads with the diameter of 0.30 ± 0.02 mm as substrate materials which can be wicked by the sample solution according to capillary action without use of external pumping devices. The threads were cut by scissors to a length of 15 cm. Complexometric analysis employed a foam sheet holder as the support which was fabricated by cutting a foam sheet with the dimension of 15 cm × 15 cm. A millimeter scale ruler was also made on the foam sheet. Step 1: threads (15 cm) were initially soaked into EBT (2.16×10^{-4} mol L^{-1}) for 10 min and then dried at room temperature (red wine color was demonstrated a whole threads). Step 2: two threads were further modified by addition of 3 µL of EDTA with different concentrations (one treated with 8.23 mmol L^{-1} of EDTA vertically aligned for detection of low range of Mg(II) concentration and the other treated with 30.86 mmol L^{-1} of EDTA horizontally aligned for the high concentration range) in CAPS solution at pH 10, which changed the thread color from red wine to blue (within 1 min) which was presented ~5 cm on 15 cm of red wine threads). Step 3: both threads were tied together with a central knot before being attached to a box prior to analysis (threads treated with 8.23 and 30.86 mmol L^{-1} of EDTA were vertically aligned for detection of low range of Mg(II) concentration and the other thread treated with 30.86 mmol L^{-1} of EDTA was horizontally aligned for detection of high range of Mg(II) concentration, respectively). Step 4: the sample (6 µL) can be added onto the crossing threads and the length of the color change can be measured with a ruler (summation of length from the central knot: Up and down for detection of low range of Mg(II) concentration, left and right for detection of high range of Mg(II) concentration). The analyte in samples then reacted with indicator reagents deposited on µTADs. This instantly produced the length of red-violet color zone on µTAD being proportional to the concentration of Mg(II) in samples within 2 min (Step 5) as demonstrated in Fig. 1. (Video related to research article appearing in Talanta)

Supplementary material related to this article can be found online at http://dx.doi.org/10.1016/j.talanta.2018.02.058.

For argentometric analysis, a polypropylene sheet was cut and made into a three-side box as a support (10 cm × 7.0 cm × 5 cm). A piece of paper printed with a ruler scale was fixed onto the base part of the box. Step 1: threads (15 cm) were stretched with the two ends attached at the rims of the box. Each thread was applied for different analysis. Step 2: the µTAD was pretreated with 0.15 M AgNO$_3$ (3 µL). Step 3: the µTAD was further treated with 5% w/v K$_2$CrO$_4$ (3 µL) producing regions of red-brown color within 1 min. Step 4: Samples containing chloride (3 µL) were applied to the prepared µTAD by using micropipette, in the middle of the scale printed on the polypropylene box. The analyte in the samples reacted with indicator reagents deposited on µTAD which instantly produced the summation of length of white color zone on the µTAD (within 1 min) being proportional to the concentration of chloride in samples (Step 5) (Fig. 2) (Video related to research article appearing in Talanta). The data of the color change length, which can be observed with naked eyes (roughly compared with the printed ruler scales) from both complexometric and argentometric titration, were then measured with a ruler and transferred to Microsoft Excel to generate calibration curves and standard scale for determination of Mg(II) and chloride, respectively.

Supplementary material related to this article can be found online at http://dx.doi.org/10.1016/j.talanta.2018.02.058.

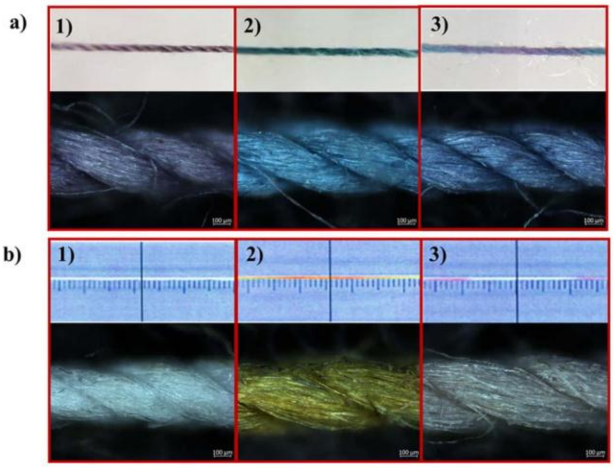

Fig. 3. Pictures (taken by camera of smartphone coupled with 20 × microscope lens) and morphology (taken by Polarized light microscope) of color distance for complexometric **a)** and argentometric titrations on μTAD **b)**.

2.6. Interferences and application of the developed μTADs for practical sample analysis on μTAD

Selectivity towards Mg(II) and chloride ion compared with potential interference ions was investigated. In complexometric analysis of Mg (II), the studied foreign cations were Fe(II), Cu(II), Mn(II), Zn(II), Ca(II), K(I), Na(I) and the anions were hydroxide, sulphate, nitrate, phosphate and chloride. Their tested concentrations were 10, 20, 30, 40, 50, 60, 70, 80, 90, 100, 150, 200, 250, 300, 350, 400, 450, 500, 750 and 1000 mg L^{-1}, respectively. Each ion solution also contained different concentration of Mg(II) (50 and 250 mg L^{-1} for low and high range of detection, respectively). Moreover, the determination of Mg(II) in real samples (as mentioned 2.4) using proposed μTAD was performed compared with classical complexometric titration method. RL sample was spiked with 50 and 100 mg L^{-1} of standard Mg(II) and tap, canal and mineral water samples were spiked with 100 mg L^{-1} of standard Mg(II) for recovery study.

In argentometric analysis of chloride ion, cations (Na(I), K(I), Cu(II), Ni(II), Fe(II), Cd(II), Mg(II), Ba(II), Mn(II), Pb(II), Ca(II), Zn(II), Hg(II)), and anions (nitrate, phosphate, sulphate, fluoride, bromide, iodide and sulphide) were investigated as the potential interferences in tap water, canal water, fish sauce and seasoning powders. These ions with different amounts (5, 10, 100, 1000, 2500, 5000, 1000 mg L^{-1}) were added to the test solution containing 100 mg L^{-1} of chloride ions. Determination of chloride in real samples (as mentioned 2.4) using proposed μTAD was carried out compared with classical complexometric titration method.

2.7. Method validation (using classical titrations)

The μTAD approaches were validated by comparison with conventional method. For complexometric analysis, water sample (10.0 mL) was transferred into a conical flask followed by addition of 0.06 mol L^{-1} NH_4Cl/NH_4OH buffer solution (2.0 mL) to control the solution pH within the range of 10.0–10.5. Next, 2.16×10^{-4} mol L^{-1} EBT indicator (1.0 mL) was dropped into the water solution. The solution was then titrated with the 5×10^{-3} mol L^{-1} EDTA standard solution (which was standardized with 5×10^{-3} mol L^{-1} $CaCO_3$) until the red solution vanished and became pure blue [12]. In addition, clear serum of RL at pH 4–5 was analyzed according to the similar procedure mentioned in water sample analysis.

For argentometric titration, sample solutions (10.0 mL) were transferred into a conical flask. After that, 5% w/v K_2CrO_4 solution (1.0 mL, indicator) was added to the sample solutions (with pH in the range of 7–10 which was adjusted by using 1 mol L^{-1} $CaCO_3$ for basic solution and 1 mol L^{-1} CH_3COOH for acidic solution. The solutions were then titrated with the 0.01 mol L^{-1} $AgNO_3$ standard (standardized with 0.01 mol L^{-1} NaCl). Although the form of AgCl is a white precipitate, addition of chromate (CrO_4^{2-}, indicator) initially resulted in the cloudy solution with a faint lemon-yellow color. The endpoint of the titration was identified as the first appearance of a red-brown color of Ag_2CrO_4.

3. Results and discussion

3.1. Study of wicking property of the threads

In this work, four different types of threads with different percentages of cotton (Fig. S2) were tested which were cotton 80% (0.30 ± 0.05), cotton 90% (0.29 ± 0.01), cotton 100% (0.30 ± 0.02) and polyester 100% (0.18 ± 0.01) (mm ± S.D., n = 10, Table S4). The fibers structures of these threads are different leading to different rates of fluid transport and penetration inside the threads. The wicking properties of the threads (untreated or treated with 10 mg L^{-1} of Na_2CO_3, which was added to remove wax cover on the thread (Fig. S3)) were examined in order to investigate the reproducibility of our results on μTAD. Note that wax was removed in order to change surface property affecting fluid wicking rate along the thread. Any surface heterogeneity will result in uneven rates of wicking. Moreover, natural cotton thread (un-mercerized) is hydrophobic [2]. To allow the wicking of aqueous solution on cotton threads, a chemical treatment is required to remove surface contaminants. Conversely, the synthetic polyester thread, which is inherently hydrophilic, allows aqueous liquid to wick by capillary action between fibers. Briefly, red color solution of food dye (3 μL) was added into central part of each thread (each with the length of 10 cm) using a micropipette within 1 min. The wicking rate data (cm/min) of threads before and after treatment measured according to a ruler scale were shown in Fig. S4. The wicking rate of 80%

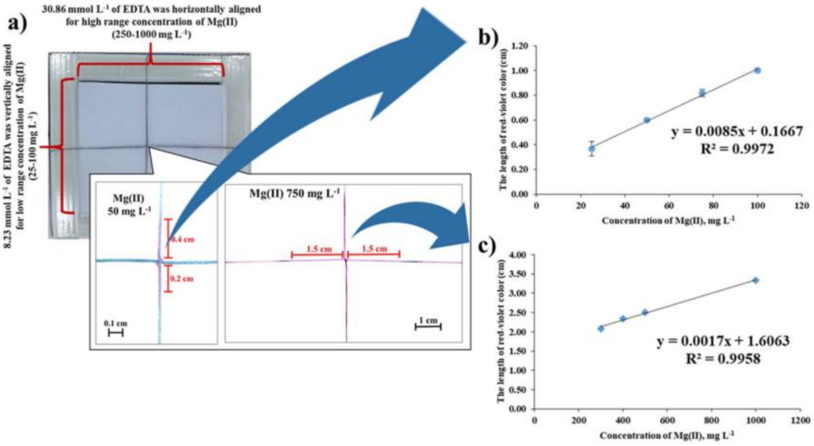

Fig. 4. The images illustrate that different concentrations of Mg(II) produced a color zone of differing length on developed μTAD for complexometric analysis **a)** and working range performed on developed μTAD of Mg(II) determination for low range concentration of Mg(II) **b)** and high range concentration of Mg(II) **c)**.

cotton before treatment was very low because of the thread hydrophobicity as mentioned above. After treatment, the rate increased. However, the wicking rates for 90% cotton, 100% cotton and 100% polyester decreased after treatment. This can be explained by the degeneration of the fiber structures after treatment. The result showed that the most suitable thread of wicking rate was 100% cotton thread due to the good wicking and dyeing properties, which was selected for μTAD fabrication in this study. Note that 100% polyester showed the best wicking property but it is difficult to dye which is not suitable for the measurement of length of color zone on μTAD.

3.2. Optimization of reagent conditions and their mechanism on μTADs

For complexometric method, the optimized reagent conditions used in our developed μTADs for determination of Mg(II) were based on the conventional ISO 17403: 2014(E) [12] and our previous approaches [14] using EBT, EDTA and NH_4Cl/NH_4OH buffer solution. A well-known reaction mechanism for Mg(II) analysis in aqueous (water and RL samples) is titration with EDTA and EBT as the indicator after the samples have been buffered to pH 10. The red complex between Mg and EBT will form before titration. At the end point, after complexation between Mg and EDTA is completed, EBT will turn to blue color as an original form. From preliminary study on μTADs (data not shown), the evaporation of ammonium buffer on μTADs was the main problem for the complexometric titration on μTADs. Thus, the ammonium buffer was replaced by CAPS for titration on μTADs.

To prove the mechanism and function of EDTA in suitable pH (threads were then tied together for clear observation), threads were pretreated with EBT. After that, μTAD was then treated with EDTA in CAPS buffer at pH 10 and EDTA in DI water at pH 6. It is clearly seen that only condition with EDTA at suitable pH (condition A) resulted in the length of red-violet color zone in the presence of Mg(II) (Fig. S5). Furthermore, effect of EDTA on μTAD based complexometric titration using the condition B (EDTA in CAPS buffer) was investigated by comparison between buffers with and without EDTA at pH 10 (Table S5). It is clearly seen that the length of purple color product generating on μTAD was proportional to the concentration of Mg(II) regardless of the presence or absence of EDTA. For each Mg(II) concentration, the length of red-violet color product in the absence of EDTA condition was longer. The concentration limit was at 750 mg L^{-1} Mg(II) due to no complexation between Mg(II) and EDTA. This observation can confirm that EDTA concentration and pH are the key factors affecting the performance of the developed complexometric titration on μTAD. The studied EDTA concentrations were within the range of 6.17–41.14 mmol L^{-1} (see also Table S6). The suitable concentrations of EDTA were 8.23 and 30.86 mmol L^{-1} for detection of low (25–100 mg L^{-1}) and high (300–1000 mg L^{-1}) ranges of Mg(II) concentrations, respectively, since these conditions provided a wide working range for Mg(II) detection. The box platform of μTAD was also designed and fabricated as mentioned in Section 2.5 (Fig. 1).

For chloride determination, optimization of reagent conditions was based on miniaturized argentometric titration using Mohr's method which was used as the conventional approach for chloride determination [13]. With sodium chromate as the indicator, chloride ions are titrated with the silver nitrate in the presence of chromate ions producing **yellow solution.** In general during the titration, Ag(I) (from $AgNO_3$ solution) is continuously added into the analyte solution containing chromate ion. Ag(I) initially reacts with chloride ion resulting in white solid of AgCl. The end point of this reaction can then be noticed when the excess amount of Ag(I) reacts with chromate ion in the solution forming red-brown solid of $Ag_2CrO_4(s)$. The concentration of the indicator is important. Ag_2CrO_4 has to start precipitating at the equivalence point, with a saturated solution of AgCl. This can be explained according to solubility product (Q) compared to K_{sp}, where $Q < K_{sp}$ and $Q > K_{sp}$ lead to soluble and precipitated products, respectively [15]. Thus, the optimization of $AgNO_3$ and K_2CrO_4 concentration for fabrication of argentometric titration on μTAD was carried out, as demonstrated in Fig. S6. The optimum $AgNO_3$ and K_2CrO_4 concentrations were 0.015 mmol L^{-1} and 5.0%w/v, respectively, obtained from the highest sensitivity (change of distance of white color on μTAD (cm) with chloride concentration). At 2.5%w/v of K_2CrO_4, the formation of insoluble Ag_2CrO_4 resulted in length of red-brown color on threads. (Fig. 3)

3.3. Analytical characteristics of μTADs

Working range performed on developed μTAD for complexometric analysis of Mg(II) was demonstrated in Fig. 4, S7 and Table S7. Two

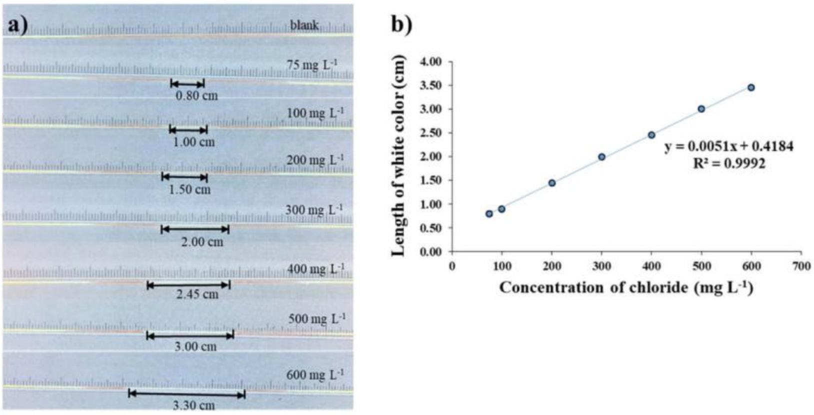

Fig. 5. The images illustrate that different concentrations of chloride produced a color zone of differing length on developed µTAD for argentometric analysis **a)** and working range performed on developed µTAD of chloride determination **b)**.

Table 1
Effect of foreign ions on the length of color change of added ions containing 50 mg L^{-1} and 250 mg L^{-1}of Mg(II) (n = 3).

Foreign ions	Compounds	Low range of Mg(II) detection at 50 mg L^{-1}		High range of Mg(II) detection at 250 mg L^{-1}	
		Tolerance concentration (mg L^{-1})	Deviation of length (cm)	Tolerance concentration (mg L^{-1})	Deviation of length(cm)
K(I)	K_2SO_4	700	0.02	750	0.11
Na(I)	Na_2SO4	90	0.05	450	0.10
Fe(II)	$FeSO_4{\cdot}7H_2O$	50	0.06	250	0.12
Mn(II)	$MnSO_4$	150	0.02	200	0.05
Ca(II)	$Ca(NO_3)_2$	20	0.01	500	0.09
Cu(II)	$CuSO_4{\cdot}5H_2O$	50	0.06	150	0.05
Zn(II)	$ZnSO_4$	80	0.01	200	0.03
Hydroxide ion	NaOH	10	−0.38	20	0.11
Sulphate ion	$MgSO_4{\cdot}7H_2O$	140	0.02	150	0.11
Nitrate ion	$Ca(NO_3)_2$	72	0.01	140	0.05
Phosphate ion	$NaH_2PO_4{\cdot}2H_2O$	50	0.01	300	0.14
Chloride ion	NaCl	250	0.01	1000	−0.20

*Length of red-violet color measurement of Mg (II) standard at 50 mg L^{-1} and 250 mg L^{-1} without foreign ions were 0.71 cm ± 0.10 cm and 2.08 cm ± 0.20 cm (n = 10), respectively.

threads were treated with two different concentrations of EDTA in CAPS buffer at pH 10. Sample solution was then applied to the µTAD. The length of red-violet color in both range on µTAD observed by naked eyes were proportional to the concentration of Mg(II) (Fig. 4a and S8a-b). The linearity ranges of the calibration curves (length of red-violet color vs concentrations of Mg(II)) for complexometric analysis of Mg(II) were found to be 25–200 mg L^{-1} (Fig. 4**b** and S7a) and 300–1000 mg L^{-1} (Fig. 4**c** and S7b) with good precision of intraday and interday (%RSD < 6) (Table S8a).

For argentometric analysis, after 3 µL of sample containing chloride was applied to the prepared µTAD. The analyte in the sample reacted with deposited red-brown indicator on the µTAD which instantly produced the length of white color zone on µTAD being proportional to the concentration of chloride in samples. The linearity range of the calibration curve (length of white color zone vs concentration of chloride) for argentometric analysis was in the range of 75–600 mg L^{-1} (**Fig. 5**) with good precision of intraday and interday (%RSD < 6). The LOQ was evaluated from lowest concentration of Mg(II) (25 mg L^{-1}) and chloride (75 mg L^{-1}) which can be observed by naked eyes (Table S8b).

3.4. Interferences study on developed µTADs

For complexometric analysis on thread, effects of foreign ions on the µTAD performance at low and high range of Mg(II) concentration were

Table 2
Effect of foreign ions on the length of color change of added ions containing 100 mg L^{-1} of chloride ion (n = 3).

Foreign ions	Compounds	Tolerance concentration (mg L^{-1})	Deviation of length (cm)
Na(I)	Na_2SO_4	10,000	−0.10
K(I)	K_2SO_4	10,000	0.10
Cu(II)	$CuSO_4{\cdot}5H_2O$	10,000	0.10
Ni(II)	$NiSO_4$	10,000	0.10
Fe(II)	$FeSO_4{\cdot}7H_2O$	10,000	0.10
Cd(II)	$Cd(NO_3)_2\,.4H_2O$	10,000	0.10
Mg(II)	$MgSO_4$	10,000	−0.10
Ba(II)	$Ba(NO_3)_2$	10,000	0.10
Mn(II)	$MnSO_4$	10,000	0.10
Pb(II)	$Pb(NO_3)_2$	10,000	−0.10
Ca(II)	$Ca(NO_3)_2$	10,000	0.10
Zn(II)	$ZnSO_4$	10,000	0.10
Hg(II)	$HgSO_4$	1	0.13
Sulphide ion	NaHS	1	0.13
Iodide ion	KI	1	0.13
Bromide ion	KBr	1	0.13
Fluoride ion	KF	10,000	0.10
Nitrate ion	$NaNO_3$	10,000	0.03
Phosphate ion	$NaH_2PO_4{\cdot}2H_2O$	10,000	−0.03
Sulphate ion	$MgSO_4{\cdot}7H_2O$	10,000	−0.10

*Length of white color measurement of chloride standard at 100 mg L^{-1} was 0.90 cm ± 0.15 cm (n = 10).

Table 3
Determination of Mg(II) in real samples using proposed μTAD compared with classical complexometric titration method and flame atomic absorption spectroscopy (FAAS) (n= 3).

Sample	FAAS				Complexometric titration[b]				Proposed method[c]		
	Concentration of (mg L^{-1})		% Recovery		Concentration of (mg L^{-1})		% Recovery		Length of red-violet color (cm)	Concentration of Mg(II) (mg L^{-1})	% Recovery
	Mg(II)	Ca(II)	Mg(II)	Ca(II)	Mg(II)	Ca(II)	Mg(II)	Ca(II)			
RL	11.6 ± 0.0014	N.D.[a]	–	–	17.8 ± 0.1	N.D.[a]	–	–	N.D.[a]	N.D.[a]	–
Spiked 100 mg L^{-1} of Mg(II)	117.7 ± 0.0027	N.D.[a]	105.5	–	121.9 ± 2.0	N.D.[a]	103.5	–	1.1 ± 0.1	109.8 ± 6.8	109.8
Tap water	0.3 ± 0.0003	7.2 ± 0.0003	–	–	N.D.[a]	9.6 ± 0.5	–	–	N.D.[a]	N.D.[a]	–
Spiked 100 mg L^{-1} of Mg(II) and 100 mg L^{-1} of Ca(II)	111.3 ± 0.0057	113.5 ± 0.0015	111.0	105.9	100.9 ± 0.7	125.5 ± 3.5	100.8	114.2	1.1 ± 0.1	113.7 ± 6.8	113.7
Drinking mineral water	5.0 ± 0.0011	38.7 ± 0.0018	–	–	5.5 ± 0.3	17.5 ± 0.0	–	–	N.D.[a]	N.D.[a]	–
Spiked 100 mg L^{-1} of Mg(II) and 100 mg L^{-1} of Ca(II)	104.3 ± 0.0028	140.5 ± 0.0028	99.3	101.4	91.6 ± 1.4	114.2 ± 3.0	86.8	97.2	1.0 ± 0.1	102.0 ± 6.8	102.0

[a] N.D.: Defined as "Not detectable".
[b] Complexometric titration.

$$Concentration\ of\ Mg(II),\ mg\ L^{-1} = \frac{V_a \times Standardized\ concentration\ of\ EDTA}{1000} \times M.W.\ of\ Mg$$

$$Concentration\ of\ Ca(II),\ mg\ L^{-1} = \frac{(V_b - V_a) \times Standardized\ concentration\ of\ EDTA}{1000} \times M.W.\ of\ Ca$$

$V_a = Volume\ of\ EDTA\ used\ for\ titration\ after\ precipitating\ out\ of\ Ca(II)\ by\ ammonium\ oxalate$

$V_b = volume\ of\ EDTA\ used\ for\ titration\ before\ precipitating\ out\ of\ Ca(II)\ by\ ammonium\ oxalate$

$M.W.\ of\ Mg = 24.3\ g\ atom^{-1}\ and\ M.W.\ of\ Ca = 40.1\ g\ atom^{-1}$

[c] Proposed method.

$Concentration\ of\ Mg(II),\ mg\ L^{-1} = Distance\ of\ sample\ after\ precipitating\ out\ of\ Ca(II)\ by\ ammonium\ oxalate$
After that fit to calibration curve of Mg(II) determination for low range concentration ($y = 0.0085x + 0.1667$).

investigated. This focuses on deviation of length of red-violet color with different foreign ions compared with the length obtained from Mg(II) standard at 50 mg L^{-1} and 250 mg L^{-1} without foreign ions, which were 0.71 cm ± 0.10 cm and 2.08 cm ± 0.20 cm (n = 10), respectively. It was found that deviation of length of color change of added ions was less than SD of the Mg(II) standard measurement without interferences with the results shown in Table 1. This indicates that insignificant interference from foreign ions except that from by hydroxide ions (Eq. S1) at low range of Mg(II) concentration. Such interference can avoided by pH adjustment before sample applications (the suitable pH of complexometric titration on developed μTAD was in range of 6–10). However, the concentrations of these ions in the real water samples and rubber latex are very much lower than the studied concentrations (Table S9 and S10).

Moreover, the effect of foreign ions on the length of white color change of added ions at various concentrations containing 100 mg L^{-1} of chloride on μTAD have been studied and demonstrated in Table 2. According to the observed high tolerance concentrations, it can be concluded that the investigated ions could not interfere the analysis of practical water samples. Note that the results revealed relatively low tolerance concentrations for Hg(II), sulphide ion, iodide ion, and bromide ion. However, the concentrations of these ions in the real water samples were much lower than the studied concentrations (Table S9). The condition of the reagent ($AgNO_3$ and K_2CrO_4 indicators) for argentometric titration on μTAD should be optimized (as mentioned in Section 3.3). Positive deviation caused by co-precipitation of white solid of AgCl and white solid formation between Ag(I) and interfering anions (such as bromide and iodide) were observed **(Eq. S2-3)** at higher tolerance concentration of added interfering ions as reported in Table 2.

3.5. *Real samples application on the developed μTADs and method validation*

The developed complexometric titration on μTAD was applied for analysis of Mg(II) in several samples shown in Table 3. Complexometric titration with complementary sample preparation (as described in footnote of Table 3.) was selected as the conventional technique for Mg (II) analysis which showed results being in agreement with our μTAD approach. Moreover, the recoveries of the developed μTAD for spiked RL and waters sample are good and acceptable. The developed argentometric titration on μTAD was applied for chloride analysis in water samples (tap and canal waters), fish sauce and seasoning powder samples compared with the conventional analysis based on argentometric titration. The result was in agreement with the conventional method as shown in Table 4.

In order to avoid potential interference in the titration based approach, such as the presence of Ca(II) in natural waters which can competitively bind with EDTA causing errors in Mg(II) analysis on our developed μTAD, and other complementary techniques were carried out to further validate the results. FAAS and ion chromatography were performed to validate the presence of Mg(II) and chloride ion, respectively. The results were shown in Tables 3, 4, which were also in agreement with that obtained from our μTAD analysis.

4. Conclusions

Novel low cost, portable and easy-to-use platforms of thread-based analytical devices (μTADs) for rapid complexometric analysis of Mg(II) and argentometric analysis of chloride ion in aqueous solutions were

Table 4
Determination of chloride in real samples using μTAD (proposed method) compared with classical argentometric titration method (n = 3) and ion chromatography (IC) (n = 1).

Sample	IC		Argentometric titration		Proposed method		
	Concentration of chloride ion (mg L^{-1})	% Recovery	Concentration of chloride ion (mg L^{-1})	% Recovery	Length of red-violet color (cm)	Concentration of chloride ion (mg L^{-1})	% Recovery
Tap water	16.91	–	21.27 ± 2.50	–	0.00	N.D.	–
Spiked 25 mg L^{-1} of chloride ions	40.22	93.2	47.27 ± 2.04	104.0		N.D.	–
Spiked 50 mg L^{-1} of chloride ions	57.15	80.5	70.90 ± 3.54	99.3	0.00	N.D.	–
Spiked 100 mg L^{-1} of chloride ions	114.80	97.9	127.62 ± 0.00	105.24	1.00	114.04 ± 0.00	114.0
Canal water	30.25	–	36.04 ± 1.30		0.00	N.D.	–
Spiked 25 mg L^{-1} of chloride ions	51.85	86.4	61.45 ± 2.04	101.6	0.00	N.D.	–
Spiked 50 mg L^{-1} of chloride ions	80.82	101.1	79.41 ± 2.04	86.7	0.00	N.D.	–
Spiked 100 mg L^{-1} of chloride ions	134.75	104.5	139.44 ± 5.38	103.4	1.00	114.04 ± 0.00	114.0
Fish sauce[a]	1490,000	-	1618,900 ± 5.82	-	2.27	1812,050 ± 0.25	-
Seasoning powder 1[a]	N.D.[b]	–	246,740 ± 3.88	–	1.00	228,080 ± 0.00	–
Seasoning powder 2[a]	N.D.[b]	–	242,480 ± 1.93	–	1.00	228,080 ± 0.00	–

Seasoning powder 1&2 (diluted 2000 fold).

Since matrix presented in seasoning powder is very complicated (e.g. organic contamination, fatty acid, protein and wax contamination in seasoning powder will be adsorbed on anion-exchange columns).

[a] Note: Fish sauce (diluted 5000 fold).

[b] Note: Chloride ion in seasoning powder 1, 2 cannot be detected by IC due to the limitation of instrument.

demonstrated. Interactions between deposited reagents and analytes in samples produce colored zones of different lengths on the threads within a few minutes. The lengths of the colored zones can be analyzed by naked eyes compared with the printed ruler scales which can be correlated with the concentrations of the analytes in the samples. The devices were evaluated with good linearity ranges and limit of detections with high tolerance limits for the interference ions. The developed μTADs were successfully applied for analysis of Mg(II) in several waters and RL samples, and analysis of chloride in tap water, canal waters and food seasoning powder samples with good precision. The results were in agreement with conventional titration, as well as other complementary techniques (FAAS and ion chromatography). Moreover, our developed μTADs with the length measurement are expected to be a pioneer platform for the development of other interesting analytes with a broad range of applications, offering a convenient and cost-effective alternative to the conventional laboratory-based equipment, as well as becoming innovative teaching tools in analytical chemistry.

Acknowledgement

This project was supported by the Thailand Research Fund (TRF: TRG5880007). The Center of Excellence for Innovation in Chemistry (PERCH-CIC), Office of the Higher Education Commission (OHEC), Ministry of Education is gratefully acknowledged. Science Achievement Scholarship of Thailand (SAST) given to Nutthaporn Malahom is also gratefully acknowledged. The research scholarships and instrumental facility of the Department of Chemistry, Faculty of Science, Ubon Ratchathani University, are also gratefully acknowledged.

Appendix A. Supplementary material

Supplementary data associated with this article can be found in the online version at http://dx.doi.org/10.1016/j.talanta.2018.02.058.

References

[1] C.E. Housecroft, E.C. Constable, Chemistry: An Introduction to Organic, Inorganic and Physical Chemistry, 3rd ed., Prentice Hall, Pearson, 2006.
[2] X. Li, J. Tian, W. Shen, Thread as a versatile material for low-Cost microfluidic diagnostics, Appl. Mater. Interfaces 2 (2010) 1–6.
[3] M. Reches, K.A. Mirica, R. Dasgupta, M.D. Dickey, M.J. Butte, G.M. Whitesides, Thread as a matrix for biomedical assays, Appl. Mater. Interfaces 2 (2010) 1722–1728.
[4] A. Nilghaz, D.R. Ballerini, W. Shen, Exploration of microfluidic devices based on multi-filament threads and textiles: a review, Biomicrofluidics 7 (2013) 051501–0515016.
[5] A. Nilghaz, D.R. Ballerini, X.-Y. Fang, W. Shena, Semiquantitative analysis on microfluidic thread-based analyticaldevices by ruler, Sens. Actuator B. 191 (2014) 586–594.
[6] D.R. Ballerini, X. Li, W. Shen, An inexpensive thread-based system for simple and rapid blood grouping, Anal. Bioanal. Chem. 399 (2011) 1869–1875.
[7] G. Zhou, X. Mao, D. Juncker, Immunochromatographic assay on thread, Anal. Chem. 84 (2012) 7736–7743.
[8] P. Jarujamrus, M. Amatatongchai, A. Thima, T. Khongrangdee, C. Mongkontong, Selective colorimetric sensors based on the monitoring of an unmodified silver nanoparticles (AgNPs) reduction for a simple and rapid determination of mercury, Spectrochim. Acta A Mol. Biomol. Spectrosc. 142 (2015) 86–93.
[9] A. Gonzalez, L. Estala, M. Gaines, F.A. Gomez, Mixed thread/paper-based microfluidic chips as a platform for glucose assays, Electrophoresis 37 (2016) 1685–1690.
[10] A. Gonzalez, M. Gaines, F.A. Gomez, Thread-based microfluidic chips as a platform to assess acetylcholinesterase activity, Electrophoresis 38 (2017) 996–1001.
[11] S. Sateanchok, S. Wangkarn, C. Saenjum, K. Grudpan, A cost-effective assay for antioxidant using simple cotton thread combining paper based device with mobile phone detection, Talanta 177 (2018) 171–175.
[12] Rubber-Determination of magnesium content of field and concentrated natural rubber latices by titration (cyanide-free method), ISO 17403:2014(E), ISO copyright office, Switzerland, 2014, pp. 16.
[13] G.H. Jeffrey, J. Bassett, J. Mendham, R.C. Denney, VOGEL's Textbook of Quantitative Chemical Analysis, 5th ed., Longman Scientific & Technical, New York, 1989.
[14] N. Malahom, P. Jarujamrus, R. Meelapsom, A. Siripinyanond, M. Amatatongchai, S. Chairam, Simple test kit based on colorimetry for quantification of magnesium content in natural rubber latex by miniaturized complexometric titration without using masking agent, Polym. Test. 59 (2017) 160–167.
[15] D.A. Skoog, D.M. West, F.J. Holler, S.R. Crouch, Fundamentals of Analytical Chemistry, 9th ed., Mary Finch, USA, 2014.

LIST OF PUBLICATIONS AND CONFERENCE PRESENTATIONS

CONFERENCE PRESENTATIONS

1 S. Puchum, N. Malahom, R. Meelapsom, M. Amatathongchai, S. Chairam A. Siripinyanond and P. Jarujamrus* "Argentometric Titration Using Thread-Based Analytical Device" **The 2018 Pure and Apllied Chemistry International Conference (PACCON 2018)**, 7 – 9 February 2018, Prince of Songkla University, Thailand.

2 S. Puchum, R. Meelapsom, S. S. Muniandy, HL. Lee, S. Pencharee, M. Amatatongchai, K. Suttisintong and P. Jarujamrus*. "Use of facile synthesized silver nanoparticles (AgNPs) as colorimetric sensors for sensitive and high sample throughput determination of Hg(II) ions in aqueous samples" **2018 International Congress for Innovation in Chemistry (PERCH-CIC Congress X)**. 4 – 7 July 2018, Jomtien Palm Beach Hotel & Resort in Pattaya, Thailand.***(Outstanding Poster Presentation award)***

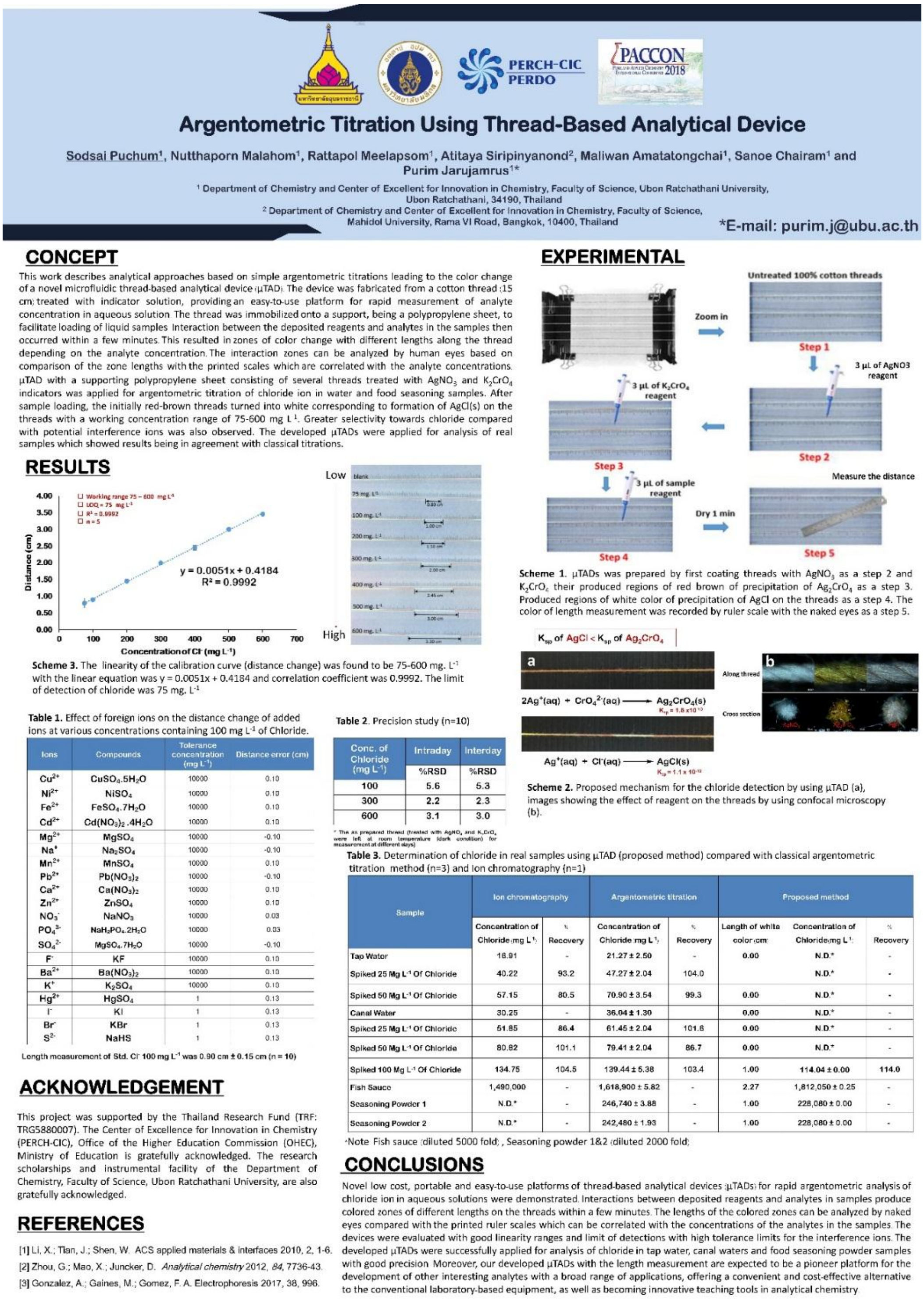

Argentometric Titration Using Thread-Based Analytical Device

Sodsai Puchum[1], Nutthaporn Malahom[1], Rattapol Meelapsom[1], Atitaya Siripinyanond[2], Maliwan Amatatongchai[1], Sanoe Chairam[1] and Purim Jarujamrus[1*]

[1] Department of Chemistry and Center of Excellent for Innovation in Chemistry, Faculty of Science, Ubon Ratchathani University, Ubon Ratchathani, 34190, Thailand
[2] Department of Chemistry and Center of Excellent for Innovation in Chemistry, Faculty of Science, Mahidol University, Rama VI Road, Bangkok, 10400, Thailand

*E-mail: purim.j@ubu.ac.th

CONCEPT

This work describes analytical approaches based on simple argentometric titrations leading to the color change of a novel microfluidic thread-based analytical device (µTAD). The device was fabricated from a cotton thread (15 cm) treated with indicator solution, providing an easy-to-use platform for rapid measurement of analyte concentration in aqueous solution. The thread was immobilized onto a support, being a polypropylene sheet, to facilitate loading of liquid samples. Interaction between the deposited reagents and analytes in the samples then occurred within a few minutes. This resulted in zones of color change with different lengths along the thread depending on the analyte concentration. The interaction zones can be analyzed by human eyes based on comparison of the zone lengths with the printed scales which are correlated with the analyte concentrations. µTAD with a supporting polypropylene sheet consisting of several threads treated with $AgNO_3$ and K_2CrO_4 indicators was applied for argentometric titration of chloride ion in water and food seasoning samples. After sample loading, the initially red-brown threads turned into white corresponding to formation of AgCl(s) on the threads with a working concentration range of 75-600 mg L^{-1}. Greater selectivity towards chloride compared with potential interference ions was also observed. The developed µTADs were applied for analysis of real samples which showed results being in agreement with classical titrations.

RESULTS

Scheme 3. The linearity of the calibration curve (distance change) was found to be 75-600 mg. L^{-1} with the linear equation was y = 0.0051x + 0.4184 and correlation coefficient was 0.9992. The limit of detection of chloride was 75 mg. L^{-1}

Table 1. Effect of foreign ions on the distance change of added ions at various concentrations containing 100 mg L^{-1} of Chloride.

Ions	Compounds	Tolerance concentration (mg L^{-1})	Distance error (cm)
Cu^{2+}	$CuSO_4.5H_2O$	10000	0.10
Ni^{2+}	$NiSO_4$	10000	0.10
Fe^{2+}	$FeSO_4.7H_2O$	10000	0.10
Cd^{2+}	$Cd(NO_3)_2.4H_2O$	10000	0.10
Mg^{2+}	$MgSO_4$	10000	-0.10
Na^{+}	Na_2SO_4	10000	-0.10
Mn^{2+}	$MnSO_4$	10000	0.10
Pb^{2+}	$Pb(NO_3)_2$	10000	-0.10
Ca^{2+}	$Ca(NO_3)_2$	10000	0.10
Zn^{2+}	$ZnSO_4$	10000	0.10
NO_3^-	$NaNO_3$	10000	0.03
PO_4^{3-}	$NaH_2PO_4.2H_2O$	10000	0.03
SO_4^{2-}	$MgSO_4.7H_2O$	10000	-0.10
F^-	KF	10000	0.10
Ba^{2+}	$Ba(NO_3)_2$	10000	0.10
K^+	K_2SO_4	10000	0.10
Hg^{2+}	$HgSO_4$	1	0.13
I^-	KI	1	0.13
Br^-	KBr	1	0.13
S^{2-}	NaHS	1	0.13

Length measurement of Std. Cl^- 100 mg L^{-1} was 0.90 cm ± 0.15 cm (n = 10)

Table 2. Precision study (n=10)

Conc. of Chloride (mg L^{-1})	Intraday	Interday
	%RSD	%RSD
100	5.6	5.3
300	2.2	2.3
600	3.1	3.0

* The as prepared thread (treated with $AgNO_3$ and K_2CrO_4 were left at room temperature (dark condition) for measurement at different days)

Table 3. Determination of chloride in real samples using µTAD (proposed method) compared with classical argentometric titration method (n=3) and Ion chromatography (n=1)

Sample	Ion chromatography		Argentometric titration		Proposed method		
	Concentration of Chloride (mg L^{-1})	% Recovery	Concentration of Chloride (mg L^{-1})	% Recovery	Length of white color (cm)	Concentration of Chloride (mg L^{-1})	% Recovery
Tap Water	16.91	-	21.27 ± 2.50	-	0.00	N.D.*	-
Spiked 25 Mg L^{-1} Of Chloride	40.22	93.2	47.27 ± 2.04	104.0		N.D.*	-
Spiked 50 Mg L^{-1} Of Chloride	57.15	80.5	70.90 ± 3.54	99.3	0.00	N.D.*	-
Canal Water	30.25	-	36.04 ± 1.30		0.00	N.D.*	-
Spiked 25 Mg L^{-1} Of Chloride	51.85	86.4	61.45 ± 2.04	101.6	0.00	N.D.*	-
Spiked 50 Mg L^{-1} Of Chloride	80.82	101.1	79.41 ± 2.04	86.7	0.00	N.D.*	-
Spiked 100 Mg L^{-1} Of Chloride	134.75	104.5	139.44 ± 5.38	103.4	1.00	114.04 ± 0.00	114.0
Fish Sauce	1,490,000	-	1,618,900 ± 5.82	-	2.27	1,812,050 ± 0.25	-
Seasoning Powder 1	N.D.*	-	246,740 ± 3.88	-	1.00	228,080 ± 0.00	-
Seasoning Powder 2	N.D.*	-	242,480 ± 1.93	-	1.00	228,080 ± 0.00	-

*Note Fish sauce (diluted 5000 fold), Seasoning powder 1&2 (diluted 2000 fold)

EXPERIMENTAL

Scheme 1. µTADs was prepared by first coating threads with $AgNO_3$ as a step 2 and K_2CrO_4 their produced regions of red brown of precipitation of Ag_2CrO_4 as a step 3. Produced regions of white color of precipitation of AgCl on the threads as a step 4. The color of length measurement was recorded by ruler scale with the naked eyes as a step 5.

K_{sp} of AgCl < K_{sp} of Ag_2CrO_4

$$2Ag^+(aq) + CrO_4^{2-}(aq) \xrightarrow{} \underset{K_{sp} = 1.8 \times 10^{-10}}{Ag_2CrO_4(s)}$$

$$Ag^+(aq) + Cl^-(aq) \xrightarrow{} \underset{K_{sp} = 1.1 \times 10^{-12}}{AgCl(s)}$$

Scheme 2. Proposed mechanism for the chloride detection by using µTAD (a), images showing the effect of reagent on the threads by using confocal microscopy (b).

ACKNOWLEDGEMENT

This project was supported by the Thailand Research Fund (TRF: TRG5880007). The Center of Excellence for Innovation in Chemistry (PERCH-CIC), Office of the Higher Education Commission (OHEC), Ministry of Education is gratefully acknowledged. The research scholarships and instrumental facility of the Department of Chemistry, Faculty of Science, Ubon Ratchathani University, are also gratefully acknowledged.

REFERENCES

[1] Li, X.; Tian, J.; Shen, W. ACS applied materials & interfaces 2010, 2, 1-6.
[2] Zhou, G.; Mao, X.; Juncker, D. *Analytical chemistry* 2012, *84*, 7736-43.
[3] Gonzalez, A.; Gaines, M.; Gomez, F. A. Electrophoresis 2017, 38, 996.

CONCLUSIONS

Novel low cost, portable and easy-to-use platforms of thread-based analytical devices (µTADs) for rapid argentometric analysis of chloride ion in aqueous solutions were demonstrated. Interactions between deposited reagents and analytes in samples produce colored zones of different lengths on the threads within a few minutes. The lengths of the colored zones can be analyzed by naked eyes compared with the printed ruler scales which can be correlated with the concentrations of the analytes in the samples. The devices were evaluated with good linearity ranges and limit of detections with high tolerance limits for the interference ions. The developed µTADs were successfully applied for analysis of chloride in tap water, canal waters and food seasoning powder samples with good precision. Moreover, our developed µTADs with the length measurement are expected to be a pioneer platform for the development of other interesting analytes with a broad range of applications, offering a convenient and cost-effective alternative to the conventional laboratory-based equipment, as well as becoming innovative teaching tools in analytical chemistry.

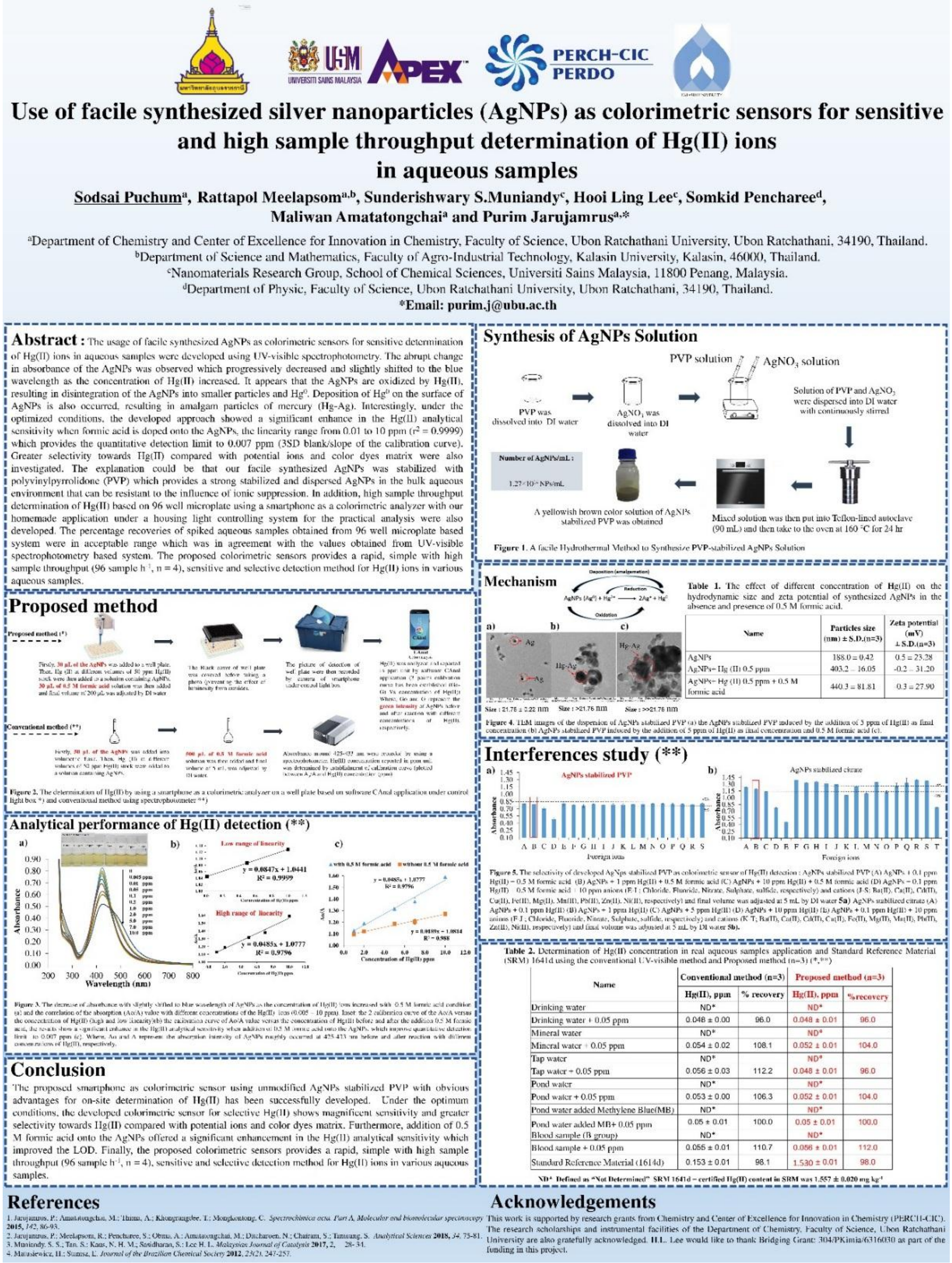

Use of facile synthesized silver nanoparticles (AgNPs) as colorimetric sensors for sensitive and high sample throughput determination of Hg(II) ions in aqueous samples

Sodsai Puchum[a], **Rattapol Meelapsom**[a,b], **Sunderishwary S.Muniandy**[c], **Hooi Ling Lee**[c], **Somkid Pencharee**[d],
Maliwan Amatatongchai[a] **and Purim Jarujamrus**[a,*]

[a]Department of Chemistry and Center of Excellence for Innovation in Chemistry, Faculty of Science, Ubon Ratchathani University, Ubon Ratchathani, 34190, Thailand.
[b]Department of Science and Mathematics, Faculty of Agro-Industrial Technology, Kalasin University, Kalasin, 46000, Thailand.
[c]Nanomaterials Research Group, School of Chemical Sciences, Universiti Sains Malaysia, 11800 Penang, Malaysia.
[d]Department of Physic, Faculty of Science, Ubon Ratchathani University, Ubon Ratchathani, 34190, Thailand.
***Email: purim.j@ubu.ac.th**

Abstract : The usage of facile synthesized AgNPs as colorimetric sensors for sensitive determination of Hg(II) ions in aqueous samples were developed using UV-visible spectrophotometry. The abrupt change in absorbance of the AgNPs was observed which progressively decreased and slightly shifted to the blue wavelength as the concentration of Hg(II) increased. It appears that the AgNPs are oxidized by Hg(II), resulting in disintegration of the AgNPs into smaller particles and Hg^0. Deposition of Hg^0 on the surface of AgNPs is also occurred, resulting in amalgam particles of mercury (Hg-Ag). Interestingly, under the optimized conditions, the developed approach showed a significant enhance in the Hg(II) analytical sensitivity when formic acid is doped onto the AgNPs, the linearity range from 0.01 to 10 ppm ($r^2 = 0.9999$) which provides the quantitative detection limit to 0.007 ppm (3SD blank/slope of the calibration curve). Greater selectivity towards Hg(II) compared with potential ions and color dyes matrix were also investigated. The explanation could be that our facile synthesized AgNPs was stabilized with polyvinylpyrrolidone (PVP) which provides a strong stabilized and dispersed AgNPs in the bulk aqueous environment that can be resistant to the influence of ionic suppression. In addition, high sample throughput determination of Hg(II) based on 96 well microplate using a smartphone as a colorimetric analyzer with our homemade application under a housing light controlling system for the practical analysis were also developed. The percentage recoveries of spiked aqueous samples obtained from 96 well microplate based system were in acceptable range which was in agreement with the values obtained from UV-visible spectrophotometry based system. The proposed colorimetric sensors provides a rapid, simple with high sample throughput (96 sample h^{-1}, n = 4), sensitive and selective detection method for Hg(II) ions in various aqueous samples.

Proposed method

Proposed method (*)

Firstly, **30 µL of the AgNPs** was added to a well plate. Then, Hg (II) at different volumes of 50 ppm Hg(II) stock were then added to a solution containing AgNPs. **30 µL of 0.5 M formic acid** solution was then added and final volume of 200 µL was adjusted by DI water

The picture of detection of well plate were then recorded by camera of smartphone under control light box

Conventional method (**)

Figure 2. The determination of Hg(II) by using a smartphone as a colorimetric analyzer on a well plate based on software CAnal application under control light box *) and conventional method using spectrophotometer **)

Analytical performance of Hg(II) detection (**)

Figure 3. The decrease of absorbance with slightly shifted to blue wavelength of AgNPs as the concentration of Hg(II) ions increased with 0.5 M formic acid condition (a) and the correlation of the absorption (Ao/A) value with different concentrations of the Hg(II) ions (0.005 – 10 ppm). Inset: the 2 calibration curve of the Ao/A versus the concentration of Hg(II) (high and low linearity)(b) the calibration curve of Ao/A value versus the concentration of Hg(II) before and after the addition 0.5 M formic acid, the results show a significant enhance in the Hg(II) analytical sensitivity when addition of 0.5 M formic acid onto the AgNPs, which improve quantitative detection limit to 0.007 ppm (c). Where, Ao and A represent the absorption intensity of AgNPs roughly occurred at 425-433 nm before and after reaction with different concentrations of Hg(II), respectively.

Conclusion

The proposed smartphone as colorimetric sensor using unmodified AgNPs stabilized PVP with obvious advantages for on-site determination of Hg(II) has been successfully developed. Under the optimum conditions, the developed colorimetric sensor for selective Hg(II) shows magnificent sensitivity and greater selectivity towards Hg(II) compared with potential ions and color dyes matrix. Furthermore, addition of 0.5 M formic acid onto the AgNPs offered a significant enhancement in the Hg(II) analytical sensitivity which improved the LOD. Finally, the proposed colorimetric sensors provides a rapid, simple with high sample throughput (96 sample h^{-1}, n = 4), sensitive and selective detection method for Hg(II) ions in various aqueous samples.

Synthesis of AgNPs Solution

PVP was dissolved into DI water

AgNO$_3$ was dissolved into DI water

Solution of PVP and AgNO$_3$ were dispersed into DI water with continuously stirred

Mixed solution was then put into Teflon-lined autoclave (90 mL) and then take to the oven at 160 °C for 24 hr

A yellowish brown color solution of AgNPs stabilized PVP was obtained

Number of AgNPs/mL :

1.27×10^{14} NPs/mL

Figure 1. A facile Hydrothermal Method to Synthesize PVP-stabilized AgNPs Solution

Mechanism

Size : 21.76 ± 0.22 nm

Size : >21.76 nm

Size : >>21.76 nm

Figure 4. TEM images of the dispersion of AgNPs stabilized PVP (a) the AgNPs stabilized PVP induced by the addition of 5 ppm of Hg(II) as final concentration (b) AgNPs stabilized PVP induced by the addition of 5 ppm of Hg(II) as final concentration and 0.5 M formic acid (c).

Table 1. The effect of different concentration of Hg(II) on the hydrodynamic size and zeta potential of synthesized AgNPs in the absence and presence of 0.5 M formic acid.

Name	Particles size (nm) ± S.D.(n=3)	Zeta potential (mV) ± S.D.(n=3)
AgNPs	188.0 ± 0.42	0.5 ± 23.28
AgNPs+ Hg (II) 0.5 ppm	403.2 ± 16.05	-0.2 ± 31.20
AgNPs+ Hg (II) 0.5 ppm + 0.5 M formic acid	440.3 ± 81.81	0.3 ± 27.90

Interferences study (**)

Figure 5. The selectivity of developed AgNps stabilized PVP as colorimetric sensor of Hg(II) detection : AgNPs stabilized PVP (A) AgNPs + 0.1 ppm Hg(II) + 0.5 M formic acid (B) AgNPs + 1 ppm Hg(II) + 0.5 M formic acid (C) AgNPs + 10 ppm Hg(II) + 0.5 M formic acid (D) AgNPs + 0.1 ppm Hg(II) + 0.5 M formic acid + 10 ppm anions (E-I ; Chloride, Fluoride, Nitrate, Sulphate, sulfide, respectively) and cations (J-S: Ba(II), Ca(II), Cd(II), Cu(II), Fe(II), Mg(II), Mn(II), Pb(II), Zn(II), Ni(II), respectively) and final volume was adjusted at 5 mL by DI water **5a)** AgNPs stabilized citrate (A) AgNPs + 0.1 ppm Hg(II) (B) AgNPs + 1 ppm Hg(II) (C) AgNPs + 5 ppm Hg(II) (D) AgNPs + 10 ppm Hg(II) (E) AgNPs + 0.1 ppm Hg(II) + 10 ppm anions (F-J ; Chloride, Fluoride, Nitrate, Sulphate, sulfide, respectively) and cations (K-T; Ba(II), Ca(II), Cd(II), Cu(II), Fe(II), Mg(II), Mn(II), Pb(II), Zn(II), Ni(II), respectively) and final volume was adjusted at 5 mL by DI water **5b).**

Table 2. Determination of Hg(II) concentration in real aqueous samples application and Standard Reference Material (SRM) 1641d using the conventional UV-visible method and Proposed method (n=3) (*,**)

Name	Conventional method (n=3)		Proposed method (n=3)	
	Hg(II), ppm	% recovery	Hg(II), ppm	%recovery
Drinking water	ND*		ND*	
Drinking water + 0.05 ppm	0.048 ± 0.00	96.0	0.048 ± 0.01	96.0
Mineral water	ND*		ND*	
Mineral water + 0.05 ppm	0.054 ± 0.02	108.1	0.052 ± 0.01	104.0
Tap water	ND*		ND*	
Tap water + 0.05 ppm	0.056 ± 0.03	112.2	0.048 ± 0.01	96.0
Pond water	ND*		ND*	
Pond water + 0.05 ppm	0.053 ± 0.00	106.3	0.052 ± 0.01	104.0
Pond water added Methylene Blue(MB)	ND*		ND*	
Pond water added MB+ 0.05 ppm	0.05 ± 0.01	100.0	0.05 ± 0.01	100.0
Blood sample (B group)	ND*		ND*	
Blood sample + 0.05 ppm	0.055 ± 0.01	110.7	0.056 ± 0.01	112.0
Standard Reference Material (1614d)	0.153 ± 0.01	98.1	1.530 ± 0.01	98.0

ND* Defined as "Not Determined" SRM 1641d – certified Hg(II) content in SRM was 1.557 ± 0.020 mg kg^{-1}

References

1. Jarujamrus, P.; Amatatongchai, M.; Thima, A.; Khongrangdee, T.; Mongkontong, C. *Spectrochimica acta. Part A, Molecular and biomolecular spectroscopy* **2015,** *142*, 86-93.
2. Jarujamrus, P.; Meelapsom, R.; Pencharee, S.; Obma, A.; Amatatongchai, M.; Ditcharoen, N.; Chairam, S.; Tamuang, S. *Analytical Sciences* **2018,** *34*. 75-81.
3. Muniandy, S. S.; Tan, S.; Kaus, N. H. M.; Sasidharan, S.; Lee H. L. *Malaysian Journal of Catalysis* **2017,** 2, 28-34.
4. Matusiewicz, H.; Stanisz, E. *Journal of the Brazilian Chemical Society* **2012,** *23(2)*, 247-257.

Acknowledgements

This work is supported by research grants from Chemistry and Center of Excellence for Innovation in Chemistry (PERCH-CIC). The research scholarships and instrumental facilities of the Department of Chemistry, Faculty of Science, Ubon Ratchathani University are also gratefully acknowledged. H.L. Lee would like to thank Bridging Grant: 304/PKimia/6316030 as part of the funding in this project.

PERCH-CIC

Center of Excellence for Innovation in Chemistry

Office of the Higher Education Commission, Ministry of Education

In recognition and appreciation to

Sodsai Puchum

for outstanding presentation in

2018 International Congress for Innovation in Chemistry

(PERCH-CIC Congress X)

July 4 - 7, 2018

Vichai Reutrakul

Professor Vichai Reutrakul

Director, PERCH-CIC

CURRICULUM VITAE

NAME	Mr. Sodsai Puchum
BORN	26 July 1994 in Sakon Nakhon, Thailand
EDUCATION	Bachelor degree of science (Chemistry), Faculty of science, Ubon Ratchathani University, 2016
SCHOLARSHIP	The Center of Excellence for Innovation in Chemistry (PERCH-CIC), Office of the Higher Education Commission (OHEC), Ministry of Education
EXPERIENCE	Department of Chemistry, Faculty of Science, Ubon Ratchathani University, Thailand **Teaching Assistant**: 1102 333 Instrumental Methods for Chemical Analysis laboratory (Semester 2/2561-62, in the year of 2018-19) **Research Assistant**: under Junior Science Talent Project (JSTP) scholarship NSTDA (Nov, 2018 - Mar, 2019) **Academic laboratory staff** of National Chemistry Olympiad, Ubon Ratchathani University (11-15, June, 2018)
REFERENCE	Asst. Prof. Purim Jarujamrus, Ph.D., Advisor, Department of Chemistry, Faculty of Science, Ubon Ratchathani University